Physics – Uspekhi **64** (3) 219 – 252 (2021)

REVIEWS OF TOPICAL PROBLEMS PACS numbers: **03.70. + k**, **04.62. + v**, 04.70.Dy, 05.30.Fk, 05.45.Ac, 05.45.Mt, 11.10.Kk, 11.10.Wx

Pedagogical introduction to the Sachdev–Ye–Kitaev model and two-dimensional dilaton gravity

D A Trunin

DOI: https://doi.org/10.3367/UFNe.2020.06.038805

Contents

Abstract. The Sachdev–Ye–Kitaev model and two-dimensional dilaton gravity have recently been attracting increasing attention of the high-energy and condensed-matter physics communities. The success of these models is due to their remarkable properties. Following the original papers, we broadly discuss the properties of these models, including the diagram technique in the limit of a large number of degrees of freedom, the emergence of conformal symmetry in the infrared limit, effective action, four-point functions, and chaos. We also briefly discuss some recent results in this field. On the one hand, we attempt to be maximally rigorous, which means considering all the details and gaps in the argument; on the other hand, we believe that this review can be suitable for those who are not familiar with the relevant models.

Keywords: Sachdev–Ye–Kitaev model, two-dimensional gravity, quantum chaos, $1/N$ expansion, AdS/CFT correspondence

D A Trunin
Moscow Institute of Physics and Technology
(National Research University),
Institutskii per. 9, 141701 Dolgoprudny, Moscow region,
Russian Federation;
National Research Center 'Kurchatov Institute',
Alikhanov Institute of Theoretical and Experimental Physics,
ul. B. Cheremushkinskaya 25, 117218 Moscow, Russian Federation
E-mail: dmitriy.trunin@phystech.edu

Received 3 March 2020, revised 28 June 2020
Uspekhi Fizicheskikh Nauk **191** (3) 225 – 261 (2021)
Translated by D A Trunin

1. Introduction

The Sachdev–Ye–Kitaev (SYK) model was proposed by A Kitaev [1] as a generalization of Sachdev–Ye model [2, 3] and was first extensively studied in [4–8]. Ever since, it has received great attention from the high-energy and condensed-matter physics communities.

The success of the SYK model is due to its remarkable properties. First, this model is exactly solvable in the limit of a large number of degrees of freedom N and the infrared (IR) limit. Second, in this limit, the model acquires conformal symmetry, and the effective action can be approximated by the Schwarzian one. Third, the leading corrections to the out-of-time ordered four-point correlation functions exponentially grow with time, with the exponent of this growth saturating the universal upper bound established in [9]. This behavior is very unusual; moreover, it coincides with the behavior of similar functions on a black hole background. Finally, the SYK model is closely related to two-dimensional

(2D) dilaton gravity, which describes excitations above the horizon of extremal black hole [10–13]. Together, these properties make the SYK model an excellent toy model for many physical phenomena, including quantum chaos [1, 9], information scrambling [14–16], traversable wormholes [17–20], and strange metals [21–23].

In this review, we give a pedagogical introduction to the SYK model and 2D dilaton gravity. We mostly follow original papers [4–13] and try to be as specific as possible, i.e., we do our best to reveal every detail and loophole in the discussion. We believe this makes the discussion clear and self-consistent. Due to this reason, we also expect the review to be suitable even for a reader who is not familiar with the phenomena under consideration.

The review is organized as follows. In Section 2, we briefly discuss quantum chaos and scrambling, the phenomena that are related to quantum black hole dynamics and motivate the study of the SYK model and 2D dilaton gravity. In particular, we introduce out-of-time ordered correlation functions (OTOCs), which are the main tool for studying these phenomena. We emphasize that in Section 2 we try to give a general motivation without focusing on details. For brevity, we postpone the discussion of specific examples until the following sections.

In Sections 3 and 4, we give a comprehensive review of the SYK model. We broadly discuss large N diagrammatics, the emergence of conformal symmetry in the IR limit, effective and Schwarzian actions, and exact two-point and four-point functions. Some technical details are discussed in the appendices. Also we briefly review recent results on the topic.

In Section 5, we attempt to give an equally comprehensive review of 2D dilaton gravity (more accurately, Jackiw–Teitelboim gravity). We show that this theory describes excitations near the horizon of extremal black hole, explain that this theory effectively reduces to the one-dimensional theory with Schwarzian action, and calculate four-point functions of the matter fields living in the corresponding space.

Finally, instead of a conclusion, in Section 6 we briefly review the most notable examples of chaotic behavior. Among them are the SYK model and 2D dilaton gravity (we briefly recall the main properties of these models), SYK-like tensor models, three-dimensional (BTZ, Bañados–Teitelboim–Zanelli) black hole, two-dimensional conformal field theory (CFT) with a large central charge, and Hermitian matrix quantum field theory with quartic self-interaction.

2. Motivation

The main motivation for studying the SYK model and 2D dilaton gravity is based on the connection to quantum chaos (see Section 2.1) and scrambling (see Section 2.2). It is also believed that these phenomena are related to the black hole information paradox [14, 15], so they have attracted a great amount of attention of the physical community.

Here, we qualitatively show that both of these phenomena are characterized by the exponential growth of OTOCs, which were first calculated in [24] and popularized by [9, 25, 26]. Therefore, systems with such a behavior of the correlators are of particular interest. The SYK model and 2D dilaton gravity are exactly such type of systems. In Section 6, we also briefly review other chaotic systems.

Note that this section may seem relatively sketchy, because we do not discuss the limits of applicability of the statements being formulated and do not provide any specific examples. Such examples will be broadly discussed in Sections 3–6. In fact, part of the original motivation to study the SYK model was exactly to find a convenient example for which the statements in Sections 2.1 and 2.2 can be verified in a controlled way [1].

2.1 Quantum chaos

In this section, we discuss the putative connection between some specific correlation functions and classical chaos [1, 9].

First of all, let us recall what classical chaos is. Consider a classical system with the following equation of motion:

$$\dot{X}^i(t) = F^i\big[X^i(t)\big]\,, \quad i = 1, \ldots, N\,, \tag{2.1}$$

where $\mathbf{X}$ is a vector in the N-dimensional phase space, $\mathbf{F}$ is a smooth vector function, and $\dot{X}^i \equiv \mathrm{d}X^i/\mathrm{d}t$. Let us introduce the norm on the phase space, $\|\cdot\|$, and expand the function $\mathbf{F}$ near a point $\mathbf{X}_0$:

$$\delta\dot{X}^i = A^i_j\,\delta X^j + B^i(\delta X^i)\,, \quad i = 1, \ldots, N\,, \tag{2.2}$$

where $\delta X^i \equiv X^i - X^i_0$, $A^i_j \equiv (\partial F^i/\partial X^j)_{\delta\mathbf{X}=\mathbf{0}}$, and B is an analytical function, such that $\|B(\delta\mathbf{X})\| \to 0$ as $\|\delta\mathbf{X}\| \to 0$. The solution of the linearized equation (i.e., the equation with B omitted) is straightforward:

$$\delta\mathbf{X} = \sum_{j=1}^{N} c_j\,\mathbf{h}_j \exp(\lambda_j t)\,, \tag{2.3}$$

where λ_j and $\mathbf{h}_j$ are eigenvalues and eigenvectors of the matrix A (for simplicity, we assume that all eigenspaces are one-dimensional), and c_j are integration constants that correspond to the initial condition $\delta\mathbf{X}(t=0) = \delta\mathbf{X}_0$. It is easy to see that, for long evolution times but small $\delta\mathbf{X}_0$, such that the condition $\|B(\delta\mathbf{X})\| \ll \|A\delta\mathbf{X}\|$ is always satisfied, the norm of the final deviation vector grows exponentially:

$$\big\|\delta\mathbf{X}(t)\big\| \leqslant \big\|\delta\mathbf{X}_0\big\| \exp(\lambda_{\max} t)\,, \tag{2.4}$$

where $\lambda_{\max}$ is the biggest eigenvalue of A. If this eigenvalue is positive, phase space trajectories rapidly diverge, i.e., a small perturbation in the initial conditions leads to a significant change in the future behavior of the system (at least for some set of initial conditions). Such sensitivity to initial conditions is sometimes called the 'butterfly effect' or 'classical chaos.'

In general, eigenvalues and eigenvectors depend on the point $\mathbf{X}_0$ and the definition of norm $\|\cdot\|$. However, the maximal eigenvalue, which is also referred to as the maximal Lyapunov exponent, can be considered as a general property of the system:

$$\lambda_{\max} \equiv \lim_{t\to\infty} \lim_{\|\delta\mathbf{X}\|\to 0} \sup \left(\frac{1}{t} \log \frac{\big\|\delta\mathbf{X}(t)\big\|}{\big\|\delta\mathbf{X}(0)\big\|}\right). \tag{2.5}$$

This definition can be applied to both linearized (2.2) and general (2.1) systems. Since the exponent (2.5) does not depend on the definition of the norm [27, 28], we can choose it as $\|\mathbf{X}\| = \sum_{i=1}^{N} |X^i|$. Then, the sensitivity to initial conditions can be reformulated as follows:

$$\left|\frac{\partial X^i(t)}{\partial X^j(0)}\right| \approx \left|\frac{\delta X^i(t)}{\delta X^j(0)}\right| \sim \exp(\lambda t) \tag{2.6}$$

for some components X^i and X^j of the vector $\mathbf{X}(t)$ which describes the phase trajectory. The first identity is approximately equal for small $\delta\mathbf{X}$.

Now, let us consider a larger system whose configuration space coincides with the phase space of the initial system: $q^i = X^i$, $i = 1, \ldots, N$. Here, q^i are generalized coordinates; corresponding generalized momenta are denoted as p^i. Introducing the Poisson bracket $\{\cdot,\cdot\}_{\mathrm{PB}}$, we can rewrite property (2.6) in a form suitable for quantum generalizations:

$$\left|\left\{q^i(t), p^j(0)\right\}_{\mathrm{PB}}\right| = \left|\sum_{k=1}^{N} \frac{\partial q^i(t)}{\partial q^k(0)} \frac{\partial p^j(0)}{\partial p^k(0)} - \frac{\partial q^i(t)}{\partial p^k(0)} \frac{\partial p^j(0)}{\partial q^k(0)}\right| = \left|\frac{\partial q^i(t)}{\partial q^j(0)}\right| \sim \exp(\lambda t)\,. \tag{2.7}$$

So far, we have considered classical mechanics. Let us now proceed to the quantum mechanical situation. We recall that in the semiclassical limit the Poisson bracket coincides with the commutator of the corresponding operators:

$$\left\{q^i(t), p^j(0)\right\}_{\mathrm{PB}} \sim -\frac{\mathrm{i}}{\hbar}\left[\hat{q}^i(t), \hat{p}^j(0)\right] \quad \text{as} \quad \hbar \to 0\,. \tag{2.8}$$

Note that the position and momentum operators on the right-hand side of (2.8) act at different moments of time, so expression (2.8) is not trivial.

This correspondence allows us to extend the concept of classical chaos and the maximal Lyapunov exponent to arbitrary quantum systems [1, 29–31]. Roughly speaking, we want to derive a quantity that correctly captures the sensitivity of the quantum system to a change in initial conditions and reproduces the exponential growth (2.6) in the limit $\hbar \to 0$ if the system is chaotic. The simplest expression of this kind is the following amplitude:

$$A_{\mathrm{in-out}} = \left\langle \mathrm{out}\right|\left[q^i(t), p^j(0)\right]\left|\mathrm{in}\right\rangle, \tag{2.9}$$

where $|\mathrm{in}\rangle$ and $|\mathrm{out}\rangle$ are initial and final wave functions of the system. Unfortunately, this expression has two drawbacks. First, due to the dependence on the specific states, the quantity (2.9) varies significantly for the same system. Second, in quantum field theory, one usually considers the analog of (2.9) for the vacuum state or thermal ensemble, for which two-point functions exponentially decay rather than grow (in quantum mechanics, correlation functions decay or grow algebraically). Thus, we need to eliminate the dependence on $|\mathrm{in}\rangle$ and $|\mathrm{out}\rangle$.

In order to do this, we sum over final states and average over a suitable initial ensemble, e.g., over the thermal one:

$$C(t) = \sum_n \sum_{\mathrm{out}} \frac{1}{Z} \exp(-\beta E_n) \times \left\langle n\right|\left[q^i(t), p^j(0)\right]^\dagger\left|\mathrm{out}\right\rangle\left\langle \mathrm{out}\right|\left[q^i(t), p^j(0)\right]\left|n\right\rangle = -\left\langle \left[q^i(t), p^j(0)\right]^2\right\rangle_\beta, \tag{2.10}$$

where β is the inverse temperature, E_n is the energy of the nth energy level, $Z = \sum_n \exp(-\beta E_n)$ is the partition function, and $\langle\ldots\rangle_\beta$ denotes averaging over the thermal ensemble. Such an average was first considered in the classical paper [24].

On the one hand, due to (2.8), we expect that this quantity exponentially grows: $C(t) \sim \hbar^2 \exp(2\lambda t)$. On the other hand, the semiclassical approximation is applicable only for small enough times, $t < t_* \sim (1/\lambda)\log(1/\hbar)$, where t_* is called the 'Ehrenfest time' [31–34]. One expects that for larger times correlator $C(t)$ approaches some constant value [9, 25]. Note that $t_* \to \infty$ as $\hbar \to 0$.

Moreover, the quantity (2.10) can be easily generalized to an arbitrary quantum system with a large number of degrees of freedom, $N \gg 1$:

$$C(t) = -\left\langle \left[V(t), W(0)\right]^2\right\rangle_\beta, \tag{2.11}$$

where V and W are Hermitian operators, each of which has vanishing one-point function ($\langle V\rangle_\beta = \langle W\rangle_\beta = 0$) and corresponds to $\mathcal{O}(1)$ degrees of freedom.[1] We call the system chaotic if quantity (2.11) grows exponentially for *all possible pairs*[2] of operators V and W with the mentioned properties. The maximal exponent of this growth is referred to as the 'quantum Lyapunov exponent.' The time t_* at which $C(t)$ saturates is referred to as 'scrambling time,' which is an analog of the Ehrenfest time. We will discuss the motivation for this terminology in more detail in Section 2.2.

Note that, in practice, the correlator (2.11) should be regularized, because it contains the product of operators at coincident times. A common approach is to uniformly smear the thermal distribution between the two commutators (which is equivalent to the smearing of operators in imaginary time):

$$C(t) = -\operatorname{tr}\left(\rho^{1/2}\left[V(t), W(0)\right]\rho^{1/2}\left[V(t), W(0)\right]\right), \tag{2.12}$$

where $\rho = (1/Z)\exp(-\beta H)$ is the density matrix. Of course, one can also consider other types of smearing, but this one has the most natural physical interpretation (see [36] for a more detailed discussion). Therefore, in this paper, we are interested in such correlators as (2.12). In Sections 3–6, we will see how such an expression arises naturally.

Let us expand the commutators in (2.12) and rewrite $C(t)$ as the sum of four four-point correlation functions:

$$\begin{aligned} C(t) &= 2\operatorname{tr}\left(V(t)\rho^{1/2}V(t)W\rho^{1/2}W\right) \\ &\quad - \operatorname{tr}\left(\rho^{1/2}V(t)W\rho^{1/2}V(t)W\right) - \operatorname{tr}\left(\rho^{1/2}WV(t)\rho^{1/2}V(t)W\right) \\ &= 2\,\mathrm{TOC}(t) - \mathrm{OTOC}\left(t - \frac{\mathrm{i}\beta}{4}\right) - \mathrm{OTOC}\left(t + \frac{\mathrm{i}\beta}{4}\right), \end{aligned} \tag{2.13}$$

where we denoted $W = W(0)$ for shortness, and introduced a time-ordered correlator (TOC) and out-of-time ordered correlator (OTOC):

$$\begin{aligned} \mathrm{TOC}(t) &\equiv \operatorname{tr}\left(V(t)\rho^{1/2}V(t)W\rho^{1/2}W\right), \\ \mathrm{OTOC}(t) &\equiv \operatorname{tr}\left(\rho^{1/4}V(t)\rho^{1/4}W\rho^{1/4}V(t)\rho^{1/4}W\right). \end{aligned} \tag{2.14}$$

There are two important time scales for $C(t)$. The first one is the dissipation time t_{d} at which two-point correlation functions exponentially decay: $\langle V(t)V\rangle_\beta \sim \langle W(t)W\rangle_\beta \sim \langle V(t)W\rangle_\beta \sim \exp(-t/t_{\mathrm{d}})$. Typically, $t_{\mathrm{d}} \sim \beta$. At this time scale, both the TOC and OTOC are approximately equal to the product of two disconnected two-point functions, so the

[1] For example, in the case of the SYK model, such operators are Majorana fermions: $V(t) = \chi_i(t)$, $W(0) = \chi_j(0)$.

[2] In integrable systems, the function $C(t)$ can grow for some, but not all, pairs of operators (see, e.g., [35]).

commutator $C(t)$ is close to zero [9, 37, 38]:

$$\begin{aligned}\mathrm{TOC}(t) &\approx \mathrm{OTOC}(t)\\ &\approx \langle VV\rangle_\beta\langle WW\rangle_\beta + \mathcal{O}\left(\exp\left(-\frac{t}{t_\mathrm{d}}\right)\right) + \mathcal{O}\left(\frac{1}{N}\right), \quad (2.15)\end{aligned}$$

where we denoted

$$\langle VV\rangle_\beta = \left\langle V\left(-\frac{\mathrm{i}\beta}{2}\right)V\right\rangle_\beta = \mathrm{tr}\,(\rho^{1/2}V\rho^{1/2}V)$$

for brevity. Let us recall that we are working in the large N limit, so the number $1/N$ plays the role of Planck's constant $\hbar$.

The second time scale is the scrambling time t_*. Typically, t_* is parametrically larger than t_d, namely $t_* \sim \beta\log N$. If the system is chaotic, well after the dissipation time and well before the scrambling time, $C(t)$ exponentially grows and the OTOC rapidly decays:

$$\begin{aligned}C(t) &\sim \frac{1}{N}\exp(\kappa t),\\ \mathrm{OTOC}(t) &\sim \langle VV\rangle_\beta\langle WW\rangle_\beta - \frac{A}{N}\exp(\kappa t),\end{aligned} \quad (2.16)$$

where A is some numerical coefficient. At greater times, $C(t)$ is saturated and the OTOC approaches zero. Since the TOC at such times is approximately constant, the growth of $C(t)$ and decay of the OTOC are qualitatively identical.

Thus, such a behavior of the OTOC and of function $C(t)$ can be considered an indicator of quantum chaos. In particular, it allows one to extract the quantum Lyapunov exponent κ, which is expected to coincide with the classical exponent (2.5) in the semiclassical limit.

However, we would like to emphasize two important points regarding OTOCs and quantum chaos. First, one should keep in mind that the argumentation of this section is quite naive, and in fact the connection between the exponential growth of $C(t)$ and classical chaos is questionable. There is evidence both in favor of this interpretation [39] and against it [40, 41]. For this reason, the notions of 'scrambling' (exponential growth of the OTOC) and 'chaos' (exponential growth of the average distance between phase trajectories) should be distinguished, although they are often considered to be the same.

Second, OTOCs are not the only possible measure of quantum chaos; in fact, there were several attempts to extend the concept of classical chaos to quantum systems. The most notable alternative approach[3] to quantum chaos is based on the level statistics at small energy separation: if this statistics agree with the Random Matrix Theory, one can consider the system to be chaotic [42–45]. This approach is also closely related to the Eigenstate Thermalization Hypothesis [46–48], which states that under some assumptions any local operator in an isolated quantum system eventually approaches its thermal form:

$$V_{ij} = \langle E_i|V|E_j\rangle = \overline{V}(E)\delta_{ij} + \exp\left(-\frac{1}{2}S(E)\right)f(E,\omega)R_{ij}, \quad (2.17)$$

where $|E_i\rangle$ is the state with energy E_i, $S(E) = -\mathrm{tr}\,(\rho\log\rho)$, $\overline{V}(E) = \mathrm{tr}\,(\rho V)$, thermal density matrix ρ is fixed by $E = \mathrm{tr}\,(\rho H)$, $f(E,\omega) = f(E,-\omega)$ is a smooth real function, and R_{ij} is a Hermitian random matrix with zero mean and unit variance. It is still unknown whether this old approach is related to OTOCs or not, although there is some evidence in favor of this assumption [49–53]. In particular, it was shown that the SYK model and 2D CFT with a large central charge under some assumptions behave like a random-matrix theory [54–56], whereas correlation functions in these models have the form (2.16).

2.2 Fast scramblers

The original motivation for studying OTOCs was based on the fast scrambling conjecture, which was proposed in [14, 15], proved in [16], and adapted for correlators in [9]. We briefly review this conjecture. Please note that this section may seem relatively vague if the reader does not have a specific example in mind. Such examples are discussed in Sections 3–6.

First of all, let us consider a complex quantum system with a large number of degrees of freedom N, prepare a pure state $|\Psi\rangle$, and let this state freely evolve under the action of unitary operator U. Due to the Eigenstate Thermalization Hypothesis, one expects that after a long enough time the system thermalizes, although its state remains pure. By this, we mean that the density matrix of every small subsystem (with the number of degrees of freedom $m < N/2$) is close to the thermal density matrix, or, equivalently, the entanglement entropy[4] of every small subsystem is close to the maximal value [57, 58]. Roughly speaking, by this time, the information about the initial state has been smeared throughout the system, so one needs to measure $\mathcal{O}(N)$ degrees of freedom to restore it. For this reason, it was proposed that such a system called 'scrambled' [14].

Let us then perturb a small number of degrees of freedom in a scrambled system and again let the system evolve freely. We expect that after some time the information about the perturbation is also smeared across all degrees of freedom, and the system returns to a scrambled state. This time is referred to as 'scrambling time.'

The fast scrambling conjecture [14–16] states that the scrambling time of any system cannot be less than $t_*^{\min} \sim \beta\log N$. Moreover, the bound is saturated for black holes (if they satisfy all the explicit and implicit assumptions of the conjecture), which makes them 'the fastest scramblers in nature by a wide margin.'[5] Later, it was argued that Rindler and de Sitter spaces also saturate this bound [15], but subsequent direct calculations in [59, 60] did not confirm this conjecture.[6] The fast scrambling conjecture has important implications for information cloning and the black hole information paradox [61–63].

To estimate the scrambling time, one needs to find how quickly a small perturbation spreads over the entire system. In some special cases, this process can be studied directly [64,

[3] In fact, this idea is old and well developed enough to be included in textbooks on chaos (see, e.g., [43–45]).

[4] Let's recall that the entanglement entropy of subsystem L is defined as $S_\mathrm{L} = -\mathrm{tr}_\mathrm{L}(\rho_\mathrm{L}\log\rho_\mathrm{L})$, where the trace is taken over the Hilbert space of L, $\rho_\mathrm{L} = \mathrm{tr}_\mathrm{R}\,|\Psi\rangle\langle\Psi|$, and R is the complement of L.

[5] For finite-dimensional systems, the bound can be tightened: $t_*^{\min} \sim \beta N^{2/d}$, where d is the dimensionality of the system [14]. For instance, in 3D, $t_*^{\min} \sim \beta N^{2/3}$. Thus, from this point of view, black holes seem to be infinite-dimensional systems.

[6] The original argumentation of [15] was based on the fact that the clock close to the event horizon goes as $\exp(2\pi t/\beta)$, where t is the asymptotic observer's time. However, later it was shown that this is not enough. This is a good reminder that it is important to clarify all the assumptions in which the hypothesis is formulated.

65], but much more often one needs to rely on implicit signs of scrambling. In essence, there are two such indicators.

One way to capture the rate of scrambling is to prepare a thermofield double (TFD) state, which describes two identical thermal subsystems,

$$|\mathrm{TFD}\rangle = \frac{1}{\sqrt{Z}}\sum_n \exp\left(-\frac{1}{2}\,\beta E_n\right)|n\rangle_{\mathrm{L}}\otimes|n\rangle_{\mathrm{R}}\,, \qquad \text{so that}\quad \rho_{\mathrm{L}} = \rho_{\mathrm{R}} = \frac{1}{Z}\sum_n \exp\left(-\beta E_n\right)|n\rangle\langle n|\,, \tag{2.18}$$

perturb one subsystem by a local operator, and check how the mutual information, $I_{\mathrm{LR}} = S_{\mathrm{L}} + S_{\mathrm{R}} - S_{\mathrm{L}\cup\mathrm{R}}$, evolves in time (see footnote 4 for the definition of S). Usually, subsystems are called 'left' (L) and 'right' (R), which explains the subscripts for S. Before the perturbation, both subsystems are highly correlated, so the mutual information is nonzero. However, gradually, the perturbation grows and affects more and more degrees of freedom. For instance, for a local operator V and a generic Hamiltonian H with local interactions, the kth term in the expansion of the evolved operator $V(t) = \exp(\mathrm{i}Ht)V\exp(-\mathrm{i}Ht)$ can lead to a product of k local operators:

$$V(t) = V + \mathrm{i}t[H,V] + \frac{(\mathrm{i}t)^2}{2!}\big[H,[H,V]\big] + \ldots + \frac{(\mathrm{i}t)^k}{k!}\big[H,\big[H,\ldots[H,V]\big]\big] + \ldots\,. \tag{2.19}$$

Thus, one expects that eventually the perturbation spreads throughout the entire system, the entanglement between the left and right subsystems disappears, and mutual information goes to zero. Therefore, the moment t_* at which $I_{\mathrm{LR}}(t_*) \approx 0$ can be considered an estimate of the scrambling time. An example of such a calculation can be found, e.g., in [26, 35, 66–68]. Notably, this calculation reproduces the conjectured bound $t_* \sim \beta\log N$ for black holes [26, 35].

Another way to evaluate t_* is based on the calculation of out-of-time-ordered correlators introduced in Section 2.1. Let us qualitatively explain why such correlators are sensitive to scrambling. As was noticed in [9, 25, 26, 35], an OTOC can be rewritten as a two-sided correlation function in a perturbed thermofield double state:

$$\mathrm{OTOC}(t) = \left\langle V\left(t-\frac{\mathrm{i}\beta}{4}\right)W(0)V\left(t+\frac{\mathrm{i}\beta}{4}\right)W\left(\frac{\mathrm{i}\beta}{2}\right)\right\rangle_\beta = \langle\psi|W_{\mathrm{L}}W_{\mathrm{R}}|\psi\rangle\,, \tag{2.20}$$

where V and W are local Hermitian operators, $W_{\mathrm{L}} = W^\dagger\otimes 1$ acts on the left subsystem, $W_{\mathrm{R}} = 1\otimes W$ acts on the right subsystem, and the perturbed state is as follows:

$$|\psi\rangle = V_{\mathrm{L}}\left(t+\frac{\mathrm{i}\beta}{4}\right)|\mathrm{TFD}\rangle = \frac{1}{\sqrt{Z}}\sum_{mn}\exp\left[-\frac{\beta}{4}(E_m+E_n)\right]V(t)_{nm}|m\rangle_{\mathrm{L}}\otimes|n\rangle_{\mathrm{R}}\,. \tag{2.21}$$

At small times, the operator V affects only $\mathcal{O}(1)$ degrees of freedom and cannot significantly change the global pattern of correlations, so the perturbed state is close to pure $|\mathrm{TFD}\rangle$. Thus, left and right subsystems are highly entangled, and the correlator is big, i.e., $\mathrm{OTOC}(t) \approx \langle VV\rangle_\beta\langle WW\rangle_\beta$. However, over time the perturbation involves other degrees of freedom and destroys the fragile pattern of correlations, so eventually the OTOC decays to zero. In this setting, scrambling time is the time at which the OTOC is saturated: $\mathrm{OTOC}(t_*) \approx 0$ or $C(t_*) \approx 2\langle VV\rangle_\beta\langle WW\rangle_\beta$.

What is interesting here is the rate at which the OTOC approaches zero. On general grounds, one expects that in the large N limit and for small evolution times the first correction to the OTOC is of the order of $\mathcal{O}(1/N)$:

$$\frac{\mathrm{OTOC}(t)}{\langle VV\rangle_\beta\langle WW\rangle_\beta} = 1 - \frac{A}{N}f(t) + \mathcal{O}\left(\frac{1}{N^2}\right), \tag{2.22}$$

where A is some positive $\mathcal{O}(1)$ numerical factor and $f(t)$ is some monotonically growing function. Extending this approximation to large times, one can qualitatively estimate the scrambling time as $t_* \sim f^{-1}(N/A)$, where f^{-1} is the inverse of f, $f\circ f^{-1} = f^{-1}\circ f = 1$. At the same time, the fast scrambling conjecture states that $t_* \gtrsim \beta\log N$. Therefore, the function f cannot grow faster than exponentially in time, $f(t) \lesssim \exp(\kappa t)$. The exponent of this growth is also bounded, $\kappa \leqslant B/\beta$, where B is a universal positive $\mathcal{O}(1)$ numerical constant. This analog of the fast scrambling conjecture for OTOCs was proven in [9] and called a 'bound on chaos':[7]

$$\frac{\mathrm{d}}{\mathrm{d}t}\big[\langle VV\rangle_\beta\langle WW\rangle_\beta - \mathrm{OTOC}(t)\big] \leqslant \frac{2\pi}{\beta}\big[\langle VV\rangle_\beta\langle WW\rangle_\beta - \mathrm{OTOC}(t)\big]\,,\ \text{i.e.,}\ \kappa \leqslant \frac{2\pi}{\beta}\,. \tag{2.23}$$

Note that, for systems that saturate the bound on f, the number κ can be considered an analog of the classical Lyapunov exponent from Section 2.1.

Furthermore, the OTOC is a very convenient measure of the spatial growth of operators. In $(d>1)$-dimensional chaotic systems (i.e., systems with $f(t)\sim\exp(\kappa t)$), the exponential growth in time is typically supplemented [70] by a coordinate-dependent factor: $f(t)\sim\exp[\kappa(t-|x|/v_{\mathrm{B}})]$, where $|x|$ is the distance to the initial perturbation caused by the operator V, and v_{B} is some positive constant. It is easy to see that the OTOC significantly deviates from the initial value only inside a ball of radius $r < v_{\mathrm{B}}t$. This ball can be interpreted as an area affected by the perturbation, i.e., the 'size' of the operator V. For this reason, constant v_{B} is called the 'butterfly velocity.' Discussions and examples of spatial operator growth can be found, for example, in [26, 70–74].

Of course, compared to mutual information, OTOCs are a very crude measure of scrambling. In particular, I_{LR} drops to zero almost immediately after t_*, whereas OTOCs at such times merely start to decay [26]. However, in practice it is much easier to calculate correlation functions than mutual information, which makes OTOCs a very popular tool. To date, OTOCs have been calculated in a large variety of models, including BTZ black hole [26, 74–76], the 2D CFT [35, 77, 78], de Sitter space [59, 60], the SYK model [1, 4–8] and its analogs [79–82], 2D dilaton gravity [10, 11], matrix models [27, 83], and, of course, in plenty of quantum many-body systems [29, 30, 71–73, 84–94]. In the following sections, we will take a closer look at the two most notable examples: the SYK model (see Sections 3 and 4) and 2D dilaton gravity (see Section 5).

Finally, let us emphasize that the arguments in [9, 14–16] work only for nearly equilibrium situations (e.g., large,

[7] In fact, for gravitational scattering of massive particles with spin $J>2$, one expects that $\kappa \sim (2\pi/\beta)(J-1)$. However, it was argued that such processes violate causality and unitarity [9, 69].

semiclassical black hole or eternal black hole in anti-de Sitter (AdS) space), assuming that a small perturbation induced by operator V cannot significantly change the initial state. Usually, OTOCs are also calculated for such situations. Due to this assumption, one can use the equilibrium (Matsubara) diagrammatic technique and apply the analytic continuation procedure to correlation functions. However, this intuition does not work if the perturbation is big or the system is far from equilibrium (e.g., for small black holes). In this case, one needs to use the nonequilibrium (Schwinger–Keldysh) diagrammatic technique and take into account that the state of the system can evolve in time [95, 96]. An example of such calculations for black holes and de Sitter space can be found in [20, 97–101], while a generalization of the nonequilibrium technique for OTOCs can be found in [84, 102]. However, it is still unknown whether the arguments in [9, 14–16] can be extended to nonequilibrium systems or not.

3. Basics of the Sachdev–Ye–Kitaev model

The SYK model is one of the most notable models for quantum chaos and holography. Due to its remarkable properties, it is an excellent toy model for many physical phenomena, including traversable wormholes [17–20] and strange metals [21–23]. For this reason, we review this model in great detail.

This section is mostly based on the pioneering papers [4–6] and talks by A Kitaev [1]. Reviews [103, 104] also contain instructive arguments. For simplicity, we consider the model with a four-fermion interaction vertex ($q = 4$), which is the simplest nontrivial and nondegenerate case. The generalization to other cases ($q \geqslant 2$) is almost straightforward and can be found in the mentioned references.

In this section, we discuss the basic properties of the SYK model: large N diagrammatics, the emergence of conformal symmetry in the IR limit, and effective and Schwarzian actions. A calculation of the four-point function is placed in a separate section (Section 4) because of its bulkiness.

3.1 Main definitions

The SYK model is a quantum mechanical model of $N \gg 1$ Majorana fermions with all-to-all random couplings:

$$I_{\mathrm{SYK}} = \int \mathrm{d}\tau \left[\frac{1}{2} \sum_{i=1}^{N} \chi_i(\tau) \dot{\chi}_i(\tau) - \frac{1}{4!} \sum_{i,j,k,l=1}^{N} J_{ijkl}\, \chi_i(\tau) \chi_j(\tau) \chi_k(\tau) \chi_l(\tau) \right], \tag{3.1}$$

where $\dot{\chi}_i = \mathrm{d}\chi_i/\mathrm{d}\tau$ and τ denotes the Euclidean time, which is related to the Lorentzian time t by the Wick rotation: $\tau = \mathrm{i}t$. In this section, we work in Euclidean time if not stated otherwise. Operators χ_i are Hermitian, $\chi_i = \chi_i^{\dagger}$, and obey the standard anticommutation relations:

$$\{\chi_i, \chi_j\} = \delta_{ij}\,, \quad i, j = 1, \ldots, N\,. \tag{3.2}$$

One can find more information about representations of the one-dimensional Clifford algebra in Appendix A. Note that in the one-dimensional case Majorana fermions are dimensionless. The couplings J_{ijkl} are distributed randomly and independently, i.e., according to the Gaussian distribution[8] with the following probability density function:

$$P(J_{ijkl}) = \exp\left(-\frac{N^3 J_{ijkl}^2}{12 J^2} \right) \quad \text{for every} \quad J_{ijkl}\,. \tag{3.3}$$

We emphasize that summation over i, j, k, and l is not assumed. This distribution leads to several important properties. First, it fixes the average and average square of couplings:

$$\overline{J_{ijkl}} = 0\,, \qquad \overline{J_{ijkl}^2} = \frac{3! J^2}{N^3}\,, \tag{3.4}$$

where J is a constant with the dimension of mass. Second, the even moments of couplings split into the sum of all possible products of the second moments (average squares), i.e., there is a Wick-type decomposition for an average of an even number of couplings. For instance,

$$\overline{J_{i_1 i_2 i_3 i_4} J_{j_1 j_2 j_3 j_4} J_{k_1 k_2 k_3 k_4} J_{l_1 l_2 l_3 l_4}} = \overline{J_{i_1 i_2 i_3 i_4} J_{j_1 j_2 j_3 j_4}}\; \overline{J_{k_1 k_2 k_3 k_4} J_{l_1 l_2 l_3 l_4}} + \overline{J_{i_1 i_2 i_3 i_4} J_{k_1 k_2 k_3 k_4}}\; \overline{J_{j_1 j_2 j_3 j_4} J_{l_1 l_2 l_3 l_4}} + \overline{J_{i_1 i_2 i_3 i_4} J_{l_1 l_2 l_3 l_4}}\; \overline{J_{j_1 j_2 j_3 j_4} J_{k_1 k_2 k_3 k_4}}\,. \tag{3.5}$$

To perform such an averaging, one should create many copies of the system with randomly chosen couplings,[9] calculate the expression in question, and average it over all copies.[10] The reasons why one requires properties (3.4) and (3.5) will become clear in Section 3.2.

Note that anticommutation relations (3.2) imply the antisymmetry of the couplings:

$$J_{ijkl} = \operatorname{sgn}\sigma J_{\sigma(i)\sigma(j)\sigma(k)\sigma(l)}\,, \quad \text{where} \quad \sigma\colon i \to \sigma(i)\,, \quad i = 1, \ldots, N\,. \tag{3.6}$$

First, this reduces the number of independent nonzero components of J_{ijkl} to $N!/[4!(N-4)!]$. Second, this allows one to define the disorder average of two arbitrary couplings:

$$\overline{J_{i_1 i_2 i_3 i_4} J_{j_1 j_2 j_3 j_4}} = \frac{3! J^2}{N^3} \sum_{\sigma} \operatorname{sgn}\sigma\, \delta_{i_1 \sigma(j_1)} \delta_{i_2 \sigma(j_2)} \delta_{i_3 \sigma(j_3)} \delta_{i_4 \sigma(j_4)}\,, \tag{3.7}$$

where the sum is performed over all possible permutations of indices. Essentially, this sum just checks whether indices of $J_{i_1 i_2 i_3 i_4}$ and $J_{j_1 j_2 j_3 j_4}$ coincide or not.

The important particular case in applications below is that of three coincident indices:

$$\sum_{k,l,m=1}^{N} \overline{J_{iklm} J_{jklm}} = \frac{3! J^2}{N^3} \sum_{k,l,m=1}^{N} \delta_{ij}\delta_{kk}\delta_{ll}\delta_{mm} + \ldots = \frac{3! J^2}{N^3} \left(N^3 \delta_{ij} + \mathcal{O}(N^2) \right) = 3! J^2 \delta_{ij} + \mathcal{O}\left(\frac{1}{N} \right). \tag{3.8}$$

Let us also specify the interval where Euclidean time τ runs. In this paper, we consider two closely related cases: Euclidean

[8] A generalization to non-gaussian distributions can be found in [105].

[9] In fact, if one is interested only in extensive quantities such as energy or entropy, in the large N limit it is sufficient to consider only one specific realization with randomly distributed couplings. Indeed, the large N system can be divided into a large number of large subsystems that automatically average themselves in extensive quantities.

[10] One can also consider a generalization of the model with dynamical couplings. In particular, large N fermionic tensor models reproduce all the main properties of the SYK model without the trick with the disorder average. For a review, see Section 6.2 and papers [106–111].

line $\tau_{\text{line}} \in (-\infty, \infty)$ and Euclidean circle $\tau_{\text{circle}} \in [-\beta/2,\ \beta/2)$, $\tau + \beta \sim \tau$. The first case describes zero-temperature quantum mechanics, whereas the second case corresponds to the thermal state with the inverse temperature $\beta = 1/T$. Below, we will use the following map to change between the Euclidean line and circle:

$$\tau_{\text{line}} = \tan \frac{\pi \tau_{\text{circle}}}{\beta} \,. \tag{3.9}$$

Note that this mapping function is real and monotonic, i.e., it preserves the order of times: $\mathrm{d}\tau_{\text{line}}/\mathrm{d}\tau_{\text{circle}} > 0$.

Finally, note that in the free theory the Hamiltonian is zero, $H_0(\tau) = 0$. Hence, operators are constant, even in the Heisenberg picture: $\chi_i(\tau) = \exp(\tau H_0)\chi_i(0)\exp(-\tau H_0) = \chi_i(0)$. Therefore, one can use anticommutation relations (3.2) to find the two-point correlation functions in the zero-temperature free theory:

$$\begin{aligned}\langle 0|\mathcal{T}\chi_i(\tau)\chi_j(0)|0\rangle &\equiv \theta(\tau)\langle 0|\chi_i\chi_j|0\rangle - \theta(-\tau)\langle 0|\chi_j\chi_i|0\rangle \\ &= \frac{1}{2}\operatorname{sgn}\tau\,\delta_{ij}\,,\end{aligned} \tag{3.10}$$

and finite-temperature free theory:

$$\big\langle \mathcal{T}\chi_i(\tau)\chi_j(0)\big\rangle_\beta = \frac{1}{2}\operatorname{sgn}\left(\sin\frac{\pi\tau}{\beta}\right)\delta_{ij}\,. \tag{3.11}$$

Here, $|0\rangle$ denotes the vacuum state in the free theory, and $\langle\ldots\rangle_\beta$ denotes averaging over the thermal distribution, together with the quantum averaging:

$$\langle\ldots\rangle_\beta \equiv \frac{\operatorname{tr}\left[\exp(-\beta H)\ldots\right]}{\operatorname{tr}\left[\exp(-\beta H)\right]}\,. \tag{3.12}$$

A more accurate derivation of the propagators can be found in Appendix A.

Note that the thermal fermion propagator is antiperiodic due to anticommutation rule (3.2). For instance, for $\tau > 0$,

$$\begin{aligned}\operatorname{tr}\left[\exp(-\beta H)\chi(\tau+\beta)\chi(0)\right] &= \operatorname{tr}\left[\chi(\tau)\exp(-\beta H)\chi(0)\right] \\ &= \operatorname{tr}\left[\exp(-\beta H)\chi(0)\chi(\tau)\right] = -\operatorname{tr}\left[\exp(-\beta H)\chi(\tau)\chi(0)\right].\end{aligned} \tag{3.13}$$

Finally, it is convenient to define the averaged correlation functions:

$$G_0(\tau) \equiv \frac{1}{N}\sum_{i=1}^{N}\big\langle \mathcal{T}\chi_i(\tau)\chi_i(0)\big\rangle = \frac{1}{2}\operatorname{sgn}\tau\,, \tag{3.14}$$

$$G_0^\beta(\tau) \equiv \frac{1}{N}\sum_{i=1}^{N}\big\langle \mathcal{T}\chi_i(\tau)\chi_i(0)\big\rangle_\beta = \frac{1}{2}\operatorname{sgn}\left(\sin\frac{\pi\tau}{\beta}\right). \tag{3.15}$$

Note that for $\tau \in [-\beta/2,\ \beta/2)$ the finite-temperature propagator (3.15) coincides with the zero-temperature propagator (3.14). Also note that any fermion Green's function is antisymmetric: $G(\tau) = -G(-\tau)$.

3.2 Two-point function and diagrammatics

Let us turn on the interaction term,

$$H(\tau) = \frac{1}{4!}\sum_{i,j,k,l} J_{ijkl}\chi_i(\tau)\chi_j(\tau)\chi_k(\tau)\chi_l(\tau)\,, \tag{3.16}$$

and calculate loop corrections — averaged over disorder — to the free propagators. For greater clarity, we turn back to the Lorentzian time for a while, expand the evolution operators, and calculate a few first orders in J. The evolution operator is given by the following expression:

$$\begin{aligned}U(t_1,t_2) &\equiv \mathcal{T}\exp\left[-\mathrm{i}\int_{t_2}^{t_1}\mathrm{d}t\,H(t)\right] \\ &= 1 - \mathrm{i}\int_{t_2}^{t_1}\mathrm{d}t\,H(t) - \int_{t_2}^{t_1}\mathrm{d}t\int_{t_2}^{t}\mathrm{d}t'\,H(t)H(t') + \ldots\,.\end{aligned} \tag{3.17}$$

The exact propagator $G(t)$ can be transformed into the following form:

$$\begin{aligned}G(t)\delta_{ij} &= \big\langle \mathcal{T}U^\dagger(t,-\infty)\chi_i(t)U(t,0)\chi_j(0)U(0,-\infty)\big\rangle \\ &= \frac{\big\langle \mathcal{T}\chi_i(t)\chi_j(0)U(+\infty,-\infty)\big\rangle}{\big\langle U(+\infty,-\infty)\big\rangle}\,.\end{aligned} \tag{3.18}$$

Here, we have used the unitarity of $U(t_1,t_2)$ and supposed that the vacuum state is not disturbed through adiabatic turning on and switching off of the interaction term [98, 112]. Note that we do not need to use the interaction picture, since $H_0 = 0$. Now, let us expand this expression and average it over the disorder:

$$\begin{aligned}G(t)\delta_{ab} = \Bigg\langle \mathcal{T}\Bigg[&\chi_a(t)\chi_b(0) \\ &- \frac{\mathrm{i}}{4!}\sum_{i,j,k,l}\overline{J_{ijkl}}\int_{-\infty}^{+\infty}\mathrm{d}t'\,\chi_a(t)\chi_b(0)\chi_i'\chi_j'\chi_k'\chi_l' \\ &- \frac{1}{2}\frac{1}{(4!)^2}\sum_{i,j,k,l,p,q,r,s}\overline{J_{ijkl}J_{pqrs}}\int_{-\infty}^{+\infty}\mathrm{d}t' \\ &\times\int_{-\infty}^{+\infty}\mathrm{d}t''\,\chi_a(t)\chi_b(0)\chi_i'\chi_j'\chi_k'\chi_l'\chi_p''\chi_q''\chi_r''\chi_s'' + \mathcal{O}(J^3)\Bigg]\Bigg\rangle,\end{aligned} \tag{3.19}$$

where we denoted $\chi_i(t') \equiv \chi_i'$ and $\chi_i(t'') \equiv \chi_i''$ for shortness. We also used the fact that in the large N limit the averaging over the disorder in the numerator and denominator in (3.19) can be done independently.

We now see that rules (3.4), (3.5), and (3.7) single out a very special type of vacuum expectation values. First, the disconnected part of the averages factorizes as usual. Second, odd orders in J_{ijkl} die out after disorder averaging. Third, the connected part of expression (3.19) reduces to the following expression:

$$\begin{aligned}G(t) - G_0(t) &= \frac{2\times 4\times 4!}{2(4!)^2}\frac{1}{N}\sum_{i,j,k,m,n}\overline{J_{ikmn}J_{jkmn}}\,\delta_{ij} \\ &\quad\times\int\mathrm{d}t'\,\mathrm{d}t''\,G_0(t-t')G_0^3(t'-t'')G_0(t'') + \mathcal{O}(J^4) \\ &= J^2\int\mathrm{d}t'\,\mathrm{d}t''\,G_0(t-t')G^3(t'-t'')G(t'') \\ &\quad + \mathcal{O}\left(\frac{J^2}{N}\right) + \mathcal{O}(J^4)\,.\end{aligned} \tag{3.20}$$

Here, we have applied Wick's theorem for the vacuum expectation values, contracted couplings with Kronecker deltas which come from the free propagators (3.10), used the antisymmetry of J_{ijkl} to find the numerical coefficient,[11] and used relation (3.8) to single out the leading order in N.

[11] All possible contractions give $4\times 4\times 3\times 2$ and the symmetry under the change $t' \leftrightarrow t''$ gives 2.

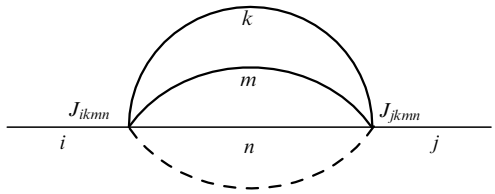

Figure 1. Melonic diagram.

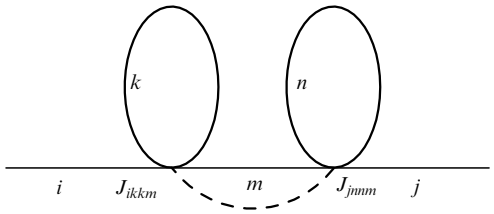

Figure 2. Double tadpole diagram that is identically zero.

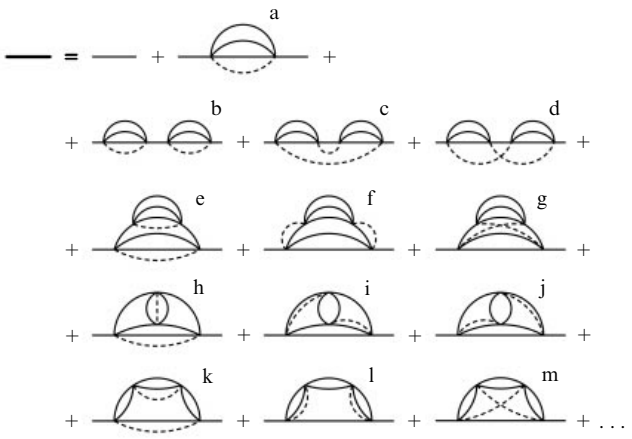

Figure 3. (a) Second-order and (b–m) fourth-order corrections to the propagator. The only diagrams that survive in the limit $N \to \infty$ are (a), (b), and (e).

Expression (3.20) can be schematically represented by a so-called melonic diagram (Fig. 1). The other second-order diagram (Fig. 2) identically equals zero, because it contains couplings with coincident indices. Solid lines in these diagrams denote fermion propagators, whereas dashed lines denote the disorder average.

Using Wick's theorem and relation (3.7), one can write higher order corrections which correspond to higher-order diagrams (Fig. 3). Each diagram is proportional to the certain power of J and N. The power of J is simply equal to the number of vertices of the diagram (each vertex gives J). The power of N has no simple connection with the shape of the diagram. However, it is easy to see that the only diagrams which survive in the limit $N \to \infty$ are melonic diagrams, because expression (3.8) is the only one of the order J^2N^0. Roughly speaking, Kronecker deltas in (3.8) are contracted directly (products of the form δ_{ii}), whereas Kronecker deltas in other averages are contracted through the other deltas (products of the form $\delta_{ij}\delta_{ji}$). The longer the 'path' of the index contraction, the lower the power of N.

For instance, compare the double melonic (Fig. 3b or 3e) and nonmelonic diagrams (e.g., Fig. 3h). The double melonic diagram contains the following disorder average:

$$\frac{J^4}{N^6}\sum \overline{J_{iklm}J_{nklm}}\;\overline{J_{npqr}J_{jpqr}} \propto \frac{J^4}{N^6}\sum \delta_{in}\delta_{kk}\delta_{ll}\delta_{mm}\delta_{jn}\delta_{pp}\delta_{qq}\delta_{rr} + \ldots = J^4 + \mathcal{O}\left(\frac{J^4}{N}\right). \tag{3.21}$$

Obviously, the contraction of six Kronecker deltas of the form δ_{nn} gives N^6, so that the overall order of the diagram is J^4N^0. At the same time, the diagram depicted in Fig. 3h contains a slightly modified average:

$$\frac{J^4}{N^6}\sum \overline{J_{iklm}J_{jqrm}}\;\overline{J_{krnp}J_{qlnp}} \propto \frac{J^4}{N^6}\sum \delta_{ij}\delta_{kq}\delta_{lr}\delta_{mm}\delta_{kq}\delta_{lr}\delta_{nn}\delta_{pp} + \ldots = \mathcal{O}\left(\frac{J^4}{N}\right). \tag{3.22}$$

Here, the power N^5 comes from the contraction of δ_{mm}, δ_{nn}, δ_{pp}, $\delta_{kq}\delta_{kq}$, and $\delta_{lr}\delta_{lr}$. One can see that two 'paths' of the contraction lengthened and one 'path' shortened, which reduced the power of N by one. Other possible products of the Kronecker deltas, which follow from (3.7), give even longer 'paths' of the contraction.

Thus, the only types of diagrams which survive in the limit $N \to \infty$ are melonic diagrams (Fig. 3a, 3b, and 3e). Moreover, one need not care about the signs and numerical coefficients in front of such diagrams, because all 'melons' come with the same numerical coefficient. In fact, the correction (see Fig. 1) can be thought of as a single block that can be inserted into any tree-level line of itself.

Recently, the dominance of melonic diagrams was also rigorously proved using a combinatorial analysis [113] and generalizations of the model [114]. We will not discuss these proofs.

Note that in this section we worked in the zero-temperature limit, $\beta = \infty$, i.e., calculated the vacuum expectation values. However, the obtained results can be easily generalized to the finite-temperature case, because the averaging over the disorder does not depend on the temperature and always singles out melonic diagrams. It does not matter whether the Feynman or Matsubara technique is used, the Kronecker delta products and numerical prefactors of the diagrams are the same.

3.3 Dyson–Schwinger equation and infrared limit

Using the results of the previous section, we can straightforwardly write the Dyson–Schwinger (DS) equation in the limit $N \to \infty$:

$$G(\tau_1,\tau_2) = G_0(\tau_1,\tau_2) + \int \mathrm{d}\tau_3\,\mathrm{d}\tau_4\, G_0(\tau_1,\tau_3)\Sigma(\tau_3,\tau_4)G(\tau_4,\tau_2)\,, \qquad \Sigma(\tau_1,\tau_2) \equiv J^2G^3(\tau_1,\tau_2)\,. \tag{3.23}$$

This equation sums up only the melonic diagrams which dominate in the limit in question. Here, we turned back to the Euclidean time and took into account that corrections to each propagator of the melon endlessly grow upwards (as in Fig. 3e) and to the right (as in Fig. 3b), so that corresponding tree-level propagators are replaced with exact ones (Fig. 4). This equation (with the appropriate limits of the integration over τ) holds for both zero- and finite-temperature propagators.

Due to translational invariance, the exact propagator depends only on the time difference: $G(\tau_1,\tau_2) = G(\tau_1 - \tau_2)$,

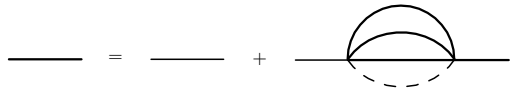

Figure 4. Dyson–Schwinger equation, which sums up melonic diagrams. Thin lines correspond to tree-level propagators, thick lines correspond to exact ones.

$\Sigma(\tau_1, \tau_2) = \Sigma(\tau_1 - \tau_2)$. Hence, we can make a Fourier transform of Eqn (3.23):

$$G^{-1}(\omega) = -\mathrm{i}\omega - \Sigma(\omega)\,, \tag{3.24}$$

where we substituted the explicit form of the tree-level propagator:

$$\begin{aligned} &G_0(\omega) \equiv \int_{-\infty}^{\infty} \mathrm{d}\tau\, \exp(\mathrm{i}\omega\tau)\, \frac{1}{2}\, \operatorname{sgn}\tau = \frac{\mathrm{i}}{\omega + \mathrm{i}0}\,, \\ &\text{i.e.,}\quad G_0^{-1}(\omega) = -\mathrm{i}\omega\,. \end{aligned} \tag{3.25}$$

Equation (3.23) can be solved numerically. Moreover, in the low frequency limit, $\omega \ll J$ (i.e., $J\tau \gg 1$), and strong coupling limit, $\beta J \gg 1$, one can also find its approximate analytical solution. Let us first consider the zero-temperature case $\beta = \infty$. On dimensional grounds, we expect that in the limit under consideration the exact propagator decays as $G(\tau) \sim \tau^{-1/2}$. Hence, the left-hand side of Eqn (3.23) is negligible, and the equation reduces to the following form (the result below shows that this assumption is correct):

$$0 = G_0(\tau_1, \tau_2) + \int_{-\infty}^{\infty} \mathrm{d}\tau_3 \int_{-\infty}^{\infty} \mathrm{d}\tau_4\, G_0(\tau_1, \tau_3)\Sigma(\tau_3, \tau_4)G(\tau_4, \tau_2)\,; \tag{3.26}$$

hence,

$$\int \mathrm{d}\tau\, \Sigma(\tau_1, \tau)G(\tau, \tau_2) = -\delta(\tau_1 - \tau_2)\,. \tag{3.27}$$

To obtain the second identity, we have differentiated (3.26) over τ_1, used the relation $\partial_1 G_0(\tau_1, \tau_2) = \delta(\tau_1 - \tau_2)$, and then taken the integral over τ_3. Obviously, the same equation arises when one throws out the inverse tree-level propagator in (3.24):

$$G^{-1}(\omega) \approx -\Sigma(\omega)\,, \quad \text{or} \quad \Sigma(\omega)G(\omega) \approx -1\,. \tag{3.28}$$

This is just a Fourier transform of Eqn (3.27). Note that in the limit in question DS equation (3.26) is invariant under reparametrizations of time, $\tau \to f(\tau)$, $f'(\tau) > 0$:

$$\begin{aligned} &G(\tau_1, \tau_2) \to G\bigl[f(\tau_1), f(\tau_2)\bigr] f'(\tau_1)^{\Delta} f'(\tau_2)^{\Delta}\,, \\ &\Sigma(\tau_1, \tau_2) \to \Sigma\bigl[f(\tau_1), f(\tau_2)\bigr] f'(\tau_1)^{3\Delta} f'(\tau_2)^{3\Delta}\,, \end{aligned} \tag{3.29}$$

where $\Delta = 1/4$. In fact,

$$\begin{aligned} &\int \mathrm{d}f(\tau)\, \Sigma\bigl[f(\tau'), f(\tau)\bigr] G\bigl[f(\tau), f(\tau'')\bigr] \\ &\quad = \frac{\int \mathrm{d}\tau\, \Sigma(\tau', \tau)G(\tau, \tau'')}{f'(\tau')^{1/4} f'(\tau'')^{3/4}} \\ &\quad = \frac{-\delta(\tau' - \tau'')}{f'(\tau')} = -\delta\bigl[f(\tau') - f(\tau'')\bigr]\,. \end{aligned} \tag{3.30}$$

We emphasize that these reparametrizations should respect the orientation of the Euclidean circle; otherwise, the last equality in (3.30) does not hold.

Thus, we conclude that in the IR limit fermions acquire an anomalous conformal dimension [12] $\Delta = 1/4$. This hints at the following ansatz to solve the DS equation:

$$G_{\mathrm{c}}(\tau_1, \tau_2) = B\, \frac{\operatorname{sgn}\tau_{12}}{|J\tau_{12}|^{2\Delta}}\,, \tag{3.31}$$

where $\tau_{12} \equiv \tau_1 - \tau_2$ and B is some numerical constant to be determined. The index 'c' stands for 'conformal'. Keeping in mind the following integral, which reduces to the gamma-function after $\pi/2$ rotation in the complex plane,

$$\int_{-\infty}^{\infty} \mathrm{d}\tau\, \exp(\mathrm{i}\omega\tau)\, \frac{\operatorname{sgn}\tau}{|\tau|^{2D}} = 2\mathrm{i}\Gamma(1 - 2D)\cos(\pi D)|\omega|^{2D-1} \operatorname{sgn}\omega\,, \tag{3.32}$$

we confirm that the proposed ansatz does solve Eqn (3.26), and find the numerical factor B:

$$G_{\mathrm{c}}(\tau) = \frac{1}{(4\pi)^{1/4}}\, \frac{\operatorname{sgn}\tau}{|J\tau|^{2\Delta}}\,. \tag{3.33}$$

Note that this solution decays as $J(\tau_1 - \tau_2) \to \infty$ which confirms the self-consistency of the approximation in which Eqn (3.26) was obtained. This solution was originally found by Sachdev and Ye in a system of randomly coupled spins [2].

Finally, reparametrization invariance (3.29) allows one to find the finite-temperature exact propagator without solving the corresponding DS equation [115]. In fact, zero- and finite-temperature propagators are connected by map (3.9), which satisfies the condition $f'(\tau) > 0$. Therefore, we can simply use this map in expression (3.33):

$$G_{\mathrm{c}}^{\beta}(\tau) = \frac{\pi^{1/4}}{\sqrt{2\beta J}}\, \frac{\operatorname{sgn}\bigl[\sin(\pi\tau/\beta)\bigr]}{|\sin(\pi\tau/\beta)|^{2\Delta}}\,, \quad \tau \in \left[-\frac{\beta}{2}, \frac{\beta}{2}\right). \tag{3.34}$$

Here, we substituted the correct sgn function from Section 3.1, which allows generalizing (3.34) to arbitrary times. At the same time, note that $\operatorname{sgn}\bigl[\sin(\pi\tau/\beta)\bigr] = \operatorname{sgn}\bigl[\tan(\pi\tau/\beta)\bigr] = \operatorname{sgn}\tau$ for $\tau \in [-\beta/2, \beta/2)$. Also note that in the limit $\tau \ll \beta$ expressions (3.33) and (3.34) coincide.

We recall that $G_{\mathrm{c}}(\tau)$ and $G_{\mathrm{c}}^{\beta}(\tau)$ are approximately equal to the exact propagators $G(\tau)$ and $G^{\beta}(\tau)$ only for relatively large times $\tau \gg 1/J$. At the same time, in the ultraviolet (UV) limit ($\tau \ll 1/J$), exact propagators are approximately equal to the bare ones, $G_0(\tau)$ and $G_0^{\beta}(\tau)$, respectively. In the intermediate region, $G(\tau)$ and $G^{\beta}(\tau)$ interpolate between these functions (see, e.g., Fig. 5).

After the analytic continuation of (3.34) to the Lorentzian time $t = -\mathrm{i}\tau$, the following two-point function is obtained: [13]

$$G_{\mathrm{c}}^{\beta}(t) = \frac{\pi^{1/4}}{\sqrt{2\beta J}}\, \frac{1}{\bigl|\sinh(\pi t/\beta)\bigr|^{2\Delta}} \propto \exp\left(-\frac{2\pi\Delta}{\beta}\, t\right), \quad t \gg \frac{1}{J}\,. \tag{3.35}$$

This function becomes exponentially small after the time $t_{\mathrm{d}} = \beta/(2\pi\Delta) \sim \beta$, which is usually called the dissipation

[12] In general, in the model with the q-fermion interaction term, fermions acquire a conformal dimension $\Delta = 1/q$.

[13] Note that in the Lorentzian signature one should specify the propagator (i.e., ordering of the operators in the correlation function) [5, 112]. The analytical behavior of different propagators is different, but the overall exponential factor is unique.

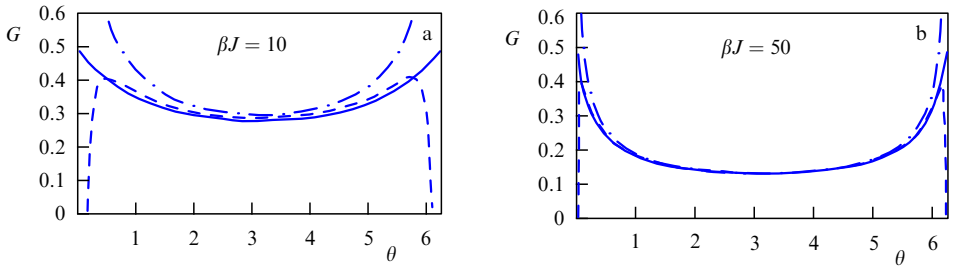

Figure 5. Numerical solutions to the large N Dyson–Schwinger equation (3.23) obtained in [5] for (a) $\beta J = 10$ and (b) $\beta J = 50$. Exact solutions are shown in solid lines, conformal approximations in dashed-dotted lines, and conformal approximations plus the first correction (which breaks the reparametrization invariance) in dashed lines. For convenience, the variable $\theta = 2\pi\tau/\beta$ is introduced.

time. We will return to this expression when we discuss four-point functions (see Section 4).

In general, this behavior is quite unusual for a one-dimensional system, but we emphasize that we consider the large $N \to \infty$ limit. In fact, it was shown in [116] that the exponential decay is replaced by the correct power-like one, $G_c^\beta(t) \sim (t/t_M)^{-3/2}$, for times larger than $t_M \sim N/J$.

3.4 Effective action

Let us derive the effective action and DS equation (3.23) directly from the path integral. Recall that we assume a Gaussian distribution for coupling constants J_{ijkl}, which gives the following averaging rule:

$$\overline{f(J_{ijkl})} \equiv \int \mathcal{D}J_{ijkl}\, f(J_{ijkl})\,, \qquad \mathcal{D}J_{ijkl} \equiv \exp\left(-\frac{N^3}{12J^2}\sum_{i<j<k<l} J_{ijkl}^2\right) \prod_{i<j<k<l} \sqrt{\frac{N^3}{3!J^2}}\,\frac{\mathrm{d}J_{ijkl}}{\sqrt{2\pi}}\,. \tag{3.36}$$

However, this rule does not specify which quantities need to be averaged, so, practically, there are two distinct ways to realize the disorder average. First, one can average the partition function itself, i.e., find $\overline{Z}$. Second, one can average the free energy using the so-called replica trick:

$$\beta\bar{F} \equiv -\overline{\log Z} = -\lim_{M\to 0} \partial_M \overline{Z^M}\,. \tag{3.37}$$

In this approach, one introduces M copies of the system ($\chi_i \to \chi_i^\alpha, i = 1,\ldots,N, \alpha = 1,\ldots,M$), calculates the extended partition function Z^M, averages over the disorder, analytically continues to noninteger M, and takes the formal limit (3.37). If one wants to find the free energy, entropy, and other thermodynamic functions that are in some sense directly observable quantities, one should use the second approach. If correlation functions are the primary target, then the first, relatively simple, approach is more viable.

However, in the SYK model, both methods of averaging give the same result [7, 23, 103], because the replica-nondiagonal contributions to the effective action are suppressed by higher powers of $1/N$, so the full partition function simply splits into the product of M naively-averaged partition functions: $\overline{Z^M} = (\overline{Z})^M + \mathcal{O}(1/N)$. One can find details about the replica calculation in [6, 7, 117, 118]. Thus, for simplicity, we consider the disorder average of the partition function itself:

$$\begin{aligned}
\overline{Z} &= \int \mathcal{D}J_{ijkl}\mathcal{D}\chi_i \exp\left[\int \mathrm{d}\tau \left(\frac{1}{2}\sum_{i=1}^N \chi_i\,\partial\chi_i - \frac{1}{4!}\sum_{i,j,k,l=1}^N J_{ijkl}\,\chi_i\chi_j\chi_k\chi_l\right)\right] \\
&= \int \mathcal{D}\chi_i \exp\left[\frac{1}{2}\sum_i \int \mathrm{d}\tau\,\chi_i\,\partial\chi_i + \frac{3!J^2}{2N^3}\,\frac{1}{4!}\sum_{i,j,k,l}\left(\int \mathrm{d}\tau\,\chi_i\chi_j\chi_k\chi_l\right)^2\right] \\
&= \int \mathcal{D}\chi_i \exp\left[\frac{1}{2}\sum_i \int \mathrm{d}\tau\,\chi_i\,\partial\chi_i + \frac{NJ^2}{8}\int \mathrm{d}\tau\,\mathrm{d}\tau'\left(\frac{1}{N}\sum_i \chi_i(\tau)\chi_i(\tau')\right)^4\right] \\
&= \int \mathcal{D}\chi_i \exp\left[\int \mathrm{d}\tau\,\mathrm{d}\tau'\left(\frac{N}{2}\,G_0^{-1}(\tau,\tau')\Xi(\tau,\tau') + \frac{NJ^2}{8}\,\Xi^4(\tau,\tau')\right)\right].
\end{aligned} \tag{3.38}$$

Here, we performed gaussian integration over J_{ijkl}, reorganized the integrals over $\mathrm{d}\tau$, and summed over fermion indices. For convenience, we also introduced the inverse tree-level propagator $G_0^{-1}(\tau,\tau')$ and mean field variable $\Xi(\tau,\tau')$:

$$G_0^{-1}(\tau,\tau') = \delta(\tau-\tau')\,\partial_\tau\,, \qquad \Xi(\tau,\tau') = \frac{1}{N}\sum_{i=1}^N \chi_i(\tau)\chi_i(\tau')\,. \tag{3.39}$$

Now, we formally apply the identity

$$f(\Xi) = \int \mathrm{d}x\, f(x)\delta(x-\Xi) = \frac{N}{2\pi}\int \mathrm{d}x\,\mathrm{d}y\, f(x)\exp\left[\mathrm{i}N(x-\Xi)y\right] \tag{3.40}$$

for the functional variables

$$x = G(\tau,\tau'), \quad y = i\Sigma(\tau,\tau') \tag{3.41}$$

with the normalization condition

$$\int \mathcal{D}G\,\mathcal{D}\Sigma \exp\left[-\frac{N}{2}\int \mathrm{d}\tau\,\mathrm{d}\tau'\,\Sigma(\tau,\tau')G(\tau,\tau')\right] = 1 \tag{3.42}$$

to the function

$$\begin{aligned}
&\exp\left[\frac{NJ^2}{8}\int \mathrm{d}\tau\,\mathrm{d}\tau'\,\Xi^4(\tau,\tau')\right] \\
&\quad = \int \mathcal{D}G\,\mathcal{D}\Sigma\, \exp\left\{\frac{N}{2}\int \mathrm{d}\tau\,\mathrm{d}\tau'\left[\frac{J^2}{4}\,G^4(\tau,\tau') - \Sigma(\tau,\tau')\big(G(\tau,\tau') - \Xi(\tau,\tau')\big)\right]\right\}.
\end{aligned} \tag{3.43}$$

In this way, we reorganize the nonlinear term $\Xi^4(\tau,\tau')$ in (3.38):

$$\begin{aligned}\overline{Z} &= \int \mathcal{D}G\,\mathcal{D}\Sigma \int \mathcal{D}\chi_i \exp\left\{\frac{N}{2}\int \mathrm{d}\tau\,\mathrm{d}\tau' \left[\left(G_0^{-1}(\tau,\tau')\right.\right.\right.\\ &\left.\left.\left.+\Sigma(\tau,\tau')\right)\Xi(\tau,\tau') + \frac{J^2}{4}\,G^4(\tau,\tau') - \Sigma(\tau,\tau')G(\tau,\tau')\right]\right\}\\ &= \int \mathcal{D}G\,\mathcal{D}\Sigma \int \mathcal{D}\chi_i \exp\left[\frac{1}{2}\sum_i \int \mathrm{d}\tau\,\mathrm{d}\tau'\,\chi_i(\tau)\big(\delta(\tau-\tau')\,\partial_\tau\right.\\ &+\Sigma(\tau,\tau')\big)\chi_i(\tau')\\ &\left.+\frac{N}{2}\int \mathrm{d}\tau\,\mathrm{d}\tau' \left(\frac{J^2}{4}\,G^4(\tau,\tau') - \Sigma(\tau,\tau')G(\tau,\tau')\right)\right]. \qquad (3.44)\end{aligned}$$

In the last expression in the square brackets, we substituted the explicit form of the inverse tree-level propagator and mean field variable (3.39). Finally, after integration over $\chi_i(\tau)$, we obtain the effective action:

$$\overline{Z} = \int \mathcal{D}G\,\mathcal{D}\Sigma \exp\left(-I_{\text{eff}}[G,\Sigma]\right), \qquad (3.45)$$

$$\begin{aligned}\frac{I_{\text{eff}}}{N} &= -\frac{1}{2}\log\det\left[-\delta(\tau-\tau')\,\partial_\tau - \Sigma(\tau,\tau')\right]\\ &+\frac{1}{2}\int \mathrm{d}\tau\,\mathrm{d}\tau' \left[\Sigma(\tau,\tau')G(\tau,\tau') - \frac{J^2}{4}\,G^4(\tau,\tau')\right]. \qquad (3.46)\end{aligned}$$

This effective action clearly reproduces the DS equations (3.23), which are simply equations of motion for G and Σ. Indeed, variation with respect to G gives the expression for the self-energy, whereas variation with respect to Σ gives the equation itself:[14]

$$\begin{aligned}\delta_\Sigma I_{\text{eff}} &= -\frac{1}{2}\,\mathrm{tr}\,\log\left(1-(-\partial_\tau-\Sigma)^{-1}\delta\Sigma\right)\\ &+\frac{1}{2}\int \mathrm{d}\tau\,\mathrm{d}\tau'\,G(\tau,\tau')\delta\Sigma(\tau,\tau')\\ &=\frac{1}{2}\int \mathrm{d}\tau\,\mathrm{d}\tau' \left\{G(\tau,\tau') - \left[G_0^{-1}(\tau,\tau')-\Sigma(\tau,\tau')\right]^{-1}\right\}\delta\Sigma(\tau,\tau'),\end{aligned}$$

$$\text{hence,}\quad G^{-1} = G_0^{-1} - \Sigma\,. \qquad (3.47)$$

Practically, this means that we do not need to rigorously explain the calculations performed above: the only important property which we require from the effective action is the correct equations of motion which reproduce the DS equations. As soon as we find such an action, we entirely define the theory in the limit $N\to\infty$. In principle, we could just guess the action (3.46) from Eqn (3.23).

We emphasize that the solution of the DS equation (3.23) is a true saddle point of the effective action (3.46), i.e., it is maximum on G and minimum on Σ. This is due to the specific choice of the integration variable y, which is purely imaginary (3.41). Such a saddle point should be treated with caution, as the system may be unstable in its vicinity. However, numerical calculations show that the solution of the DS equation does converge on this point [5, 7, 8, 118, 119].

Note that the functional integration over one-dimensional Majorana fermions is defined badly, because such fermions cannot be described by either normal or Grassmann numbers. In practice, one should redefine Majorana fermions in terms of ordinary Dirac fermions and reduce integral (3.38) to an integral over Grassmann variables. For details on this calculation, see Appendix B.

[14] On the third line, we used the fact that $G_0^{-1}(\tau',\tau) = G_0^{-1}(\tau,\tau')$ and $\Sigma(\tau',\tau) = -\Sigma(\tau,\tau')$.

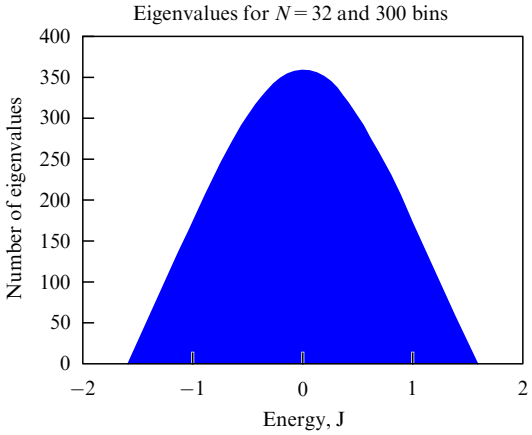

Figure 6. Energy spectrum numerically calculated in [5] for a single realization of the couplings in model (3.1) with $N = 32$ fermions.

Also note that the number $1/N$ plays the role of Planck's constant $\hbar$ in functional integral (3.45), i.e., the limit $N\to\infty$ is equivalent to the classical limit $\hbar\to 0$.

Finally, the effective action (3.46) allows one to calculate the entropy and free energy of the system, which determine its thermodynamic properties [5, 8, 120]:

$$\begin{aligned}\beta F &= \beta E_0 + N\left[-S_0 - \frac{2\pi^2 C}{\beta J} + \mathcal{O}\left(\frac{1}{(\beta J)^2}\right)\right]\\ &+\frac{3}{2}\log(\beta J) + \text{const} + \mathcal{O}\left(\frac{1}{N}\right), \qquad (3.48)\end{aligned}$$

where E_0 is the ground state energy, $S_0\approx 0.232$ is the zero temperature entropy per site, and C is a numerical coefficient, the origin of which will be explained in Section 3.5. Note that the entropy of the system is large ($S\sim N$), even at low temperatures, which is not a common property. This is due to the specific form of the density of states, which resembles a random matrix semicircle and smoothly goes to zero at low energies (Fig. 6). In other words, even near the ground state, the density of states is large ($\rho\sim\exp(S_0 N)$), and energy gaps are small ($\sim\exp(-S_0 N)$).

3.5 Schwarzian action

As we have seen in Section 3.3, the presence of the inverse tree-level propagator in (3.23) breaks the reparametrization invariance of DS equation (3.29). Let us study this break more carefully. First, let us make the change $\Sigma\to\Sigma - G_0^{-1}$ in the effective action (3.46) and separate the conformally-invariant and noninvariant parts, $I_{\text{eff}} = I_{\text{CFT}} + I_{\text{S}}$:

$$\begin{aligned}\frac{I_{\text{CFT}}}{N} &= -\frac{1}{2}\log\det\left(-\Sigma(\tau,\tau')\right)\\ &+\frac{1}{2}\int \mathrm{d}\tau\,\mathrm{d}\tau' \left[\Sigma(\tau,\tau')G(\tau,\tau') - \frac{J^2}{4}\,G^4(\tau,\tau')\right], \qquad (3.49)\end{aligned}$$

$$\frac{I_{\text{S}}}{N} = -\frac{1}{2}\int \mathrm{d}\tau\,\mathrm{d}\tau'\,G_0^{-1}(\tau,\tau')G(\tau,\tau'). \qquad (3.50)$$

Now, it is easy to see that the conformal part $I_{\rm CFT}$ reproduces DS equation (3.26) or (3.28), which is invariant with respect to reparametrizations $\tau \to f(\tau)$, $f'(\tau) > 0$. Furthermore, the delta-function in $G_0^{-1}(\tau, \tau')$ picks up small time differences $|\tau - \tau'| \ll J^{-1}$; therefore, it can be disregarded in the IR limit. Hence, conformal invariance emerges in the deep IR limit and disappears when one moves away from it.

However, one cannot simply throw away the noninvariant part of the effective action, even in this limit, because it contains essential information about the theory. In order to see this, let us consider fluctuations of the effective action (3.46) near the saddle point $(\tilde{G}, \tilde{\Sigma})$. We emphasize that $\tilde{G} \neq G_{\rm c}$; $G_{\rm c}$ is only the IR limit of $\tilde{G}$. It is convenient to parametrize the fluctuations[15] in the form $G = \tilde{G} + \delta G/|\tilde{G}|$, $\Sigma = \tilde{\Sigma} + |\tilde{G}|\delta\Sigma$:

$$\begin{aligned}\frac{I_{\rm eff}}{N} &\approx \frac{1}{4}\int \mathrm{d}\tau_1\,\mathrm{d}\tau_2\,\mathrm{d}\tau_3\,\mathrm{d}\tau_4\,\delta\Sigma(\tau_1,\tau_2)\\ &\times\Big(\big|\tilde{G}(\tau_1,\tau_2)\big|\tilde{G}(\tau_1,\tau_3)\tilde{G}(\tau_2,\tau_4)\big|\tilde{G}(\tau_3,\tau_4)\big|\Big)\delta\Sigma(\tau_3,\tau_4)\\ &+\frac{1}{2}\int \mathrm{d}\tau_1\,\mathrm{d}\tau_2\left[\delta G(\tau_1,\tau_2)\delta\Sigma(\tau_1,\tau_2) - \frac{3J^2}{2}\,\delta G^2(\tau_1,\tau_2)\right]\\ &\equiv -\frac{1}{12J^2}\langle\delta\Sigma|K|\delta\Sigma\rangle + \frac{1}{2}\langle\delta G|\delta\Sigma\rangle - \frac{3J^2}{4}\langle\delta G|\delta G\rangle\,. \end{aligned} \tag{3.51}$$

Here, K is the operator that acts on the space of antisymmetric two-point functions (and generates ladder diagrams, as we will see in Section 4.2). The integral kernel of this operator appears as follows:

$$\begin{aligned}&K(\tau_1,\tau_2,\tau_3,\tau_4) \equiv -3J^2\big|\tilde{G}(\tau_1,\tau_2)\big|\tilde{G}(\tau_1,\tau_3)\tilde{G}(\tau_2,\tau_4)\big|\tilde{G}(\tau_3,\tau_4)\big|,\\ &K|A\rangle = \int \mathrm{d}\tau_3\,\mathrm{d}\tau_4\,K(\tau_1,\tau_2,\tau_3,\tau_4)A(\tau_3,\tau_4)\,.\end{aligned} \tag{3.52}$$

It is straightforward to see that this kernel is antisymmetric under the changes $\tau_1 \leftrightarrow \tau_2$ and $\tau_3 \leftrightarrow \tau_4$ but symmetric under the change $(\tau_1,\tau_2) \leftrightarrow (\tau_3,\tau_4)$ (recall that $G(\tau_2,\tau_1) = -G(\tau_1,\tau_2)$). Also, we introduce the identity operator [6, 121]:

$$\begin{aligned}&I(\tau_1,\tau_2,\tau_3,\tau_4) \equiv \frac{1}{2}\big[\delta(\tau_1-\tau_3)\delta(\tau_2-\tau_4) - \delta(\tau_1-\tau_4)\delta(\tau_2-\tau_3)\big],\\ &I|A\rangle = |A\rangle\,,\end{aligned} \tag{3.53}$$

and the inner product of two-point functions:

$$\langle A|B\rangle \equiv \int \mathrm{d}\tau_1\,\mathrm{d}\tau_2\,A^*(\tau_1,\tau_2)B(\tau_1,\tau_2)\,. \tag{3.54}$$

Recall that Σ is a Lagrange multiplier, i.e., it does not appear in physical quantities. Hence, we can just integrate out its fluctuations from the functional integral with action (3.46) to obtain the following semiclassical approximation:

$$\begin{aligned}\frac{I_{\rm eff}[\delta G]}{N} &= -\log\int \mathcal{D}\delta\Sigma\,\exp\big(-I_{\rm eff}[\delta G,\delta\Sigma]\big)\\ &\simeq \frac{3J^2}{4}\big\langle\delta G\big|(K^{-1}-I)\big|\delta G\big\rangle\,.\end{aligned} \tag{3.55}$$

Let us check what happens with action (3.55) in the conformal (IR) limit. It would seem that it can be expected that the noninvariant part of the action is negligible in this limit, i.e., action (3.46) approximately equals (3.49). This means that the conformally invariant propagator replaces the exact saddle point, $\tilde{G} \approx G_{\rm c}$. The fluctuations of the effective action in this limit are as follows:

$$\frac{I_{\rm eff}[\delta G]}{N} \approx \frac{I_{\rm CFT}[\delta G]}{N} \approx \frac{3J^2}{4}\,\langle\delta G|K_{\rm c}^{-1} - I|\delta G\rangle\,, \tag{3.56}$$

where the operator $K_{\rm c}$ has the form (3.52) with the functions $G_{\rm c}$ instead of $\tilde{G}$. Unfortunately, such a naively truncated effective action does not appropriately treat all fluctuations around the saddle point. Indeed, let us consider such fluctuations δG that conserve the conformal symmetry (3.29). In this case, $G = G_{\rm c} + \delta G/|G_{\rm c}|$ and $\Sigma = J^2 G_{\rm c}^3 + 3J^2|G_{\rm c}|\delta G$ solve the conformal Dyson–Schwinger equation (3.27):

$$\begin{aligned}&\int \mathrm{d}\tau_4\left(\Sigma_{\rm c}(\tau_3,\tau_4) + 3J^2\big|G_{\rm c}(\tau_3,\tau_4)\big|\delta G(\tau_3,\tau_4)\right)\\ &\quad\times\left(G_{\rm c}(\tau_4,\tau_2) + \frac{\delta G(\tau_4,\tau_2)}{\big|G_{\rm c}(\tau_4,\tau_2)\big|}\right) = -\delta(\tau_3-\tau_2)\,.\end{aligned} \tag{3.57}$$

Subtracting the DS equation for the conformal functions $G_{\rm c}$ and $\Sigma_{\rm c}$, multiplying by $G_{\rm c}(\tau_3,\tau_1)$, and integrating over τ_3, we obtain the following identity:

$$\begin{aligned}&\int \mathrm{d}\tau_3\,\mathrm{d}\tau_4\left(\frac{\delta G(\tau_4,\tau_2)}{\big|G_{\rm c}(\tau_4,\tau_2)\big|}\,\Sigma_{\rm c}(\tau_3,\tau_4)G_{\rm c}(\tau_3,\tau_1)\right.\\ &\left.+\,3J^2 G_{\rm c}(\tau_1,\tau_3)G_{\rm c}(\tau_2,\tau_4)\big|G_{\rm c}(\tau_3,\tau_4)\big|\delta G(\tau_3,\tau_4)\right) = 0\,,\end{aligned} \tag{3.58}$$

which straightforwardly reduces to

$$(I - K_{\rm c})\delta G = 0\,. \tag{3.59}$$

Thus, in such fluctuations, the conformally-invariant action (3.56) or (3.49) is zero, i.e., the noninvariant part (3.50) cannot be omitted. Therefore, we have to move away from the IR limit and estimate how action (3.50) changes under conformal transformations (3.29).

Let us first consider the zero temperature case ($\beta = \infty$). As the first approximation, we expand the conformal propagator

$$\begin{aligned}G_{\rm c}(\tau_1,\tau_2) &\to G_{\rm c}\big[f(\tau_1),f(\tau_2)\big]\\ &\approx \frac{\mathrm{sgn}\,(\tau_1-\tau_2)}{(4\pi)^{1/4}J^{2\Delta}}\,\frac{f'^{\Delta}(\tau_1)f'^{\Delta}(\tau_2)}{\big|f(\tau_1)-f(\tau_2)\big|^{2\Delta}}\end{aligned} \tag{3.60}$$

near $\tau = (\tau_1+\tau_2)/2$ into the powers of $\tau_{12} = \tau_1 - \tau_2$:

$$\begin{aligned}&G(\tau_1,\tau_2) = G_{\rm c}(\tau_1,\tau_2)\left(1 + \frac{\Delta}{6}\,\tau_{12}^2\,\mathrm{Sch}\,\big[f(\tau),\tau\big] + \mathcal{O}(\tau_{12}^3)\right),\\ &\mathrm{Sch}\,\big[f(\tau),\tau\big] \equiv \frac{f'''}{f'} - \frac{3}{2}\left(\frac{f''}{f'}\right)^2.\end{aligned} \tag{3.61}$$

We do this expansion because the delta-function from $G_0^{-1}(\tau_1,\tau_2)$ in (3.50) picks up values around $\tau_{12} \approx 0$. We will use this property below. Then, we subtract the untransformed part from (3.61) and substitute the final result into

[15] Note that the measure of the functional integration does not change if we choose fluctuations in this form.

the action (3.50) to obtain

$$\frac{I_S}{N} = -\frac{1}{2}\langle G_0^{-1}|\delta G\rangle = -\frac{1}{2}\int d\tau\, d\tau_{12}\, G_0^{-1}(\tau_{12})\tilde{G}(\tau_{12}) \times \left[\frac{\Delta}{6}\tau_{12}^2\ \mathrm{Sch}\left[f(\tau),\tau\right] + \mathcal{O}(\tau_{12}^3)\right]$$
$$\approx -\frac{\Delta}{12}\int d\tau_{12}\,\delta(\tau_{12})\partial_{\tau_{12}}\left(\tau_{12}^2\tilde{G}(\tau_{12})\right)\int d\tau\,\mathrm{Sch}\left[f(\tau),\tau\right]$$
$$= -\frac{1}{J}\underbrace{\frac{\Delta}{12}\int d\eta\,\delta(\eta)\partial_\eta\left(\eta^2\tilde{G}(\eta)\right)}_{C}\int d\tau\,\mathrm{Sch}\left[f(\tau),\tau\right], \quad (3.62)$$

where we have changed to the dimensionless variable $\eta = J\tau_{12}$. It is now easy to see that the integral over $d\eta$ is undefined:

$$C = \frac{\Delta}{12}\int d\eta\,\delta(\eta)\left[\left(\eta^2 g(\eta)\right)'\operatorname{sgn}\eta + \eta^2 g(\eta)\delta(\eta)\right]$$
$$= \frac{\Delta}{12}\int d\eta\, g(\eta)\eta^2\delta(\eta)^2 = \frac{\Delta}{12}\,\delta(0)\,g(0)\times 0^2 = 0\times\infty, \quad (3.63)$$

where we singled out the relevant part of the saddle point value, $\tilde{G}(\eta) = g(\eta)\operatorname{sgn}\eta$.

There is no simple way to resolve this uncertainty, because we cannot analytically find the function $g(\eta)$ for all times. However, this problem can be solved by smearing the delta-function (i.e., by replacing the term G_0^{-1} with another suitable source, which is big at small times, $\eta \ll 1$) and introducing gentle UV and IR cut-offs for integral (3.63). This was done in [6].

The other way is to calculate the leading nonconformal corrections to the eigenfunctions and eigenvalues of the operator K, substitute them into the action (3.55), and directly evaluate $I_S = I_{\mathrm{eff}} - I_{\mathrm{CFT}} \approx \delta I_{\mathrm{CFT}}$. This calculation was performed in [5, 8]. Both these methods lead to an action of the form (3.62) with the coefficient $C \approx 0.48\,\Delta/12 > 0$. In summary, for the zero-temperature theory, we obtain

$$\frac{I_S}{N} \approx -\frac{C}{J}\int_{-\infty}^{\infty}\mathrm{Sch}\left[f(\tau),\tau\right]d\tau. \quad (3.64)$$

As usual, one can change to the finite-temperature version of (3.64) using the map (3.9):

$$\frac{I_S}{N} = -\frac{C}{J}\int_{-\beta/2}^{\beta/2}\mathrm{Sch}\left[\tan\frac{\pi\varphi(\tau)}{\beta},\tau\right]d\tau. \quad (3.65)$$

In this case, the saddle point values of the effective action are parametrized by the function $\varphi(\tau)$, which maps the time circle to itself and preserves its orientation. Note that the coefficient C is exactly the coefficient in the thermodynamic identity (3.48). This is because the low energy dynamics of the SYK model are determined by the Schwarzian action.

Note that conformal invariance does not completely disappear when one moves away from the IR limit. Indeed, exact propagators and the effective action must be invariant under the transformations from the $\mathrm{SL}(2,\mathbb{R})$ group: these transformations are the rotations of the time circle (or time line in the limit $\beta\to\infty$) and do not correspond to any physical degrees of freedom. Both the action (3.55) and the Schwarzian action (3.65) are zero on the reparametrizations from the $\mathrm{SL}(2,\mathbb{R})$ group.

Thus, the apparent conformal symmetry of the IR theory is actually broken down into the symmetry with respect to the transformations from the $\mathrm{SL}(2,\mathbb{R})$ group. The dynamics of the pseudo-Goldstone boson which is associated with this broken symmetry (the so-called 'soft mode') are approximately described by the Schwarzian action (3.65).

4. Sachdev–Ye–Kitaev spectrum and four-point functions

This section has two main purposes. First, by way of a simple example, we show how to calculate quantum corrections (which are suppressed by the powers of $1/N$) to many-point correlation functions. For pedagogical reasons, we keep as many details of the calculation as possible. Second, we show that OTOCs exponentially decay with time, with the main contribution being provided by the Schwarzian action. This is one of the most striking properties of the SYK model, as soon as this growth saturates the 'bound on chaos' and coincides with the behavior of similar correlators calculated on the black hole background (see Section 2.2 and paper [9]). This section is mostly based on pioneering papers [4–6]. A generalization to n-point functions with arbitrary n can be found in [122].

Let us consider the following four-point correlation function:

$$\frac{1}{N^2}\sum_{i,j=1}^{N}\left\langle\mathcal{T}\chi_i(\tau_1)\chi_i(\tau_2)\chi_j(\tau_3)\chi_j(\tau_4)\right\rangle$$
$$= \frac{1}{Z}\int\mathcal{D}G\,\mathcal{D}\Sigma\Big[G(\tau_1,\tau_2)G(\tau_3,\tau_4) + \frac{1}{N}\big(G(\tau_1,\tau_4)G(\tau_2,\tau_3)$$
$$- G(\tau_1,\tau_3)G(\tau_2,\tau_4)\big)\Big]\exp\left(-I_{\mathrm{eff}}[G,\Sigma]\right), \quad (4.1)$$

where we have used the approach from Section 3.4 to transform from the functional integrals over $\mathcal{D}\chi_i$ on the left-hand side to those over $\mathcal{D}G$ and $\mathcal{D}\Sigma$ on the right-hand side. The letter Z denotes partition function (3.45). As usual, we work in the limit $J\tau \gg 1$, $N \gg 1$ and keep the leading quantum correction ($\sim 1/N$) in the classical expression

$$\mathcal{F}(\tau_1,\tau_2,\tau_3,\tau_4) \equiv \frac{1}{N^2}\sum_{i,j=1}^{N}\left\langle\mathcal{T}\chi_i(\tau_1)\chi_i(\tau_2)\chi_j(\tau_3)\chi_j(\tau_4)\right\rangle - \tilde{G}(\tau_1,\tau_2)\tilde{G}(\tau_3,\tau_4), \quad (4.2)$$

where $\tilde{G}$ denotes the saddle point value of the effective action (3.46), which in the IR limit approximately equals the conformal propagator (3.34). For clarity, we consider the theory at finite temperature, i.e., $\tau_{1,2,3,4}\in[-\beta/2,\,\beta/2)$.

Without loss of generality, we restrict ourselves to the regions $\tau_1>\tau_2$, $\tau_3>\tau_4$, and $\tau_1>\tau_3$. First, function $\mathcal{F}(\tau_1,\tau_2,\tau_3,\tau_4)$ does not depend on the choice of the coordinates on the time circle, i.e., does not change under the cyclic permutation of its arguments. Second, this function is antisymmetric under the changes $\tau_1\leftrightarrow\tau_2$ and $\tau_3\leftrightarrow\tau_4$ and symmetric under the simultaneous change $(\tau_1,\tau_2)\leftrightarrow(\tau_3,\tau_4)$, which follows from the anticommutation relations of χ_i. Together, these two symmetries allow one to recover the behavior of this function in the regions with the other order of $\tau_{1,2,3,4}$.

As we have shown in Section 3.5, it is convenient to separate conformally-invariant and noninvariant fluctua-

tions near the saddle point value $\tilde{G}$. We denote these fluctuations as $\delta G^{\parallel}$ and $\delta G^{\perp}$, respectively. Unlike Section 3.5, in this section we do not divide the fluctuations by $\tilde{G}^{-1}$, i.e., the fluctuations $\delta G^{\parallel}$ are defined in such way that the function $G_{\mathrm{c}} + \delta G^{\parallel}$ solves the conformal DS equation (3.27), and the subspace of noninvariant fluctuations $\delta G^{\perp}$ is the orthogonal complement to the subspace of conformally-invariant fluctuations. Note that, due to symmetry (3.29), all conformal fluctuations can be parametrized by the function $\varphi(\tau)$, which maps the time circle onto itself:

$$\delta G^{\parallel}_{\varphi}(\tau_1, \tau_2) = G^{\beta}_{\mathrm{c}}\big[\varphi(\tau_1), \varphi(\tau_2)\big] - G^{\beta}_{\mathrm{c}}(\tau_1, \tau_2)$$
$$\text{for some reparametrization} \quad \tau \to \varphi(\tau)\,. \tag{4.3}$$

In these notations, the functional integral for the four-point function looks like the following:

$$\begin{aligned}\mathcal{F} &\approx \mathcal{F}_0 + \frac{1}{Z}\int \mathcal{D}\delta G^{\parallel}\,\mathcal{D}\delta G^{\perp}\,\mathcal{D}\Sigma\,\big(\delta G^{\parallel}(\tau_1,\tau_2) + \delta G^{\perp}(\tau_1,\tau_2)\big)\\ &\times\big(\delta G^{\parallel}(\tau_3,\tau_4) + \delta G^{\perp}(\tau_3,\tau_4)\big)\exp\left(-I_{\mathrm{CFT}} - I_{\mathrm{S}}\right)\\ &= \mathcal{F}_0 + \mathcal{F}_{\mathrm{S}} + \mathcal{F}_{\mathrm{CFT}} + \mathcal{O}\left(\frac{1}{N^2}\right),\end{aligned} \tag{4.4}$$

where we expanded the integrand near the saddle point and introduced the following expectation values:

$$\mathcal{F}_0 \equiv \frac{1}{N}\big(\tilde{G}(\tau_1,\tau_4)\tilde{G}(\tau_2,\tau_3) - \tilde{G}(\tau_1,\tau_3)\tilde{G}(\tau_2,\tau_4)\big)\,, \tag{4.5}$$

$$\begin{aligned}\mathcal{F}_{\mathrm{S}} &\equiv \big\langle \delta G^{\parallel}(\tau_1,\tau_2)\delta G^{\parallel}(\tau_3,\tau_4)\big\rangle_{\mathrm{S}}\\ &= \frac{\int \mathcal{D}\varphi\;\delta G^{\parallel}_{\varphi}(\tau_1,\tau_2)\delta G^{\parallel}_{\varphi}(\tau_3,\tau_4)\exp\big(-I_{\mathrm{S}}[\varphi]\big)}{\int \mathcal{D}\varphi\;\exp\big(-I_{\mathrm{S}}[\varphi]\big)}\,,\end{aligned} \tag{4.6}$$

$$\begin{aligned}\mathcal{F}_{\mathrm{CFT}} &\equiv \big\langle \delta G^{\perp}(\tau_1,\tau_2)\delta G^{\perp}(\tau_3,\tau_4)\big\rangle_{\mathrm{CFT}}\\ &= \frac{\int \mathcal{D}\delta G^{\perp}\;\delta G^{\perp}(\tau_1,\tau_2)\delta G^{\perp}(\tau_3,\tau_4)\exp\big(-I_{\mathrm{eff}}[\delta G^{\perp}]\big)}{\int \mathcal{D}\delta G^{\perp}\;\exp\big(-I_{\mathrm{eff}}[\delta G^{\perp}]\big)}\,.\end{aligned} \tag{4.7}$$

We will clarify the meaning of these notations in Sections 4.1 and 4.2. To obtain average (4.6), we used the fact that the Jacobian

$$J = \left[\frac{\mathcal{D}G^{\parallel}_{\varphi}}{\mathcal{D}\varphi}\right]_{\varphi(\tau)=2\pi\tau/\beta} \tag{4.8}$$

is constant and nonzero, because, for reparametrisations which are infinitesimally close to the identity, $\varphi(\tau) = 2\pi\tau/\beta + \delta\varphi(\tau)$, fluctuations $\delta G^{\parallel}_{\varphi}$ depend only on $\delta\varphi$ (see Eqn (4.11)). The integral $\int \mathcal{D}\delta G^{\perp}\mathcal{D}\Sigma\,\exp\left(-I_{\mathrm{CFT}}\right)$ in the numerator and denominator of (4.6) is also constant and nonzero. For average (4.7), we repeated the argumentation around formula (3.55) and used the action I_{eff} evaluated on the conformal functions $\tilde{G} = G^{\beta}_{\mathrm{c}}$. Recall that for the conformally-invariant fluctuations $(I - K)\delta G^{\parallel} = 0$; hence, $I_{\mathrm{eff}}[\delta G^{\perp} + \delta G^{\parallel}] = I_{\mathrm{eff}}[\delta G^{\perp}]$.

For convenience, in this section, we rescale the fields and map the finite-temperature time circle into the unit circle:

$$\begin{aligned}&\tau \to \frac{2\pi\tau}{\beta}\,, \quad \chi_i \to \left(\frac{\beta J}{2\pi}\right)^{\Delta}\chi_i\,,\\ &G(\tau,\tau') \to \left(\frac{\beta J}{2\pi}\right)^{2\Delta} G(\tau,\tau')\,, \quad \Sigma(\tau,\tau') \to \frac{1}{J^2}\left(\frac{\beta J}{2\pi}\right)^{6\Delta}\Sigma(\tau,\tau')\,.\end{aligned} \tag{4.9}$$

In this case, the Schwarzian and conformally-invariant actions acquire the following form:

$$\begin{aligned}\frac{I_{\mathrm{CFT}}}{N} &= -\frac{1}{2}\log\det\big(-\Sigma(\tau,\tau')\big)\\ &\quad + \frac{1}{2}\int_{-\pi}^{\pi}\mathrm{d}\tau\int_{-\pi}^{\pi}\mathrm{d}\tau'\left(\Sigma(\tau,\tau')G(\tau,\tau') - \frac{1}{4}\,G^4(\tau,\tau')\right),\\ \frac{I_{\mathrm{S}}}{N} &= -\frac{2\pi C}{\beta J}\int_{-\pi}^{\pi}\mathrm{Sch}\left(\tan\frac{\varphi(\tau)}{2},\,\tau\right)\mathrm{d}\tau\,.\end{aligned} \tag{4.10}$$

The prefactors in (4.10) explicitly depend on N, J, and β, whereas other quantities are dimensionless. It is now easy to see that both contributions from the conformally-invariant and noninvariant parts are of the order $\mathcal{O}(1/N)$, because both actions I_{S} and I_{CFT} are proportional to N. However, in the case of strong coupling, $\beta J \gg 1$, the leading contribution to the correlation function comes from the Schwarzian action due to the additional small factor. Roughly speaking, due to this small factor, soft mode fluctuations are the easiest to excite. We calculate this contribution in Section 4.1 and compare it with the contribution from the conformal part in Section 4.2.

4.1 Soft mode contribution

Let us review the argumentation of [6] to estimate correlator (4.6) in the limit $1 \ll \tau J < \beta J \ll N$. In this limit, the fluctuations are small, so we use the Gaussian approximation for the functional integrals. Note that this limit does not hold in the zero temperature case. In fact, we have to work in the limit of small but nonzero temperatures: $J/N \ll T \ll J$.

Consider conformally-invariant fluctuations of the saddle point value $\tilde{G} \approx G^{\beta}_{\mathrm{c}}$. For infinitesimal transformations $\delta\varphi(\tau) \equiv \varphi(\tau) - \tau$, the fluctuations look like this:

$$\begin{aligned}\delta G^{\parallel}_{\varphi}(\tau_1,\tau_2) &= G^{\beta}_{\mathrm{c}}\big[\varphi(\tau_1),\varphi(\tau_2)\big] - G^{\beta}_{\mathrm{c}}(\tau_1,\tau_2)\\ &= \left[\delta\varphi(\tau_1)\partial_{\tau_1} + \frac{1}{4}\,\delta\varphi'(\tau_1) + \delta\varphi(\tau_2)\partial_{\tau_2} + \frac{1}{4}\,\delta\varphi'(\tau_2)\right]G^{\beta}_{\mathrm{c}}(\tau_1,\tau_2)\\ &= \frac{1}{4}\left[\delta\varphi'(\tau_1) + \delta\varphi'(\tau_2) - \frac{\delta\varphi(\tau_1) - \delta\varphi(\tau_2)}{\tan\big[(\tau_1-\tau_2)/2\big]}\right]G^{\beta}_{\mathrm{c}}(\tau_1,\tau_2)\,.\end{aligned} \tag{4.11}$$

To obtain the last line, we have used expression (3.34).

Let us expand the function $\delta\varphi$ in Fourier modes,

$$\delta\varphi(\tau) = \sum_{m\in\mathbb{Z}}(\delta\varphi)_m\exp\left(\mathrm{i}m\tau\right), \tag{4.12}$$

and rewrite expression (4.11) as

$$\begin{aligned}\frac{\delta G^{\parallel}_{\varphi}(\tau_1,\tau_2)}{G^{\beta}_{\mathrm{c}}(\tau_1,\tau_2)} &= -\frac{\mathrm{i}}{2}\sum_{m\in\mathbb{Z}}\exp\left(\mathrm{i}m\,\frac{\tau_1+\tau_2}{2}\right)\\ &\quad\times\left[\frac{\sin\left(m\tau_{12}/2\right)}{\tan\left(\tau_{12}/2\right)} - m\cos\left(\frac{m\tau_{12}}{2}\right)\right](\delta\varphi)_m\,,\end{aligned} \tag{4.13}$$

where $\tau_{12} \equiv \tau_1 - \tau_2$. Then, we use the following integral:

$$\begin{aligned}\int_{\tau_2}^{\tau_1}\frac{s_{10}s_{02}}{s_{12}}\exp\left(\mathrm{i}m\tau_0\right)\frac{\mathrm{d}\tau_0}{2\pi} &= \frac{2}{\pi}\,\frac{1}{m(m^2-1)}\exp\left(\mathrm{i}m\,\frac{\tau_1+\tau_2}{2}\right)\\ &\quad\times\left[\frac{\sin\left(m\tau_{12}/2\right)}{\tan\left(\tau_{12}/2\right)} - m\cos\left(\frac{m\tau_{12}}{2}\right)\right],\end{aligned} \tag{4.14}$$

which allows us to write

$$\frac{\delta G_\varphi^{\parallel}(\tau_1,\tau_2)}{G_{\mathrm{c}}^{\beta}(\tau_1,\tau_2)} = -\frac{\mathrm{i}\pi}{2}\sum_{m\in\mathbb{Z}}\int_{\tau_2}^{\tau_1}\frac{s_{10}s_{02}}{s_{12}}\,m(m^2-1)(\delta\varphi)_m \times \exp(\mathrm{i}m\tau_0)\,\frac{\mathrm{d}\tau_0}{2\pi}\,. \tag{4.15}$$

Here, we have denoted $s_{12}\equiv 2\sin[(\tau_1-\tau_2)/2]$ and assumed that $2\pi>\tau_1-\tau_2>0$. Finally, we introduce the $\mathrm{SL}(2,\mathbb{R})$-invariant observable,

$$O(\tau)=\mathrm{Sch}\left(\tan\frac{\varphi(\tau)}{2},\tau\right)=\frac{1}{2}+\delta\varphi'+\delta\varphi'''+\frac{1}{2}(\delta\varphi')^2 - (\delta\varphi')(\delta\varphi''')-\frac{3}{2}(\delta\varphi'')^2+\mathcal{O}(\delta\varphi^3)\,, \tag{4.16}$$

do the Fourier transformation of the noninvariant part,

$$\delta O(\tau)\equiv O(\tau)-\frac{1}{2} = -\mathrm{i}\sum_{m\in\mathbb{Z}} m(m^2-1)(\delta\varphi)_m\exp(\mathrm{i}m\tau)+\mathcal{O}(\delta\varphi^2)\,, \tag{4.17}$$

and compare this expression to expression (4.15). As a result, we obtain the following integral representation for the variation in the variable G:

$$\frac{\delta G_\varphi^{\parallel}(\tau_1,\tau_2)}{G_{\mathrm{c}}^{\beta}(\tau_1,\tau_2)}=\frac{\pi}{2}\int_{\tau_2}^{\tau_1}\frac{s_{10}s_{02}}{s_{12}}\,\delta O(\tau_0)\,\frac{\mathrm{d}\tau_0}{2\pi}\,. \tag{4.18}$$

Using this representation, we can rewrite correlator (4.6):

$$\frac{\mathcal{F}_{\mathrm{S}}(\tau_1,\tau_2,\tau_3,\tau_4)}{G_{\mathrm{c}}^{\beta}(\tau_1,\tau_2)G_{\mathrm{c}}^{\beta}(\tau_3,\tau_4)}=\frac{\big\langle\delta G_\varphi^{\parallel}(\tau_1,\tau_2)\delta G_\varphi^{\parallel}(\tau_3,\tau_4)\big\rangle_{\mathrm{S}}}{G_{\mathrm{c}}^{\beta}(\tau_1,\tau_2)G_{\mathrm{c}}^{\beta}(\tau_3,\tau_4)} =\frac{\pi^2}{4}\int_{\tau_2}^{\tau_1}\frac{\mathrm{d}\tau_5}{2\pi}\int_{\tau_4}^{\tau_3}\frac{\mathrm{d}\tau_6}{2\pi}\big\langle\delta O(\tau_5)\delta O(\tau_6)\big\rangle_{\mathrm{S}}\frac{s_{15}s_{52}}{s_{12}}\frac{s_{36}s_{64}}{s_{34}}\,. \tag{4.19}$$

Recall that we have restricted ourselves to the regions $\tau_1>\tau_2$, $\tau_3>\tau_4$, and $\tau_1>\tau_3$, because the expressions for other regions can be restored by a simple transformation.

Let us estimate the correlation function of two δO's in the Gaussian approximation. Using expansion (4.16), we find the Schwarzian action (3.65) up to the boundary and $\mathcal{O}(\delta\varphi^3)$ terms:

$$\frac{I_{\mathrm{S}}}{N}=-\frac{2\pi C}{\beta J}\int_{-\pi}^{\pi}\left[\frac{1}{2}+\frac{(\delta\varphi')^2-(\delta\varphi'')^2}{2}\right]\mathrm{d}\tau =-\frac{\pi C}{\beta J}+\frac{\pi C}{\beta J}\sum_{m\in\mathbb{Z}}m^2(m^2-1)(\delta\varphi)_m(\delta\varphi)_{-m}\,. \tag{4.20}$$

Therefore, in the Gaussian approximation, the correlation function of two $\delta\varphi$'s appears as follows:

$$\big\langle(\delta\varphi)_m(\delta\varphi)_n\big\rangle_{\mathrm{S}}=\frac{1}{2\pi C}\frac{\beta J}{N}\frac{\delta_{m,-n}}{m^2(m^2-1)},\quad m,n\neq -1,0,1\,. \tag{4.21}$$

Note that modes with $m=-1,0,1$ are $\mathrm{SL}(2,\mathbb{R})$ generators, i.e., they correspond to the nonphysical degrees of freedom and cancel out from all physical observables. They are zero modes of the Schwarzian action, which we mentioned at the end of Section 3.5.

Using identity (4.21), we find the correlation function of two δO's:

$$\begin{aligned}\big\langle\delta O(\tau_5)\delta O(\tau_6)\big\rangle_{\mathrm{S}} &= -\sum_{m,n\in\mathbb{Z}} m(m^2-1)n(n^2-1) \times\big\langle(\delta\varphi)_m(\delta\varphi)_n\big\rangle_{\mathrm{S}}\exp(\mathrm{i}m\tau_5+\mathrm{i}n\tau_6)\\ &=\frac{1}{2\pi C}\frac{\beta J}{N}\sum_{m\neq 0}(m^2-1)\exp\big[\mathrm{i}m(\tau_5-\tau_6)\big]\\ &=\frac{1}{2\pi C}\frac{\beta J}{N}\big[1-2\pi\delta(\tau_{56})-2\pi\delta''(\tau_{56})\big]\,,\end{aligned} \tag{4.22}$$

where we have used the fact that $\delta(\tau)=(1/2\pi)\sum\exp(\mathrm{i}m\tau)$. Note that delta-functions in (4.22) are zero if the integration intervals over $\mathrm{d}\tau_5$ and $\mathrm{d}\tau_6$ do not overlap. Therefore, it is convenient to separately consider two different orderings:

$$\begin{aligned}&\text{OPE:}\quad 2\pi>\tau_1>\tau_2>\tau_3>\tau_4>0\,,\\ &\text{OTO:}\quad 2\pi>\tau_1>\tau_3>\tau_2>\tau_4>0\,.\end{aligned} \tag{4.23}$$

The abbreviation OPE stands for 'operator product expansion,' which is applicable for the corresponding time ordering (see [5, 103, 123] and Section 4.2.4 for details). The abbreviation OTO stands for 'out of time ordered' for obvious reasons.

For the OPE ordering, the integrals over $\mathrm{d}\tau_5$ and $\mathrm{d}\tau_6$ decouple, and the result of the integration in (4.19) reduces to

$$\frac{\mathcal{F}_{\mathrm{S}}(\tau_1,\tau_2,\tau_3,\tau_4)}{G_{\mathrm{c}}^{\beta}(\tau_1,\tau_2)G_{\mathrm{c}}^{\beta}(\tau_3,\tau_4)} =\frac{1}{8\pi C}\frac{\beta J}{N}\left(\frac{\tau_{12}}{2\tan(\tau_{12}/2)}-1\right)\left(\frac{\tau_{34}}{2\tan(\tau_{34}/2)}-1\right). \tag{4.24}$$

In fact, this correlator describes the fluctuations of the total energy in the thermal ensemble, so it could be expected to factorize. A more detailed explanation can be found in Appendix B and paper [5].

On the other hand, for the OTO ordering, we obtain [16] the contribution (4.24) plus the additional term due to the delta-functions in (4.22):

$$\begin{aligned}\frac{\mathcal{F}_{\mathrm{S}}(\tau_1,\tau_2,\tau_3,\tau_4)}{G_{\mathrm{c}}^{\beta}(\tau_1,\tau_2)G_{\mathrm{c}}^{\beta}(\tau_3,\tau_4)} &=\frac{1}{8\pi C}\frac{\beta J}{N}\bigg[-\frac{3\pi}{8}\frac{\sin(\Delta\tau)}{\sin(\tau_{12}/2)\sin(\tau_{34}/2)}\\ &+\frac{\pi}{16}\frac{\sin(\Delta\tau-\tau_{12})}{\sin(\tau_{12}/2)\sin(\tau_{34}/2)}+\frac{\pi}{16}\frac{\sin(\Delta\tau-\tau_{34})}{\sin(\tau_{12}/2)\sin(\tau_{34}/2)}\\ &-\frac{\pi}{8}\frac{2\Delta\tau-\tau_{12}-\tau_{34}}{\tan(\tau_{12}/2)\tan(\tau_{34}/2)}+\frac{3\pi}{8}\frac{1}{\tan(\tau_{12}/2)}+\frac{3\pi}{8}\frac{1}{\tan(\tau_{34}/2)}\\ &+\left(\frac{\tau_{12}}{2\tan(\tau_{12}/2)}-1\right)\left(\frac{\tau_{34}}{2\tan(\tau_{34}/2)}-1\right)\bigg]\,,\end{aligned} \tag{4.25}$$

where we have introduced the time $\Delta\tau\equiv(\tau_1+\tau_2)/2-(\tau_3+\tau_4)/2$. It is convenient to take $\tau_1-\tau_2=\pi$ and $\tau_3-\tau_4=\pi$, because, in this case, the expression for correlator (4.25) significantly simplifies:

$$\frac{\mathcal{F}_{\mathrm{S}}(\tau_1,\tau_2,\tau_3,\tau_4)}{G_{\mathrm{c}}^{\beta}(\beta/2)G_{\mathrm{c}}^{\beta}(\beta/2)} =\frac{1}{8\pi C}\frac{\beta J}{N}\left[1-\frac{\pi}{2}\sin\left(\frac{2\pi\Delta\tau}{\beta}\right)\right]. \tag{4.26}$$

Here, we have restored β in the exponent, i.e., mapped the unit circle back to the β circle (4.9).

[16] A useful relation is $\partial^2_{\tau_{56}}=(1/4)\partial^2_{\tau_5}+(1/4)\partial^2_{\tau_6}-(1/2)\partial_{\tau_5}\partial_{\tau_6}$.

To understand the physical relevance of the obtained result, let us analytically continue the four-point function to Lorentzian time and check the behavior of the correlator at large values of $t = -\mathrm{i}\Delta\tau \gg J^{-1}$. A particularly important case is when $\tau_1 = \beta/4 + \mathrm{i}t$, $\tau_2 = -\beta/4 + \mathrm{i}t$, $\tau_3 = 0$, $\tau_4 = -\beta/2$, which describes the regularized out-of-time-ordered correlation function (see Section 2.1):

$$\begin{aligned}\mathrm{OTOC}(t) &\equiv \frac{1}{N^2}\sum_{i,j=1}^{N}\mathrm{tr}\left[\rho^{1/4}\chi_i(t)\rho^{1/4}\chi_j(0)\rho^{1/4}\chi_i(t)\rho^{1/4}\chi_j(0)\right]\\ &= \tilde{G}\left(\frac{\beta}{2}\right)\tilde{G}\left(\frac{\beta}{2}\right) + \mathcal{F}\left(\frac{\beta}{4}+\mathrm{i}t,\, -\frac{\beta}{4}+\mathrm{i}t,\, 0,\, -\frac{\beta}{2}\right)\\ &= \tilde{G}\tilde{G} + \mathcal{F}_{\mathrm{S}} + \mathcal{F}_{\mathrm{CFT}} + \mathcal{F}_0 + \mathcal{O}\left(\frac{1}{N^2}\right), \end{aligned} \tag{4.27}$$

where we have defined the density matrix as $\rho \equiv (1/Z)\times \exp(-\beta H)$. For brevity, we omitted arguments of correlation functions in the last line. At $t = 0$, this choice corresponds to the OTO region, so the correlator is given by the analytical continuation of (4.26) to the nonzero real t. Now, it is straightforward to see that in the leading order the corrected OTOC rapidly decays:

$$\begin{aligned}\mathrm{OTOC}(t) &\approx \tilde{G}\left(\frac{\beta}{2}\right)\tilde{G}\left(\frac{\beta}{2}\right) + \mathcal{F}_{\mathrm{S}}\left(\frac{\beta}{4}+\mathrm{i}t,\, -\frac{\beta}{4}+\mathrm{i}t,\, 0,\, -\frac{\beta}{2}\right)\\ &\approx \frac{\sqrt{\pi}}{2\beta J}\left[1 + \frac{1}{8\pi C}\frac{\beta J}{N}\left(1 - \frac{\pi}{2}\cos\left(\frac{2\pi \mathrm{i}t}{\beta}\right)\right)\right]\\ &\approx \frac{\sqrt{\pi}}{2\beta J}\left[1 - \frac{\Delta^2}{2C}\frac{\beta J}{N}\exp\left(\frac{2\pi}{\beta}t\right)\right] \quad \text{for} \quad \beta \ll t \ll \beta\log\frac{N}{\beta J}. \end{aligned} \tag{4.28}$$

Here, we have restored the conformal dimension $\Delta = 1/4$ and substituted the approximate saddle value, $\tilde{G} \approx G_{\mathrm{c}}^{\beta}$. However, for larger times, the Gaussian approximation breaks down and one has to take into account corrections to (4.28). In general, one expects that the decay is eventually saturated due to the contribution of multiple parallel ladders (see Section 4.2). However, we will not discuss this point here.

At the same time, the contribution of the soft mode to the regularized time-ordered correlation function (TOC) does not change with t:

$$\begin{aligned}\mathrm{TOC}(t) &\equiv \frac{1}{N^2}\sum_{i,j=1}^{N}\mathrm{tr}\left[\chi_i(t)\rho^{1/2}\chi_i(t)\chi_j(0)\rho^{1/2}\chi_j(0)\right]\\ &= \tilde{G}\left(\frac{\beta}{2}\right)\tilde{G}\left(\frac{\beta}{2}\right) + \mathcal{F}\left(\frac{\beta}{2}+\mathrm{i}t,\, \mathrm{i}t,\, 0,\, -\frac{\beta}{2}\right)\\ &\approx \tilde{G}\left(\frac{\beta}{2}\right)\tilde{G}\left(\frac{\beta}{2}\right) + \mathcal{F}_{\mathrm{S}}\left(\frac{\beta}{2}+\mathrm{i}t,\, \mathrm{i}t,\, 0,\, -\frac{\beta}{2}\right) \approx \frac{\sqrt{\pi}}{2\beta J} + \frac{\mathrm{const}}{N}. \end{aligned} \tag{4.29}$$

This contribution is small compared to the tree-level value, even at very large times.

Finally, one should also take into account the $\mathcal{F}_0$ and $\mathcal{F}_{\mathrm{CFT}}$ corrections to the connected four-point function which are also of the order $\mathcal{O}(1/N)$. However, at the end of Section 3.3, we showed that two-point correlation functions exponentially decay for large Lorentzian times, $t \gg \beta$; for such times, the contribution of $\mathcal{F}_0$ to the OTOC and TOC also exponentially decays and therefore can be ignored. The contribution of $\mathcal{F}_{\mathrm{CFT}}$ will be discussed in Section 4.2.

4.2 Conformal action contribution

Let us estimate the conformal contribution to the four-point correlation function, which is given by (4.7). As usual, we work in the IR and large N limit. Let us keep in mind that in this limit the theory is conformally invariant in the sense (3.29), so we can freely change between the zero temperature and finite temperature cases using the map (3.9). Due to this reason, in most of this section we work with zero-temperature functions.

At the same time, integrands in both the numerator and denominator of (4.7) are invariant with respect to arbitrary reparametrizations and I_{S} is nonzero for all but $\mathrm{SL}(2,\mathbb{R})$ reparametrizations. Therefore, one can integrate such reparametrizations out and obtain a nonzero constant that coincides for the numerator and denominator. Therefore, the full reparametrization symmetry of the four-point function is effectively broken down to $\mathrm{SL}(2,\mathbb{R})$.

Taking the integral over the fluctuations[17] of the variable G in functional integral (4.7) with the effective action (3.55), we obtain

$$\begin{aligned}\mathcal{F}_{\mathrm{CFT}} &= \frac{2}{3J^2N}\frac{(K_{\mathrm{c}}^{-1} - I)^{-1}I}{\left|G_{\mathrm{c}}(\tau_1,\tau_2)G_{\mathrm{c}}(\tau_3,\tau_4)\right|}\\ &= \frac{2}{3J^2N}\frac{(I - K_{\mathrm{c}})^{-1}K_{\mathrm{c}}I}{\left|G_{\mathrm{c}}(\tau_1,\tau_2)G_{\mathrm{c}}(\tau_3,\tau_4)\right|}. \end{aligned} \tag{4.30}$$

Here, K_{c} denotes the conformal kernel that is defined by (3.52) with conformal two-point functions $\tilde{G} = G_{\mathrm{c}}$. From (3.52), (3.53), and (4.5), it follows that

$$K_{\mathrm{c}}I = \frac{3J^2N}{2}\,\mathcal{F}_0(\tau_1,\tau_2,\tau_3,\tau_4)\left|G_{\mathrm{c}}(\tau_1,\tau_2)G_{\mathrm{c}}(\tau_3,\tau_4)\right|. \tag{4.31}$$

It is now easy to see that $\mathcal{F}_{\mathrm{CFT}}$ is simply the sum of all possible ladder diagrams (Fig. 7):

$$\mathcal{F}_{\mathrm{CFT}} = \sum_{n=0}^{\infty}\mathcal{F}_n = (I - K_{\mathrm{c}})^{-1}\mathcal{F}_0, \tag{4.32}$$

where $\mathcal{F}_n \equiv K_{\mathrm{c}}^n\mathcal{F}_0$ corresponds to the n-ladder diagram. Indeed, one can check that, in the diagrammatic technique introduced in Section 3.2, ladder diagrams as in Fig. 7 are the only contributions to the four-point correlation functions of the order $1/N$.

Note that the kernel K_{c}, which we use, is conjugated to the natural kernel, which follows from the diagrams in Fig. 7, by the power of the propagator:

$$\begin{aligned}&K_{\mathrm{c}}(\tau_1,\tau_2,\tau_3,\tau_4)\\ &\quad = \left|G_{\mathrm{c}}(\tau_1,\tau_2)\right|K_{\mathrm{diagram}}(\tau_1,\tau_2,\tau_3,\tau_4)\left|G_{\mathrm{c}}(\tau_3,\tau_4)\right|^{-1}. \end{aligned} \tag{4.33}$$

Such a conjugation is necessary to make the symmetry $(\tau_1,\tau_2) \leftrightarrow (\tau_3,\tau_4)$ explicit. In addition, it is straightforward to check that under reparametrizations $\tau \to f(\tau)$, $f'(\tau) > 0$ operator K_{c} transforms as a four-point function of fields with conformal dimension $\Delta = 1/2$.

Note that the diagrammatics with conformal two-point functions naively lead to a divergent expression, because in the conformal limit operator K has a unit eigenvalue: $(I - K_{\mathrm{c}})\delta G = 0$ (see Section 3.5). In Section 4.1, we treated

[17] We recall that in this section we parametrize fluctuations as $G = \tilde{G} + \delta G$, while in Section 3.5 we used the notation $G = \tilde{G} + \delta G/|\tilde{G}|$.

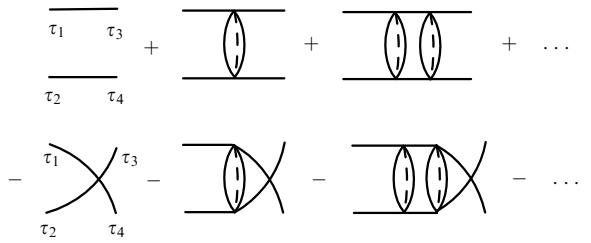

Figure 7. Sum of the ladder diagrams which contribute to $\mathcal{F}_{\rm CFT}$.

this divergence directly, moving away from the IR limit and considering nonconformal corrections to the effective action. The alternative approach is to calculate the leading correction to the unit eigenvalue and corresponding eigenfunctions (this approach is implemented in [5]).

To calculate expression (4.30), we need to determine a complete set[18] of antisymmetric eigenfunctions $\Psi_h(\tau_1,\tau_2)$, find eigenvalues $K_c\Psi_h = k(h)\Psi_h$, and calculate the following sum:

$$(I-K_c)^{-1}K_cI = \sum_{k(h)\neq 1}\frac{k(h)}{1-k(h)}\frac{1}{\langle\Psi_h|\Psi_h\rangle}|\Psi_h\rangle\langle\Psi_h|\,, \quad (4.34)$$

where h is an abstract label that numerates eigenvalues and eigenfunctions (this label will be specified in Section 4.2.3). In other words, we need to find the spectrum of the conformal kernel K_c. Let us recall that we have to exclude the unit eigenvalue subspace, because, during the integration over this subspace, the effective action (3.55) is zero, i.e., the dominant contribution to the full four-point function is given by (4.6).

4.2.1 $\mathrm{SL}(2,\mathbb{R})$ generators and the Casimir operator. It is difficult to directly solve the integral equation $K_c\Psi_h = k(h)\Psi_h$. Fortunately, the $\mathrm{SL}(2,\mathbb{R})$ invariance significantly simplifies this task. This invariance implies that K_c commutes with the Casimir C of the $\mathrm{SL}(2,\mathbb{R})$ group; therefore, eigenfunctions of K_c and C coincide. This allows us to find eigenfunctions and eigenvalues separately: first, we solve the simpler equation[19] $C\Psi_h = h(h-1)\Psi_h$, and then determine the eigenvalues $k(h)$ for the known functions Ψ_h.

The $\mathrm{SL}(2,\mathbb{R})$ algebra can be defined using the following generators:

$$L_0^\tau = -\tau\partial_\tau - \Delta, \quad L_{-1}^\tau = \partial_\tau, \quad L_1^\tau = \tau^2\partial_\tau + 2\Delta\tau\,. \quad (4.35)$$

It is straightforward to check that these operators obey the proper commutation relations:

$$\big[L_m^\tau, L_n^\tau\big] = (m-n)L_{m+n}^\tau\,, \qquad m,n=-1,0,1\,. \quad (4.36)$$

Note that in this definition an operator with conformal dimension Δ is annihilated by the generator L_0^τ.

Please note that in the case $\Delta = 1/2$ these generators should commute with the kernel K_c:

$$\begin{aligned}&\big\langle(L_m^{\tau_1}+L_m^{\tau_2})K_c(\tau_1,\tau_2,\tau_3,\tau_4)|\Psi_h(\tau_3,\tau_4)\big\rangle\\ &\quad=\big\langle K_c(\tau_1,\tau_2,\tau_3,\tau_4)(L_m^{\tau_3}+L_m^{\tau_4})|\Psi_h(\tau_3,\tau_4)\big\rangle\\ &\quad+2\int_{-\infty}^{\infty}\mathrm{d}\tau_4\big[\tau_3^{m+1}K_c(\tau_1,\tau_2,\tau_3,\tau_4)\Psi_h(\tau_3,\tau_4)\big]_{\tau_3=-\infty}^{\tau_3=\infty}\,, \quad (4.37)\end{aligned}$$

where $\langle\cdot|\cdot\rangle$ denotes the inner product (3.54). This condition implies that $\mathrm{SL}(2,\mathbb{R})$ generators are zero modes of the operator K_c. To ensure this commutation relation, the term on the second line must vanish for all basis functions Ψ_h and all generators. In Section 4.2.2, we will see that this condition imposes an important restriction on the functions Ψ_h.

Finally, using generators (4.35), we build the Casimir operator,

$$\begin{aligned}C &= \big(L_0^{\tau_1}+L_0^{\tau_2}\big)^2 - \frac{1}{2}\big(L_{-1}^{\tau_1}+L_{-1}^{\tau_2}\big)\big(L_1^{\tau_1}+L_1^{\tau_2}\big)\\ &\quad-\frac{1}{2}\big(L_1^{\tau_1}+L_1^{\tau_2}\big)\big(L_{-1}^{\tau_1}+L_{-1}^{\tau_2}\big)\\ &= 2\big(\Delta^2-\Delta\big)+2L_0^{\tau_1}L_0^{\tau_2}-L_{-1}^{\tau_1}L_1^{\tau_2}-L_1^{\tau_1}L_{-1}^{\tau_2}\,, \quad (4.38)\end{aligned}$$

which defines the differential equation on the eigenfunctions.

4.2.2 Eigenfunctions and eigenvalues. Let us solve the equation $C\Psi_h = h(h-1)\Psi_h$. Substituting generators (4.35) and $\Delta = 1/2$, we obtain the following differential equation:

$$\begin{aligned}&\big[-(\tau_1-\tau_2)^2\partial_{\tau_1}\partial_{\tau_2}+(\tau_1-\tau_2)(\partial_{\tau_1}-\partial_{\tau_2})\big]\Psi_h(\tau_1,\tau_2)\\ &\qquad= h(h-1)\Psi_h(\tau_1,\tau_2)\,. \quad (4.39)\end{aligned}$$

We propose the following ansatz to solve this equation:

$$\begin{aligned}\Psi_{h\omega}(\tau_1,\tau_2) &= \frac{\mathrm{sgn}\,(\tau_1-\tau_2)}{\sqrt{|\tau_1-\tau_2|}}\,\psi_h\!\left(\frac{|\omega(\tau_1-\tau_2)|}{2}\right)\\ &\quad\times\exp\left(-\mathrm{i}\omega\,\frac{\tau_1+\tau_2}{2}\right). \quad (4.40)\end{aligned}$$

This ansatz is inspired by the following properties of the Casimir operator and function Ψ_h. First, Ψ_h is an antisymmetric function with the conformal weight $\Delta = 1/2$, which explains the factor $\mathrm{sgn}\,(\tau_1-\tau_2)/\sqrt{|\tau_1-\tau_2|}$. Second, the structure of Eqn (4.39) demonstrates that it is convenient to use variables $\tau \equiv \tau_1-\tau_2$ and $T \equiv (1/2)(\tau_1+\tau_2)$ rather than τ_1 and τ_2. Third, the result of the action of Casimir operator (4.39) on (4.40) does not depend on ω, and, finally, ψ_h solves the Bessel equation:

$$\begin{aligned}&\left[x^2\partial_x^2+x\partial_x+\left(x^2-h(h-1)-\frac{1}{4}\right)\right]\psi_h(x)=0\,,\\ &\text{where}\quad x\equiv\frac{|\omega\tau|}{2}\,. \quad (4.41)\end{aligned}$$

This means that for each h one has an infinite set of eigenfunctions parametrized by the frequency ω. In the zero temperature case, frequency is continuous ($\omega\in\mathbb{R}$); in the finite temperature case, it is discrete ($\omega = (\pi/\beta)(2n+1)$, $n\in\mathbb{Z}$). This also implies that in the decomposition (4.34) one has to sum over the set $\Psi_{h\omega}$ instead of the set Ψ_h:

$$\begin{aligned}&(I-K_c)^{-1}K_cI\\ &\quad=\sum_{k(h)\neq 1}\sum_{\omega}\frac{k(h,\omega)}{1-k(h,\omega)}\frac{1}{\langle\Psi_{h\omega}|\Psi_{h\omega}\rangle}|\Psi_{h\omega}\rangle\langle\Psi_{h\omega}|\,. \quad (4.42)\end{aligned}$$

The general solution of Eqn (4.41) is the sum of Bessel functions:

$$\begin{aligned}\psi_h(x) &= -A_hJ_{h-1/2}(x)-B_hY_{h-1/2}(x)\\ &= \frac{B_{1-h}}{\cos(\pi h)}\,J_{h-1/2}(x)-\frac{B_h}{\cos(\pi h)}\,J_{1/2-h}(x)\,. \quad (4.43)\end{aligned}$$

Here, B_h is some function of h. To obtain the second equality, we required that $\Psi_{1-h} = \Psi_h$, because Eqn (4.41) is invariant

[18] That is such a set where $I = \sum_h (1/\langle\Psi_h|\Psi_h\rangle)|\Psi_h\rangle\langle\Psi_h|$.

[19] It is convenient but not necessary to choose the eigenvalue of the Casimir operator as $h(h-1)$.

under the change $h \to 1-h$. Also, we have used the following relation between Bessel functions of the first and second kinds:

$$Y_\alpha(x) = \frac{J_\alpha(x)\cos(\pi\alpha) - J_{-\alpha}(x)}{\sin(\pi\alpha)}\,. \tag{4.44}$$

Then, we recall that the kernel K_c must commute with $\mathrm{SL}(2,\mathbb{R})$ generators. This implies that the term in the third line of (4.37) should be identically zero for $m=-1,0,1$ and all h. For $m=-1,0$, this condition is always satisfied, so it does not restrict anything. Indeed, the expression under the square brackets is proportional to $|\tau_3|^{m-1}$ as $\tau_3 \to \pm\infty$, i.e., in the case $m=-1,0$ the integrand is identically zero. However, in the case $m=1$ this condition imposes an additional restriction on the coefficients B_h:

$$\begin{aligned}
&\int_{-\infty}^{\infty} \mathrm{d}\tau_4 \Bigg[\tau_3^2 K(\tau_1,\tau_2,\tau_3,\tau_4)\\
&\times \frac{1}{\sqrt{|\tau_3-\tau_4|}}\,\psi_{h\omega}\left(\frac{|\omega(\tau_3-\tau_4)|}{2}\right)\cos\left(\frac{\omega(\tau_3+\tau_4)}{2}\right)\Bigg]_{\tau_3=-\infty}^{\tau_3=\infty}\\
&= -3\sqrt{\pi}\,J^2\int_{-\infty}^{\infty}\mathrm{d}\tau_4\,\frac{\operatorname{sgn}(\tau_2-\tau_4)}{\sqrt{|\tau_1-\tau_2||\tau_2-\tau_4|}}\\
&\times \sin\frac{\omega\tau_4}{2}\left[\frac{B_h}{\cos(\pi h)}\cos\frac{\pi h}{2} - \frac{B_{1-h}}{\cos(\pi h)}\sin\frac{\pi h}{2}\right] = 0\,;
\end{aligned} \tag{4.45}$$

hence,

$$\frac{B_h}{B_{1-h}} = \tan\frac{\pi h}{2}\,. \tag{4.46}$$

Putting all these relations together, we conclude that the eigenfunctions have the following form (up to the numerical factor to be fixed below):

$$\begin{aligned}
\Psi_{h\omega}(\tau_1,\tau_2) = \frac{\operatorname{sgn}\tau}{\sqrt{|\tau|}}\exp(-\mathrm{i}\omega T)\Bigg[&\frac{\cos(\pi h/2)}{\cos(\pi h)}\,J_{h-1/2}\left(\frac{|\omega\tau|}{2}\right)\\
&-\frac{\sin(\pi h/2)}{\cos(\pi h)}\,J_{1/2-h}\left(\frac{|\omega\tau|}{2}\right)\Bigg]\,.
\end{aligned} \tag{4.47}$$

Integrating function (4.47) with kernel K_c (similarly to (3.52)), one finds the corresponding eigenvalue, $K_c\Psi_h = k(h,\omega)\Psi_h$:

$$k(h,\omega) = -\frac{3}{2}\,\frac{\tan\left[(\pi/2)(h-1/2)\right]}{h-1/2}\,. \tag{4.48}$$

This calculation is cumbersome but straightforward, so we do not reproduce it here. A detailed calculation[20] can be found in Appendices C and D of [4].

Note that eigenvalue (4.48) does not depend on the frequency ω due to the conformal invariance of the kernel. However, it does depend on the frequency when one moves away from the IR limit. In paper [5], this dependence was established and used to calculate the leading nonconformal correction to the four-point correlation functions. The result of this calculation coincides with the one in Section 4.1.

4.2.3 Complete set of eigenfunctions. Eigenfunctions of the Hermitian operator form a complete set (see, e.g., [124]). Keeping this fact in mind, we require the hermiticity of the Casimir operator with respect to the inner product (3.54):

$$\big\langle C\Psi_{h\omega}(\tau_1,\tau_2)\big|\Psi_{h'\omega'}(\tau_1,\tau_2)\big\rangle = \big\langle \Psi_{h\omega}(\tau_1,\tau_2)\big|C\Psi_{h'\omega'}(\tau_1,\tau_2)\big\rangle\,. \tag{4.49}$$

On the one hand, the hermiticity means that eigenvalues of the Casimir operator are real:

$$\operatorname{Im}\big[h(h-1)\big] = 0\,,\quad \text{i.e.,}\quad \operatorname{Im} h\,(2\operatorname{Re} h - 1) = 0\,. \tag{4.50}$$

In other words, variable h is either purely real or has a fixed real part: $h = 1/2 + \mathrm{i}s$, $s\in\mathbb{R}$, $s>0$ (without the last inequality, the eigenfunctions are ambiguous: $\Psi_{1/2+\mathrm{i}s,\,\omega} = \Psi_{1/2-\mathrm{i}s,\,\omega}$). On the other hand, identity (4.49) implies that the corresponding boundary term vanishes for arbitrary ω, ω' and h, h' from the spectrum:

$$\begin{aligned}
&\big\langle C\Psi_{h\omega}(\tau_1,\tau_2)\big|\Psi_{h'\omega'}(\tau_1,\tau_2)\big\rangle - \big\langle \Psi_{h\omega}(\tau_1,\tau_2)\big|C\Psi_{h'\omega'}(\tau_1,\tau_2)\big\rangle\\
&= \frac{8\pi\delta(\omega-\omega')}{\omega}\Big[x\big(\psi_{h'}(x)\partial_x\psi_h^*(x) - \psi_h^*(x)\partial_x\psi_{h'}(x)\big)\Big]_{x=0}^{x=\infty} = 0\,.
\end{aligned} \tag{4.51}$$

Here, we substituted ansatz (4.40) and denoted $x = |\omega\tau|/2$. Substituting the asymptotics of the Bessel function [125], we find that

$$\lim_{x\to\infty}\Big[x\big(\psi_{h'}(x)\partial_x\psi_h^*(x) - \psi_h^*(x)\partial_x\psi_{h'}(x)\big)\Big] = 0 \tag{4.52}$$

for arbitrary h and h', and

$$\begin{aligned}
&\lim_{x\to 0}\Big[x\big(\psi_{h'}(x)\partial_x\psi_h^*(x) - \psi_h^*(x)\partial_x\psi_{h'}(x)\big)\Big]\\
&= \lim_{x\to 0}\frac{\cos(\pi h^*/2)\cos(\pi h'/2)}{\cos(\pi h^*)\cos(\pi h')}\\
&\times\Bigg[\frac{h^*-h'}{\Gamma(h^*+1/2)\Gamma(h'+1/2)}\left(\frac{x}{2}\right)^{h^*+h'-1}\\
&-\tan\frac{\pi h^*}{2}\tan\frac{\pi h'}{2}\,\frac{h^*-h'}{\Gamma(3/2-h^*)\Gamma(3/2-h')}\left(\frac{x}{2}\right)^{1-h^*-h'}\\
&+\tan\frac{\pi h^*}{2}\,\frac{h^*+h'-1}{\Gamma(3/2-h^*)\Gamma(h'+1/2)}\left(\frac{x}{2}\right)^{h'-h^*}\\
&-\tan\frac{\pi h'}{2}\,\frac{h^*+h'-1}{\Gamma(h^*+1/2)\Gamma(3/2-h')}\left(\frac{x}{2}\right)^{h^*+h'-1}\Bigg] = 0
\end{aligned} \tag{4.53}$$

for values of the form $h = 1/2 + \mathrm{i}s$, $s\in\mathbb{R}$, $s>0$ (in this case, an oscillating expression is obtained) or $h = 2n$, $n = 1,2,3,\ldots$ (in this case, the divergent terms are multiplied by zeroes). We conclude that together these two sets form a complete set in the space of antisymmetric two-point functions.

Finally, let us find the normalization in decomposition (4.42), i.e., calculate the inner product of two eigenfunctions:

$$\begin{aligned}
&\big\langle \Psi_{h\omega}(\tau_1,\tau_2)\big|\Psi_{h'\omega'}(\tau_1,\tau_2)\big\rangle\\
&= 2\int_{-\infty}^{\infty}\mathrm{d}T\int_0^\infty\frac{\mathrm{d}\tau}{\tau}\,\psi_h^*\left(\frac{|\omega|\tau}{2}\right)\psi_{h'}\left(\frac{|\omega'|\tau}{2}\right)\exp\big[\mathrm{i}(\omega-\omega')T\big]\\
&= 4\pi\delta(\omega-\omega')\int_0^\infty\frac{\mathrm{d}\tau}{\tau}\Bigg[\frac{\sin(\pi h/2)}{\cos(\pi h)}\,J_{1/2-h}\left(\frac{\omega\tau}{2}\right)\\
&-\frac{\cos(\pi h/2)}{\cos(\pi h)}\,J_{h-1/2}\left(\frac{\omega\tau}{2}\right)\Bigg]^*\\
&\times\left[\frac{\sin(\pi h'/2)}{\cos(\pi h')}\,J_{1/2-h'}\left(\frac{\omega\tau}{2}\right) - \frac{\cos(\pi h'/2)}{\cos(\pi h')}\,J_{h'-1/2}\left(\frac{\omega\tau}{2}\right)\right].
\end{aligned} \tag{4.54}$$

[20] The authors of [4] use a different kernel and obtain slightly different eigenfunctions, but the integral for the eigenvalue coincides with our case.

For a discrete set, this integral gives the Kronecker delta,

$$\left\langle \Psi_{h\omega}(\tau_1,\tau_2)|\Psi_{h'\omega'}(\tau_1,\tau_2)\right\rangle = \frac{2\pi^2}{2h-1}\,\delta_{hh'}\,2\pi\delta(\omega-\omega')\,, \tag{4.55}$$

and, for the continuum set, it gives the Dirac delta,[21]

$$\left\langle \Psi_{h\omega}(\tau_1,\tau_2)|\Psi_{h'\omega'}(\tau_1,\tau_2)\right\rangle = \frac{2\pi\tan(\pi h)}{2h-1}\,2\pi\delta(h-h')\,2\pi\delta(\omega-\omega')\,. \tag{4.56}$$

Furthermore, identity operator (3.53) in the space of antisymmetric two-point functions can be represented as the following decomposition:

$$I(\tau_1,\tau_2,\tau_3,\tau_4) = \frac{1}{2}\int_{-\infty}^{\infty}\frac{\mathrm{d}\omega}{2\pi}\left[\int_0^{\infty}\frac{\mathrm{d}s}{2\pi}\,\frac{2h-1}{\pi\tan(\pi h)}\right.$$
$$\times\,\Psi_{h\omega}(\tau_1,\tau_2)\Psi^*_{h\omega}(\tau_3,\tau_4)\Big|_{h=1/2+is}$$
$$\left.+\sum_{n=1}^{\infty}\frac{2h-1}{\pi^2}\,\Psi_{h\omega}(\tau_1,\tau_2)\Psi^*_{h\omega}(\tau_3,\tau_4)\Big|_{h=2n}\right]. \tag{4.57}$$

Substituting ansatz (4.47) and integrating over the frequencies, we obtain the decomposition which explicitly looks as the conformal four-point function of fields with $\Delta = 1$:

$$I(\tau_1,\tau_2,\tau_3,\tau_4) = \frac{1}{2}\,\frac{\operatorname{sgn}(\tau_{12})\operatorname{sgn}(\tau_{34})}{|\tau_{12}||\tau_{34}|}$$
$$\times\left[\int_0^{\infty}\frac{\mathrm{d}s}{2\pi}\,\frac{2h-1}{\pi\tan(\pi h)}\,\Psi_{1/2+is}(\chi)\Big|_{h=1/2+is}\right.$$
$$\left.+\sum_{n=1}^{\infty}\frac{2h-1}{\pi^2}\,\Psi_{2n}(\chi)\Big|_{h=2n}\right], \tag{4.58}$$

where we have denoted $\tau_{12}\equiv\tau_1-\tau_2$, introduced the $\mathrm{SL}(2,\mathbb{R})$-invariant cross-ratio,

$$\chi \equiv \frac{\tau_{12}\tau_{34}}{\tau_{13}\tau_{24}}\,, \tag{4.59}$$

and defined the function $\Psi_h(\chi)$,

$$\Psi_h(\chi)\equiv\begin{cases}\dfrac{\Gamma(h/2)\Gamma((1-h)/2)}{\sqrt{\pi}}\;{}_2F_1\left[\dfrac{h}{2},\dfrac{1-h}{2},\dfrac{1}{2},\left(\dfrac{2-\chi}{\chi}\right)^2\right],\\ \text{if}\quad \chi>1\,,\\ \dfrac{\cos^2(\pi h/2)}{\cos(\pi h)}\,\dfrac{\Gamma^2(h)}{\Gamma(2h)}\,\chi^h\,{}_2F_1\big(h,h,2h,\chi\big)+(h\to 1-h)\,,\\ \text{if}\quad 0<\chi<1\,,\end{cases} \tag{4.60}$$

where $\Gamma(\ldots)$ is the gamma function and ${}_2F_1(\ldots)$ is the hypergeometric function. For details on this calculation, see Appendix D and papers [4, 5].

Finally, decomposition (4.58) can be rewritten as the single contour integral,

$$I(\tau_1,\tau_2,\tau_3,\tau_4) = \frac{1}{2}\,\frac{\operatorname{sgn}(\tau_{12})\operatorname{sgn}(\tau_{34})}{\tau_{12}\tau_{34}}$$
$$\times\int_{\mathcal{C}}\frac{\mathrm{d}h}{2\pi\mathrm{i}}\,\frac{h-1/2}{\pi\tan(\pi h/2)}\,\Psi_h(\chi)\,, \tag{4.61}$$

[21] We introduce UV cutoff $\epsilon\to 0$ and use $\lim_{\epsilon\to 0}[2/(p-s)]\times\sin[(1/2)(s-p)\log(\epsilon/2)] = \pi\delta(s-p)$. More details can be found in [4].

where the contour $\mathcal{C}$ is defined in the following way:

$$\int_{\mathcal{C}}\frac{\mathrm{d}h}{2\pi\mathrm{i}} \equiv \int_{1/2-\mathrm{i}\infty}^{1/2+\mathrm{i}\infty}\frac{\mathrm{d}h}{2\pi\mathrm{i}} + \sum_{n=1}^{\infty}\operatorname{Res}_{h=2n}\,. \tag{4.62}$$

In order to rewrite the integral over $\mathrm{d}s$, we used the symmetry of the integrand under the change $h\to 1-h$ along with the following identity:

$$\frac{2}{\tan(\pi h)} = \frac{1}{\tan(\pi h/2)} - \frac{1}{\tan\left[\pi(1-h)/2\right]}\,. \tag{4.63}$$

Of course, the decomposition for the identity operator can also be deduced from the representation theory of the $\mathrm{SL}(2,\mathbb{R})$ group. More details on this method can be found in [121].

4.2.4 Four-point function and operator expansion. To find the conformal contribution to the four-point function, we substitute the eigenvalues and the decomposition of identity operator (4.61) into Eqn (4.30),

$$\mathcal{F}_{\mathrm{CFT}}(\tau_1,\tau_2,\tau_3,\tau_4) = \frac{\sqrt{4\pi}}{3N}\,\frac{\operatorname{sgn}(\tau_{12})}{|J\tau_{12}|^{2\Delta}}\,\frac{\operatorname{sgn}(\tau_{34})}{|J\tau_{34}|^{2\Delta}}\,\mathcal{F}_{\mathrm{CFT}}(\chi)\,, \tag{4.64}$$

where $\Delta = 1/4$, and we have introduced the $\mathrm{SL}(2,\mathbb{R})$-invariant function $\mathcal{F}_{\mathrm{CFT}}(\chi)$,

$$\mathcal{F}_{\mathrm{CFT}}(\chi) = \int_{\mathcal{C}}\frac{\mathrm{d}h}{2\pi\mathrm{i}}\,\frac{k(h)}{1-k(h)}\,\frac{h-1/2}{\pi\tan(\pi h/2)}\,\Psi_h(\chi)\Big|_{h\neq 2}\,. \tag{4.65}$$

In the finite temperature case, expression (4.64) transforms into

$$\mathcal{F}_{\mathrm{CFT}}(\tau_1,\tau_2,\tau_3,\tau_4) = \frac{\sqrt{4\pi}}{3N}\,\frac{1}{\beta J}\,\frac{\operatorname{sgn}\left[\sin(\pi\tau_{12}/\beta)\right]}{\left|\sin(\pi\tau_{12}/\beta)\right|^{2\Delta}}\,\frac{\operatorname{sgn}\left[\sin(\pi\tau_{34}/\beta)\right]}{\left|\sin(\pi\tau_{34}/\beta)\right|^{2\Delta}}\,\mathcal{F}_{\mathrm{CFT}}(\tilde{\chi})\,,$$
$$\tilde{\chi} = \frac{\sin(\pi\tau_{12}/\beta)\sin(\pi\tau_{34}/\beta)}{\sin(\pi\tau_{13}/\beta)\sin(\pi\tau_{24}/\beta)}\,. \tag{4.66}$$

Recall that we had to exclude the value $h=2$ in integral (4.62), because it corresponds to the zero mode of the operator K_{c}, i.e., to the soft mode discussed in Section 4.1. However, $h=2$ is not the only solution to the equation $k(h)=1$ with $k(h)$ from (4.48). In fact, this equation has infinitely many real solutions of the form $h_m = 2\Delta + 2m + 1 + \epsilon_m$, where ϵ_m goes to zero for a large integer m as

$$\epsilon_m \approx \frac{3}{2\pi m}\quad\text{for}\quad m\gg 1\,. \tag{4.67}$$

These solutions do not belong to the spectrum of the operator K_{c}, but they correspond to the simple poles of the function $k(h)/(1-k(h))(h-1/2)/[\pi\tan(\pi h/2)]\Psi_h(\chi)$. Hence, we can push the contour $\mathcal{C}$ to the right (Fig. 8) and obtain a different decomposition for the function $\mathcal{F}_{\mathrm{CFT}}$:

$$\mathcal{F}_{\mathrm{CFT}}(\chi) = \sum_{m=0}^{\infty}\operatorname{Res}_{h=h_m}\left[\frac{k(h)}{1-k(h)}\,\frac{h-1/2}{\pi\tan(\pi h/2)}\,\Psi_h(\chi)\right], \tag{4.68}$$

where $h_0=2$ and h_m for $m>0$ have the form mentioned above. However, the contribution from the $h_0=2$ pole cancels if one moves away from the IR limit and considers corrections to $k(h,\omega)$ near $h_0=2$ (we will not discuss how this happens: for details, see [5]). Thus, for $\chi<1$, this expansion

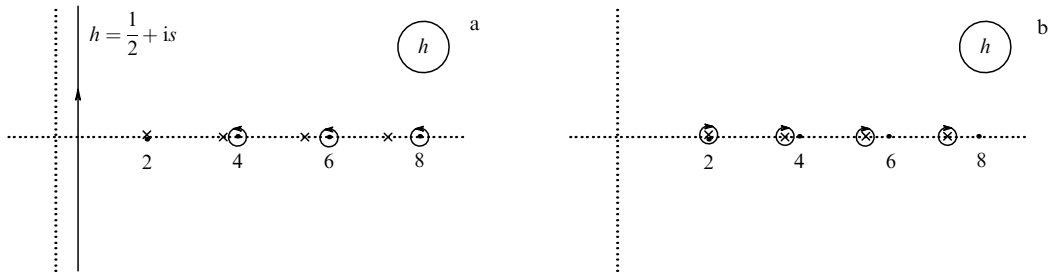

Figure 8. (a) Contour $\mathcal{C}$ from sum (4.65). (b) Contour from sum (4.68). Dots denote poles that correspond to the solutions of $\tan(\pi h/2) = 0$, crosses denote poles that correspond to solutions of $k(h) = 1$. Note the double pole at $h = 2$.

reproduces the four-point function OPE [5, 103]:

$$\mathcal{F}_{\rm CFT}(\chi) = \sum_{m=1}^{\infty} c_m^2 \chi^{h_m}\, {}_2F_1\left(h_m, h_m, 2h_m, \chi\right) = \sum_{m=0}^{\infty} c_m^2 \quad \mathcal{O}_m \quad , \tag{4.69}$$

where h_m are conformal weights of the corresponding intermediate operators, and the coefficients c_m are found from the decomposition of (4.61) around $\chi = 0$. The asymptotic behavior of the conformal weights shows that the operators of the OPE are built from two fermion fields, $(2m+1)$ derivatives and the anomalous part that corresponds to the interactions

$$\mathcal{O}_m \approx \sum_{i=1}^{N} \sum_{k=0}^{2m+1} d_{mk} \partial_\tau^k \chi_i \partial_\tau^{2m+1-k} \chi_i \,, \tag{4.70}$$

where d_{mk} are some numerical coefficients. The explicit form of the operators $\mathcal{O}_m$ can be found in [123].

4.2.5 OTOC and TOC. Let us estimate the conformal contributions to the OTOC (4.27), which corresponds to the function $\mathcal{F}(\beta/4 + it, -\beta/4 + it, 0, -\beta/2)$, and the TOC (4.29), which corresponds to the function $\mathcal{F}(\beta/2 + it, it, 0, -\beta/2)$. On the tree level, both of these correlators behave as

$$\mathrm{OTOC}(t) = \mathrm{TOC}(t) = \tilde{G}\left(\frac{\beta}{2}\right)\tilde{G}\left(\frac{\beta}{2}\right) \approx \frac{\sqrt{\pi}}{2\beta J} + \mathcal{O}\left(\frac{1}{N}\right) \tag{4.71}$$

in the limit $t \to \infty$. In Section 4.1, we estimated the leading $1/N$ corrections to these correlators, which are ensured by the so-called soft mode. Here, we find the subleading corrections that have the same order in $1/N$ but are suppressed by the small factor $1/(\beta J)$. We denote such corrections as $\delta\mathrm{OTOC}(t)$ and $\delta\mathrm{TOC}(t)$.

In the limit $t \to \infty$, choices of times for both the OTOC and TOC give small cross-ratios (4.59), $\chi \to 0$. However, in the limit $t \to 0$, times of the OTOC correspond to the cross-ratio $\chi \to 2 - 4\pi i t/\beta$, whereas times of the TOC correspond to $\chi \to 1 - \pi^2 t^2/\beta^2$. Hence, for the OTOC, we need to analytically continue the $\chi > 1$ version of expression (4.65) to small imaginary cross-ratios $\chi \sim -4i \exp(-2\pi t/\beta)$:

$$\delta\mathrm{OTOC}(t) = \frac{\sqrt{4\pi}}{3N}\frac{1}{\beta J}\int_{\mathcal{C}} \frac{dh}{2\pi i}\, \frac{k(h)}{1-k(h)}\, \frac{h-1/2}{\pi \tan(\pi h/2)} \times \frac{\Gamma(h/2)\Gamma\left((1-h)/2\right)}{\sqrt{\pi}}\, {}_2F_1\left[\frac{h}{2}, \frac{1-h}{2}, \frac{1}{2}, \left(\frac{2-\chi}{\chi}\right)^2\right]_{h\neq 2} . \tag{4.72}$$

For the TOC, we just need to take the limit $\chi \sim 4\exp(-2\pi t/\beta) \to 0$:

$$\delta\mathrm{TOC}(t) = \frac{\sqrt{4\pi}}{3N}\frac{1}{\beta J}\int_{\mathcal{C}} \frac{dh}{2\pi i}\, \frac{k(h)}{1-k(h)}\, \frac{h-1/2}{\pi \tan(\pi h/2)} \times \left[\frac{\cos^2(\pi h/2)}{\cos(\pi h)}\, \frac{\Gamma^2(h)}{\Gamma(2h)}\, \chi^h\, {}_2F_1(h,h,2h,\chi) + (h \to 1-h)\right]_{h\neq 2} . \tag{4.73}$$

To evaluate the integral along the contour $\mathcal{C}$, we use the following trick. First of all, we define the function $k_{\rm R}(h)$,

$$k_{\rm R}(h) \equiv \frac{\cos[\pi(2h-1)/4]}{\cos[\pi(2h+1)/4]}\, k(h) \,, \tag{4.74}$$

which has two important properties. On the one hand, for any real even h, this function coincides with the eigenvalue $k(h)$, so we can substitute $k(h) \to k_{\rm R}(h)$ into the discrete sum in (4.65). On the other hand, $k_{\rm R}(h) = 1$ in the unique point of the complex plane, $h = 2$. Hence, we can freely [22] pull the contour that circles $h = 2, 4, 6, \ldots$ back to the line $h = 1/2 + is$ (Fig. 9). After this operation, we get the single integral over the line $h = 1/2 + is$ plus the pole at $h = 2$:

$$\mathcal{F}_{\rm CFT}(\chi) = \int_{-\infty}^{\infty} \frac{ds}{2\pi}\left[\frac{k(h)}{1-k(h)} - \frac{k_{\rm R}(h)}{1-k_{\rm R}(h)}\right] \times \frac{h-1/2}{\pi\tan(\pi h/2)}\, \Psi_h(\chi) - \mathrm{Res}_{h=2}\left[\frac{k_{\rm R}(h)}{1-k_{\rm R}(h)}\, \frac{h-1/2}{\pi\tan(\pi h/2)}\, \Psi_h(\chi)\right] . \tag{4.75}$$

The integral on the first line rapidly converges and does not grow in the limit $\chi \to 0$, because in this limit function $\Psi_{1/2+s}(\chi) \sim \chi^{1/2}$ (this asymptotic behavior holds for both the TOC and OTOC). Therefore, for our purposes this integral can be disregarded.

At the same time, the pole on the right-hand side of (4.75) makes a growing contribution to the OTOC. Moreover, this is a double pole, which gives a combination of the function Ψ_h and its derivative $\partial_h \Psi_h$. This combination grows faster than exponentially:

$$\delta\mathrm{OTOC}(t) \approx \frac{C_1}{\beta J N}\exp\left(\frac{2\pi t}{\beta}\right) + \frac{C_2}{\beta J N}\frac{2\pi t}{\beta}\exp\left(\frac{2\pi t}{\beta}\right) , \tag{4.76}$$

where C_1 and C_2 are some positive numerical constants. At first sight, such fast growth violates bound [9], but accurate

[22] $\Psi_h(\chi)$ has simple poles at the points $h = 1, 3, 5, \ldots$, but these poles are canceled by the zeroes of $[\tan(\pi h/2)]^{-1}$.

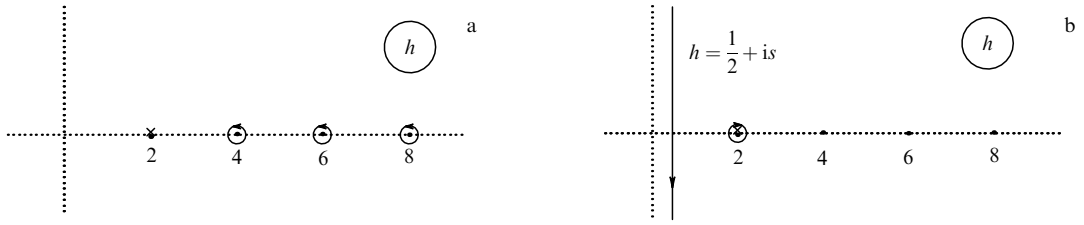

Figure 9. (a) Sum over the poles into (4.65) with $k(h) \to k_{\rm R}(h)$. (b) Result of pushing the contour to the left. Note that $k_{\rm R}(h) = 1$ only for $h = 2$, so we do not get contributions as in Fig. 8b.

consideration shows that this is not the case. An apparent contradiction is explained by the sign of (4.76) (we expect the OTOC to decay, not grow) and small factor $1/(\beta J)$. Due to this factor, the contribution of the conformal part is parametrically smaller than the contribution of the soft mode, at least until the growth of the OTOC is saturated. This means that expression (4.76) can be interpreted as the leading correction to the Lyapunov exponent [5, 6, 103]:

$$\mathrm{OTOC}(t) \to \mathrm{OTOC}(t) + \delta\mathrm{OTOC}(t) \approx \frac{\sqrt{\pi}}{2\beta J} \times \left[1 - \mathrm{const}\,\frac{\beta J}{N}\exp(\kappa t)\right] \quad \text{for} \quad \beta \ll t \ll \beta \log\frac{N}{\beta J}\,, \tag{4.77}$$

where const is a positive $\mathcal{O}(1)$ numerical factor and κ is the corrected Lyapunov exponent; both factor and exponent are equal to the corresponding quantities from (4.28) with $\mathcal{O}(1/(\beta J))$ corrections:

$$\kappa \approx \frac{2\pi}{\beta}\left(1 - \frac{6.05}{\beta J} + \dots\right). \tag{4.78}$$

Note that the conformally corrected Lyapunov exponent is *smaller* that the upper bound $\kappa = 2\pi/\beta$ predicted in [9].

One can also check that the pole on the right-hand side of (4.75) does not generate any growth with time contributions to the TOC. Similarly to the soft mode case, this contribution is of the order of $1/N$, i.e., the approximate identity for the whole TOC is nearly the same as in (4.29).

We emphasize that the OTOC rapidly decays only at times well before the scrambling time $t_* \sim \beta \log[N/(\beta J)]$. At larger times, our approximations do not work, and other types of diagrams (e.g., multiple parallel ladders) also generate significant corrections to (4.28). So, one expects that the rate of the decay slows down before the OTOC is eventually saturated [5, 6, 9, 103]. This conjecture was confirmed in [126], where SYK OTOCs were evaluated for arbitrary times. Namely this paper established a new time scale, $t_M = N\log N/(64\sqrt{\pi}J)$, after which exponential decay of OTOCs is replaced by a power law: $\mathrm{OTOC}(t) \sim (t/t'_M)^{-6}$, where $t'_M = t_M$ if $\beta \ll t_M$ and $t'_M = \beta^{-1}$ in the opposite case.

Let us also emphasize again that identities (4.77) and (4.78) were obtained in the limit $1 \ll \tau J < \beta J \ll N$, i.e., only for small but nonzero temperatures. However, recently it was argued that in the large $q \gg 1$ limit, where q is the number of fermions in the interaction vertex, similar identities hold for arbitrary temperatures and couplings [127, 128].

5. Two-dimensional dilaton gravity

The other remarkable theory which exhibits a chaotic behavior is two-dimensional dilaton gravity coupled to matter. Correlation functions of the boundary operators corresponding to bulk matter fields in this model behave similarly to the correlation functions of the fermion fields in the SYK model. However, we emphasize that the behavior of these models coincides only in the low energy limit. This aspect of two-dimensional dilaton gravity has been extensively studied in [10–13]. In Sections 5.1–5.5, we review the reasoning of these papers.

5.1 Dilaton gravity as the near-horizon limit of extremal black hole

First of all, let us show that in the near-horizon limit the spacetime of a 4D extremal black hole factorizes into the product of two-dimensional anti-de Sitter space (AdS_2) and a two-dimensional sphere (S_2). The metric and the electromagnetic field of the charged Reissner–Nordström black hole are as follows:

$$\mathrm{d}s^2 = -\frac{(r-r_+)(r-r_-)}{r^2}\,\mathrm{d}t^2 + \frac{r^2}{(r-r_+)(r-r_-)}\,\mathrm{d}r^2 + r^2\,\mathrm{d}\Omega^2, \tag{5.1}$$
$$r_\pm = Ql_{\rm P} + El_{\rm P}^2 \pm \sqrt{2QEl_{\rm P}^3 + E^2 l_{\rm P}^4}\,, \quad F_{rt} = \frac{Q}{r^2}\,.$$

Here, M is the mass and Q is the electrical charge of the black hole, $\mathrm{d}\Omega^2$ is the metric on the two-sphere with unit radius. Also, $l_{\rm P} = \sqrt{G}$ is the Planck length (G is the usual four-dimensional Newton constant), and the excitation energy above extremality is $E = M - Q/l_{\rm P}$. Obviously, for $E = 0$ horizons r_+ and r_- coincide, and the black hole becomes extremal. Note that in this case M and Q are not independent, so the Planck length is the only dimensionful parameter of the extremal black hole.

In order to take the near-horizon limit of the extremal black hole, we introduce the variable

$$z \equiv \frac{Q^2 l_{\rm P}^2}{r - r_+} \tag{5.2}$$

and take the limit $r \to r_+$, $l_{\rm P} \to 0$ while keeping $z = \mathrm{const}$. This is the simplest combination of $r - r_+$ and $l_{\rm P}$ with a length dimensionality which does not vanish in the limit $r \to r_+$ (we introduce the factor Q^2 for convenience). It is straightforward to see that metric (5.1) factorizes into the sum of AdS_2 and S_2 in the limit in question:

$$\mathrm{d}s^2 \approx Q^2 l_{\rm P}^2\left(\frac{-\,\mathrm{d}t^2 + \mathrm{d}z^2}{z^2} + \mathrm{d}\Omega^2\right). \tag{5.3}$$

Now, let us show that some type of excitation above the horizon of an extremal black hole (5.3) is described by two-dimensional dilaton gravity [103, 129–131]. Namely, we consider a static, spherically symmetric ansatz for the metric:

$$\mathrm{d}s^2 = h_{ij}(x^0, x^1)\,\mathrm{d}x^i\,\mathrm{d}x^j + \Phi^2(x^0, x^1)\,\mathrm{d}\Omega^2\,, \tag{5.4}$$

where $i, j = 0, 1$, $x^0 = t$, $x^1 = r$, and h_{ij} and Φ are some functions to be determined. The determinant of the metric ($g = \det g_{\mu\nu}$), Ricci-scalar (R_g), and square of the electromagnetic tensor ($F^2_{\mu\nu}$) are as follows:

$$\begin{aligned}
&\sqrt{-g} = \sqrt{-h}\,\Phi^2 \sin\theta\,,\\
&R_g = R_h + \frac{2}{\Phi^2} - 4\nabla^2 \log\Phi - 6h^{mn}\nabla_m \log\Phi\,\nabla_n \log\Phi\,, \quad (5.5)\\
&F^2_{\mu\nu} = \frac{2Q^2}{\Phi^4}\,,
\end{aligned}$$

where ∇_k denotes the covariant derivative with respect to the metric h_{ij}. On the second line, we used the fact that the unit sphere has constant curvature $R_{(\theta,\phi)} = 2$. Substituting these formulas into the Einstein–Hilbert action,

$$I = -\frac{1}{16\pi l_{\mathrm{P}}^2}\int \mathrm{d}^4x\,\sqrt{-g}\left[R_h - \frac{l_{\mathrm{P}}^2}{4}\,F^2_{\mu\nu}\right], \quad (5.6)$$

using Stokes' theorem (we assume that corresponding boundary terms at flat spacetime infinity vanish), and integrating over the angular degrees of freedom, we obtain the following two-dimensional theory:[23]

$$I = -\frac{1}{4l_{\mathrm{P}}^2}\int \mathrm{d}^2x\,\sqrt{-h}\left[\Phi^2 R_h + 2(\nabla\Phi)^2 + 2 - \frac{2Q^2 l_{\mathrm{P}}^2}{\Phi^2}\right]. \quad (5.7)$$

The field Φ is usually referred to as the dilaton field. Note that the Weyl transformation shifts the potential and the coefficient in front of the kinetic term:

$$\begin{aligned}
&h_{ij} \to h_{ij}\Phi^{-\lambda/2} \quad \text{leads to} \quad 2 \to 2 - \lambda\,,\\
&2 - \frac{2Q^2 l_{\mathrm{P}}^2}{\Phi^2} \to \Phi^{-\lambda/2}\left(2 - \frac{2Q^2 l_{\mathrm{P}}^2}{\Phi^2}\right); \quad (5.8)
\end{aligned}$$

so, we can get rid of the kinetic term for the field Φ:

$$I = -\frac{1}{4l_{\mathrm{P}}^2}\int \mathrm{d}^2x\,\sqrt{-h}\left[\Phi^2 R_h + 2 - \frac{2Q^2 l_{\mathrm{P}}^2}{\Phi^2}\right]. \quad (5.9)$$

Since the dilaton is now nondynamical, the extremum of this action is achieved at some constant value Φ_0 which determines the curvature of the spacetime. Moreover, the curvature is always negative, i.e., the extremum corresponds to the AdS_2 space:

$$\delta_\Phi I = 0 \quad \text{implies} \quad R_h = -\frac{2Q^2 l_{\mathrm{P}}^2}{\Phi_0^4} = -\frac{2}{L^2}\,, \quad (5.10)$$

where we have defined the radius of the AdS_2 as $L = \Phi_0^2/(|Q|l_{\mathrm{P}})$. Substituting $L^2 \approx Q^2 l_{\mathrm{P}}^2$ from (5.3), one can estimate the critical value of the dilaton field: $\Phi_0 \approx |Q|l_{\mathrm{P}}$. As expected, in the leading order this theory reproduces the near-horizon limit of an extremal black hole with the gravitational radius $r_\pm \approx \Phi_0$. Let us consider excitations above the extremality, which in this picture correspond to small deformations of the dilaton field,

$$\Phi^2 = \Phi_0^2 + \phi(x,t)\,, \quad \phi(x,t) \ll \Phi_0^2\,, \quad (5.11)$$

and expand action (5.9) up to the second order in ϕ/Φ_0^2:

$$\begin{aligned}
I \approx -\frac{1}{2l_{\mathrm{P}}^2}\int \mathrm{d}^2x\,\sqrt{-h} - \frac{\Phi_0^2}{4l_{\mathrm{P}}^2}\left[\int \mathrm{d}^2x\,\sqrt{-h}\left(R_h + \frac{2}{L^2}\right)\right.\\
\left. + 2\int_{\mathrm{bdy}} \mathcal{K}\right] - \frac{1}{4l_{\mathrm{P}}^2}\left[\int \mathrm{d}^2x\,\sqrt{-h}\,\phi\left(R_h + \frac{2}{L^2}\right) + 2\int_{\mathrm{bdy}} \phi_b\mathcal{K}\right] \quad (5.12)
\end{aligned}$$

(where 'bdy' stands for 'boundary'). Here, we have restored the appropriate boundary terms at the AdS_2 boundary[24] to make the minimal action finite (we will check this below) and introduced the trace of the extrinsic curvature,

$$\mathcal{K} = -\frac{h_{ab}T^a T^c \nabla_c n^b}{h_{ab}T^a T^b}\,, \quad (5.13)$$

where T^a and n^a are tangent and unit normal vectors to the boundary curve[25] of AdS_2. We have also denoted $\phi|_{\mathrm{bdy}} = \phi_b$ for brevity.

The first term in (5.12) is proportional to the volume of the AdS_2 space, which is infinite but constant. The second term is the ordinary two-dimensional Einstein gravity. This expression is purely topological, i.e., it just gives the Euler characteristic of the manifold due to the Gauss–Bonnet theorem. Hence, neither of the terms under discussion affects the equations of motion.

At the same time, the last term in sum (5.12) does describe the nontrivial dynamics of the remaining fields. The corresponding action

$$I_{\mathrm{JT}} = -\frac{1}{16\pi G}\left[\int \mathrm{d}^2x\,\sqrt{-h}\,\phi\left(R_h + \frac{2}{L^2}\right) + 2\int_{\mathrm{bdy}} \phi_b\mathcal{K}\right] \quad (5.14)$$

is usually referred to as the Jackiw–Teitelboim 2D gravity theory [132, 133]. Note that we have rescaled the Newton constant. Also note that ϕ and G^{-1} always come together and form a dimensionless combination, so it is convenient to define a dimensionless dilaton and Newton constant. In Sections 5.2–5.5, we will study the dynamical implications of action (5.14) more thoroughly.

A more detailed derivation of the theory (5.14) from the near-horizon limit of an extremal black hole can be found, e.g., in [129, 130]. Also note that this theory can be obtained by reducing some other higher-dimensional models [131, 134].

5.2 Pure two-dimensional anti-de Sitter space and its symmetries

Before discussing the Jackiw–Teitelboim theory, let us first consider pure AdS_2 space to set up the notations and reveal some useful properties of the space.

First of all, it is convenient to set the radius of the space to unity, $L = 1$, because it can be easily restored on dimensional grounds. Below, we will consider such space if it is not stated otherwise.

[23] Of course, one can also consider other theories of 2D dilaton gravity, e.g., theories with a different type of potential. A comprehensive review of such theories can be found in [131].

[24] Note that this is not the same as the flat spacetime boundary of the four-dimensional theory.

[25] In the higher dimensional case, the boundary surface has two tangent vectors, T_1^a and T_2^a, so this expression must be modified to

$$\mathcal{K} = -\frac{h_{ab}T_1^a T_2^c \nabla_c n^b}{h_{ab}T_1^a T_2^b}\,.$$

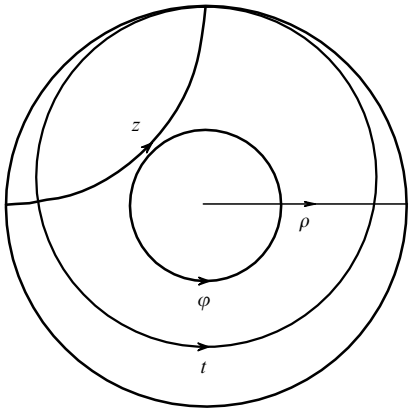

Figure 10. Curves of constants t, z, φ, and ρ. Arrows show the direction in which the complementary coordinate increases.

Second, we will work in the Euclidean signature. On the one hand, this is natural from the holographic point of view, because eventually we are interested in correlation functions of operators in the dual boundary theory (see Section 5.5). Similarly to the SYK case (see Section 4), we evaluate some types of correlation functions in the Euclidean signature and then analytically continue them to Lorentzian times (see [135] for a discussion of the analytical continuation of AdS correlation functions).

On the other hand, in the Euclidean signature, AdS_2 is just a hyperbolic disk (Lobachevsky space[26]), which is fully covered by the Poincaré and Rindler coordinates (see Fig. 10):

$$\begin{aligned} &ds^2 = \frac{dt^2 + dz^2}{z^2} \quad \text{(Poincaré)}\,, \\ &ds^2 = d\rho^2 + \sinh^2\rho\, d\varphi^2 \quad \text{(Rindler)}\,. \end{aligned} \tag{5.15}$$

One can change between these coordinates using the following identities:

$$\begin{aligned} &\tanh\frac{\rho}{2}\cos\varphi = -\frac{2t}{t^2 + (z+1)^2}\,, \\ &\tanh\frac{\rho}{2}\sin\varphi = \frac{t^2 + z^2 - 1}{t^2 + (z+1)^2}\,. \end{aligned} \tag{5.16}$$

Note that t runs from $-\infty$ to ∞ and φ runs from $-\pi$ to π (in fact, this coordinate is periodic: $\varphi \sim \varphi + 2\pi$). Also note that in the Lorentzian signature Poincaré coordinates ($ds^2 = (-d\hat{t}^2 + dz^2)/z^2$) cover only half of the spacetime, and Rindler coordinates ($ds^2 = d\rho^2 - \sinh^2\rho\, d\hat{\varphi}^2$) cover an even smaller region (see, e.g., [10, 136]).

Finally, in practice, one should cut off AdS_2 space at some curve that is close to the boundary (Fig. 11). Otherwise, the volume of the space and the length of the boundary–boundary geodesics are infinite. This cutoff corresponds to the UV cutoff in the proposed dual boundary theory. To

[26] We do not distinguish between the upper half-plane and unit disk because they can be mapped onto each other by the Möbius transformation: $w \to (iw + 1)/(w + i)$, where $w = t + iz$. The metrics on the plane and the disk are related by the same transformation. In particular, curves of constant t and z in Fig. 10 should be interpreted as the mappings of the corresponding curves on the hyperbolic plane.

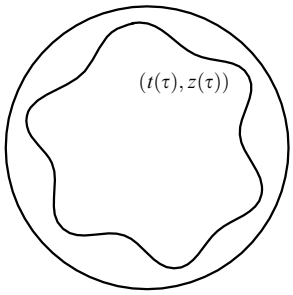

Figure 11. Cutoff of the AdS_2 space.

implement such a cutoff, we fix the boundary value of the metric,

$$ds\big|_{\text{bdy}} = \sqrt{\frac{ds^2}{d\tau^2}}\,d\tau = \sqrt{\frac{(t')^2 + (z')^2}{z^2}}\,d\tau = \frac{d\tau}{\epsilon}\,, \tag{5.17}$$

which implies that the boundary curve has large proper length,

$$S = \int ds = \int_0^\beta \frac{d\tau}{\epsilon} = \frac{\beta}{\epsilon} \to \infty\,, \tag{5.18}$$

where the time on the boundary theory runs in the interval $\tau \in [0, \beta)$ and the prime denotes the derivative over τ. The limit $S \to \infty$ corresponds to $\epsilon \to 0$. Note that in this limit coordinates of the curve are not independent:

$$\begin{aligned} &\frac{(t')^2 + (z')^2}{z^2} = \frac{1}{\epsilon^2}\,; \quad \text{hence}\,, \\ &z(\tau) = \epsilon t'(\tau) + \mathcal{O}(\epsilon^3)\,. \end{aligned} \tag{5.19}$$

Thus, the function $t(\tau)$ unambiguously determines the boundary curve.

As soon as the interior of the space is the same for all boundary curves, the geometry of the clipped space is determined by the shape of the boundary curve, i.e., by the single function $t(\tau)$. However, recall that Euclidean AdS_2 space is invariant under the transformations from the isometry group $SO(2,1) \simeq SL(2,\mathbb{R})/\mathbb{Z}_2$, i.e., under translations and rotations. Hence, the functions $t(\tau)$ and $\tilde{t}(\tau)$, which are related by such a transformation,

$$t(\tau) \to \tilde{t}(\tau) = \frac{at(\tau) + b}{ct(\tau) + d}\,, \text{ where } ad - bc = 1\,,\ a, b, c, d \in \mathbb{R}\,, \tag{5.20}$$

describe the same geometry. This statement is obvious if we rewrite the Poincaré metric in terms of complex coordinates, $w = t + iz$. The transformations that map the upper half-plane onto itself are as follows:

$$w \to \frac{aw + b}{cw + d}\,, \quad \text{where} \quad ad - bc = 1\,,\ a, b, c, d \in \mathbb{R}\,, \tag{5.21}$$

which gives (5.20) in the limit $\epsilon \to 0$.

5.3 Schwarzian theory

Let us consider the Jackiw–Teitelboim theory (5.14) on a clipped Poincaré disk and show that it effectively reduces to the one-dimensional theory with Schwarzian action. First, we

consider the bulk part of action (5.14):

$$I_{\text{bulk}} = -\frac{1}{16\pi G}\int \mathrm{d}^2x\,\sqrt{h}\,\phi(R_h+2)\,. \tag{5.22}$$

The equation of motion for the dilaton establishes the constraint $R_h + 2 = 0$, i.e., simply tells us that the metric is that of AdS_2. This is true even if we add matter fields, because they are not directly coupled to the dilaton. The equation of motion for the metric are as follows:

$$T^{\phi}_{ij} \equiv \frac{1}{8\pi G}\left(\nabla_i\nabla_j\phi - h_{ij}\nabla^2\phi + h_{ij}\phi\right) = 0\,, \tag{5.23}$$

which determines the behavior of the dilaton field:

$$\phi = \frac{a+bt+c(t^2+z^2)}{z}\,, \tag{5.24}$$

where a, b, and c are integration constants. Note that near the boundary dilaton blows up:

$$\phi\big|_{\text{bdy}} \approx \frac{1}{\epsilon}\,\frac{a+bt(\tau)+ct^2(\tau)}{t'(\tau)} \equiv \frac{\phi_{\text{r}}(\tau)}{\epsilon}\,, \tag{5.25}$$

where we have used (5.19) and for convenience defined the 'renormalized' boundary field $\phi_{\text{r}}(\tau)$. However, we assume that this large field is still smaller than the extremal value, $\phi_{\text{r}}/\epsilon \ll \Phi_0^2 \approx Q^2 l_{\text{P}}^2$, due to (5.11).

Let us now evaluate the boundary term. The tangent and normal vectors to the curve $(t(\tau), z(\tau))$ in the Poincaré metric are

$$T^a = \begin{pmatrix} t' \\ z' \end{pmatrix}, \qquad n^a = \frac{z}{\sqrt{(t')^2+(z')^2}}\begin{pmatrix} -z' \\ t' \end{pmatrix},$$

respectively. Hence, using (5.13) and (5.19), one readily obtains the trace of the extrinsic curvature:

$$\begin{aligned}\mathcal{K} &= \frac{t'(t'^2+z'^2+zz'') - zz't''}{(t'^2+z'^2)^{3/2}} \\ &= 1 + \epsilon^2\,\mathrm{Sch}\left[t(\tau),\tau\right] + \mathcal{O}(\epsilon^4)\,.\end{aligned} \tag{5.26}$$

Substituting (5.25) and (5.26) into the boundary part of action (5.14) and changing to integration over the time on the boundary, we obtain the following action:

$$\begin{aligned}I^{\text{min}}_{\text{JT}} &= 0 + I_{\text{bdy}} = -\frac{1}{8\pi G}\int_{\text{bdy}} \mathrm{d}s\,\frac{\phi_{\text{r}}(\tau)}{\epsilon}\,\mathcal{K} \\ &= -\frac{1}{8\pi G}\int_0^{\beta}\frac{\mathrm{d}\tau}{\epsilon}\,\frac{\phi_{\text{r}}(\tau)}{\epsilon}\left[1+\epsilon^2\,\mathrm{Sch}\left[t(\tau),\tau\right]+\mathcal{O}(\epsilon^4)\right].\end{aligned} \tag{5.27}$$

The divergent term (of the order of $\mathcal{O}(\epsilon^{-2})$) contributes to the ground state energy of the theory and should be treated using the holographic renormalizations [137–139]. This method as applied to two-dimensional dilaton gravity was extensively studied in [11, 140–142]. Here, we just assume that the divergent term can be omitted.[27] Thus, in the leading order in ϵ we obtain the following action:

$$I^{\text{min}}_{\text{JT}} \approx -\frac{1}{8\pi G}\int_0^{\beta}\mathrm{d}\tau\,\phi_{\text{r}}(\tau)\,\mathrm{Sch}\left[t(\tau),\tau\right]. \tag{5.28}$$

It is straightforward to check that the variation of this action over $t(\tau)$ reproduces relation (5.25).

Moreover, the time dependence of $\phi_{\text{r}}(\tau)$ can be removed by rescaling the time in the boundary theory. In order to do this, we define a new coordinate $\tilde{\tau}$, such that $\mathrm{d}\tilde{\tau} = \bar{\phi}_{\text{r}}\,\mathrm{d}\tau/\phi_{\text{r}}^2(\tau)$, where $\bar{\phi}_{\text{r}}$ is some positive dimensionless constant (let us keep in mind that we are considering a dimensionless dilaton and Newton constant), and use the composition law for the Schwarzian:[28]

$$I_{\text{bdy}} \approx -\frac{\bar{\phi}_{\text{r}}}{8\pi G}\int_0^{\tilde{\beta}}\mathrm{d}\tilde{\tau}\,\mathrm{Sch}\left[t(\tilde{\tau}),\tilde{\tau}\right]. \tag{5.29}$$

The integral of the second term, $\phi_{\text{r}}\,\mathrm{Sch}\left[\tilde{\tau},\tau\right] = -2\phi_{\text{r}}''$, is zero due to the periodicity $\phi_{\text{r}}'(\tau+\beta) = \phi_{\text{r}}'(\tau)$ (the boundary curve is smooth and closed). So, in what follows, we consider constant boundary values of the dilaton without loss of generality.

It is also convenient to change to the Rindler coordinates using the map $t(\tau) = \tan(\varphi(\tau)/2)$ which follows from the near-boundary limit $(z \to 0)$ of identities (5.16):

$$\mathrm{Sch}\left[t,\tau\right] = \mathrm{Sch}\left[\varphi,\tau\right] + \frac{(\varphi')^2}{2}\,. \tag{5.30}$$

Varying the corresponding action with respect to φ, we obtain the following equation of motion:

$$\frac{\mathrm{Sch}\left[\varphi,\tau\right]'}{\varphi'} - \varphi'' = 0\,, \tag{5.31}$$

which has a solution linear in time:

$$\varphi(\tau) = \frac{2\pi\tau}{\beta}\,. \tag{5.32}$$

We choose the coefficient of the linear dependence in such a way that the Rindler time is periodic with the period 2π: $\varphi \sim \varphi + 2\pi$. This solution can be associated with the boundary theory at the temperature β. In what follows, we will consider excitations over this solution. For convenience, we set $\beta = 2\pi$.

Note that equation (5.31) is a fourth-order nonlinear differential equation that potentially has many sophisticated solutions. We do not know all of them. As a consequence, we cannot explicitly check whether solution (5.32) is the true minimum of action (5.29) or not. However, we expect the latter to be true on physical grounds.

Finally, let us consider fluctuations of the boundary curve near the minimal solution (5.32):

$$\varphi(\tau) \approx \tau + \delta\varphi(\tau)\,. \tag{5.33}$$

As in the SYK model (see Section 4.1), we find the effective action for such fluctuations,

$$I_{\text{S}} = -\frac{\bar{\phi}_{\text{r}}}{16\pi G}\int_0^{2\pi}\mathrm{d}\tau\left[(\delta\varphi')^2 - (\delta\varphi'')^2\right] + \mathcal{O}\big(\delta\varphi^3\big)\,, \tag{5.34}$$

[27] We emphasize that the only safe way to get the correct action and observables is honest holographic renormalization, because the mentioned crude method is sometimes misleading [140, 143]. However, for theory (5.14), this crude method gives the correct result. A thorough discussion of boundary conditions, boundary counterterms, and derivation of the Schwarzian action in 2D dilaton gravity can be found in [140, 141, 144–146].

[28] $\mathrm{Sch}\left[f(g(\tau)),\tau\right] = (g')^2\,\mathrm{Sch}\left[f(g),g\right] + \mathrm{Sch}\left[g,\tau\right]$.

and estimate their correlation function (compare it with (4.21)),

$$\begin{aligned}\left\langle \delta\varphi(\tau)\delta\varphi(0)\right\rangle_{\mathrm{S}} &\approx \frac{4G}{\bar{\phi}_{\mathrm{r}}}\sum_{m\neq -1,0,1}\frac{\exp(\mathrm{i}m\tau)}{m^2(m^2-1)}\\ &= \frac{4G}{\bar{\phi}_{\mathrm{r}}}\left[-\frac{(|\tau|-\pi)^2}{2}+(|\tau|-\pi)\sin|\tau|+1+\frac{\pi^2}{6}+\frac{5}{2}\cos|\tau|\right].\end{aligned} \tag{5.35}$$

Note that we excluded the modes that correspond to translations and rotations (i.e., $\mathrm{SL}(2,\mathbb{R})$ transformations), because they are not dynamical. We will need this expression to evaluate the corrections to the correlators in the boundary theory (see Section 5.5).

5.4 Matter fields

Let us add matter fields to theory (5.14). The simplest action would be

$$I_{\mathrm{m}} = \frac{1}{2}\int \mathrm{d}^2x\,\sqrt{h}\left[h^{ab}\partial_a\xi\partial_b\xi + m^2\xi^2\right]. \tag{5.36}$$

The solution to the corresponding equation of motion, which is finite in the bulk but divergent in the limit $z\to 0$, is as follows:

$$\xi(t,z) = z^{1-\Delta}\xi_{\mathrm{r}}(t)+\ldots,\ \text{ where }\ \Delta = \frac{1}{2}+\sqrt{\frac{1}{4}+m^2}, \tag{5.37}$$

$\xi_{\mathrm{r}}(t)$ is the boundary value of the field $\xi(t,z)$; the function $\xi_{\mathrm{r}}(t)$ unambiguously determines the field $\xi(t,z)$ if it is finite in the bulk. The ellipsis denotes the subleading contribution in the limit $z\to 0$. According to the AdS/CFT prescription [147–150], the function $\xi_{\mathrm{r}}(t)$ can be interpreted as the source for the operator with the conformal dimension Δ. Hence, the effective theory for matter fields[29] which propagate in AdS_2 and satisfy boundary conditions (5.37) is as follows (for the derivation, see, e.g., [151]):

$$\begin{aligned} I_{\mathrm{m-bdy}} &= -D\int \mathrm{d}t\,\mathrm{d}t'\frac{\xi_{\mathrm{r}}(t)\xi_{\mathrm{r}}(t')}{|t-t'|^{2\Delta}},\\ \text{where}\quad D &= \frac{(\Delta-1/2)\Gamma(\Delta)}{\sqrt{\pi}\Gamma(\Delta-1/2)}. \end{aligned} \tag{5.38}$$

This action implicitly depends on the form of the boundary curve. In order to reveal this dependence, we use (5.19) and rewrite the boundary condition in terms of the time on the boundary,

$$\xi_{\mathrm{r}}(t,z)\approx z^{1-\Delta}\xi_{\mathrm{r}}(t) = \epsilon^{1-\Delta}\left[t'(\tau)\right]^{1-\Delta}\xi_{\mathrm{r}}\left[t(\tau)\right] = \epsilon^{1-\Delta}\xi_{\mathrm{r}}(\tau), \tag{5.39}$$

where we have introduced the 'renormalized' field $\xi_{\mathrm{r}}(\tau)\equiv[t'(\tau)]^{1-\Delta}\xi_{\mathrm{r}}[t(\tau)]$. Substituting this definition into action (5.38), we obtain

$$I_{\mathrm{m-bdy}} = -D\int \mathrm{d}\tau\,\mathrm{d}\tau'\left[\frac{t'(\tau)t'(\tau')}{\left(t(\tau)-t(\tau')\right)^2}\right]^{\Delta}\xi_{\mathrm{r}}(\tau)\xi_{\mathrm{r}}(\tau'). \tag{5.40}$$

[29] We recall that matter fields do not affect the constraint $R_h+2=0$ (see the beginning of Section 5.3).

Thus, in the quasiclassical limit $G\to 0$, the boundary partition function with the source $\xi_{\mathrm{r}}(\tau)$ appears as follows:

$$Z\left[\xi_{\mathrm{r}}(\tau)\right] = \exp\left(-I_0 - I_{\mathrm{Sch}} - I_{\mathrm{m-bdy}}\right), \tag{5.41}$$

where I_0 denotes the ground state free energy. This term is naively divergent (in particular, it includes the divergent term which we obtained in Section 5.3), so it should be renormalized [11, 103, 142]. However, it does not depend on the shape of the boundary, and we just omit it in what follows.

Moreover, in the limit $G\to 0$ the contribution of the matter term is negligible (at least if Δ grows more slowly than $G^{-2/3}$ (see [10, 103])), so the partition function (5.41) is saturated at the extremum of the Schwarzian action. This limit corresponds to the large N limit in the dual boundary CFT. Hence, the two-point correlation function of operators in the dual theory in the leading order is as follows:

$$\begin{aligned}\left\langle V(\tau)V(\tau')\right\rangle &= \frac{1}{Z[\xi_{\mathrm{r}}]}\frac{\partial^2 Z[\xi_{\mathrm{r}}]}{\partial\xi_{\mathrm{r}}(\tau)\partial\xi_{\mathrm{r}}(\tau')}\bigg|_{\xi_{\mathrm{r}}=0}\\ &= \left[\frac{t'(\tau)t'(\tau')}{\left(t(\tau)-t(\tau')\right)^2}\right]^{\Delta} = \frac{1}{\left\{2\sin\left[(\tau-\tau')/2\right]\right\}^{2\Delta}},\end{aligned} \tag{5.42}$$

where we substituted the saddle point solution (5.32) and set $\beta=2\pi$. Here, operator $V(\tau)$ is the conjugate to $\xi_{\mathrm{r}}(\tau)$ according to the AdS/CFT terminology. Of course, this argumentation also holds for a many-point correlation function.

There are two possible types of corrections to this expression. The first is the corrections due to interactions in the bulk, including interaction between matter fields and the backreaction to the shape of the boundary. The second one is 'quantum gravity' loop corrections due to fluctuations in $t(\tau)$ and $\xi(t,z)$ near the classical values (we recall that for finite G the right-hand side of (5.41) is the functional integral over the bulk fields). In the limit $G\to 0$, the leading corrections come from fluctuations in the boundary shape (5.33). In Section 5.5, we evaluate the contribution of such fluctuations to four-point correlation functions.

5.5 Four-point correlation function, time-ordered and out-of-time ordered correlators

Following [10, 11], in this section we evaluate the first 'quantum gravity' correction to the four-point function in the 'nearly AdS_2' theory. The calculations in this section are very similar to those that we already discussed for the SYK model in Section 4. As in the SYK model, it is convenient to define the connected part of the four-point function:

$$\begin{aligned}\mathcal{F}(\tau_1,\tau_2,\tau_3,\tau_4) &\equiv \left\langle V(\tau_1)V(\tau_2)W(\tau_3)W(\tau_4)\right\rangle\\ &\quad -\left\langle V(\tau_1)V(\tau_2)\right\rangle\left\langle W(\tau_3)W(\tau_4)\right\rangle.\end{aligned} \tag{5.43}$$

For simplicity, we consider operators V and W, which have the same conformal dimension Δ and are dual to different free fields in the bulk. First, we thus avoid cross-channels. Second, two-point correlation functions of such operators rapidly decay with evolution in the Lorentzian time: $\langle V(\tau_1+\mathrm{i}t)W(\tau_2)\rangle\sim\exp\left[(-2\pi\Delta/\beta)t\right]\approx 0$ for $t\gg\beta$ (here, we restored β in (5.42)). We will need this property to evaluate the OTOC and TOC.

Let us find the first order in G correction to the function $\mathcal{F}$. To do this, we consider small fluctuations[30] on top of the

[30] Due to action (5.34), such fluctuations are of the order of $\delta\varphi\sim\sqrt{G/\bar{\phi}_{\mathrm{r}}}$.

'classical' boundary curve,

$$t(\tau) = \tan\frac{\varphi(\tau)}{2} = \tan\frac{\tau + \delta\varphi(\tau)}{2}\,, \tag{5.44}$$

and expand the two-point function (5.42) to the third order in $\delta\varphi$:

$$\left[\frac{t'(\tau)t'(\tau')}{\big(t(\tau)-t(\tau')\big)^2}\right]^{\Delta} = \frac{1}{\big\{2\sin\big[(\tau-\tau')/2\big]\big\}^{2\Delta}} \times \big[1 + \mathcal{B}(\tau,\tau') + \mathcal{C}(\tau,\tau') + \mathcal{O}(\delta\varphi^3)\big]\,, \tag{5.45}$$

where

$$\mathcal{B}(\tau_1,\tau_2) = \Delta\left(\delta\varphi'(\tau_1) + \delta\varphi'(\tau_2) - \frac{\delta\varphi(\tau_1)-\delta\varphi(\tau_2)}{\tan(\tau_{12}/2)}\right),$$

$$\mathcal{C}(\tau_1,\tau_2) = \frac{\Delta}{\big[2\sin(\tau_{12}/2)\big]^2}\Big[(1+\Delta+\Delta\cos\tau_{12}) \times \big(\delta\varphi(\tau_1)-\delta\varphi(\tau_2)\big)^2 + 2\Delta\sin\tau_{12}\big(\delta\varphi(\tau_1)-\delta\varphi(\tau_2)\big) \times \big(\delta\varphi'(\tau_1)+\delta\varphi'(\tau_2)\big) - (\cos\tau_{12}-1) \times \Big(\Delta\big(\delta\varphi'(\tau_1)+\delta\varphi'(\tau_2)\big)^2 - \delta\varphi'^2(\tau_1) - \delta\varphi'^2(\tau_2)\Big)\Big]. \tag{5.46}$$

Here, we denoted $\tau_{12} = \tau_1 - \tau_2$. Using this expansion, we average the generating functional (5.41) over the fluctuations of the boundary shape and find the effective action:

$$\begin{aligned}
-I_{\text{eff}}[\xi_V,\xi_W] &= \log\Big\langle \exp\big(-I_{\text{m-bdy}}[\xi_V] - I_{\text{m-bdy}}[\xi_W]\big)\Big\rangle_{\text{S}} \\
&= D\int \mathrm{d}\tau_1\,\mathrm{d}\tau_2\,\Big[1 + \big\langle\mathcal{C}(\tau_1,\tau_2)\big\rangle_{\text{S}}\Big] \\
&\times \frac{\xi_V(\tau_1)\xi_V(\tau_2) + (\xi_V\leftrightarrow\xi_W)}{\big\{2\sin\big[(\tau_1-\tau_2)/2\big]\big\}^{2\Delta}} \\
&+ \frac{D^2}{2}\int \mathrm{d}\tau_1\,\mathrm{d}\tau_2\,\mathrm{d}\tau_3\,\mathrm{d}\tau_4\,\big\langle\mathcal{B}(\tau_1,\tau_2)\mathcal{B}(\tau_3,\tau_4)\big\rangle_{\text{S}} \\
&\times \frac{\xi_V(\tau_1)\xi_V(\tau_2)\xi_V(\tau_3)\xi_V(\tau_4) + (\xi_V\leftrightarrow\xi_W)}{\big\{2\sin\big[(\tau_1-\tau_2)/2\big]\big\}^{2\Delta}\big\{2\sin\big[(\tau_3-\tau_4)/2\big]\big\}^{2\Delta}} \\
&+ D^2\int \mathrm{d}\tau_1\,\mathrm{d}\tau_2\,\mathrm{d}\tau_3\,\mathrm{d}\tau_4\,\big\langle\mathcal{B}(\tau_1,\tau_2)\mathcal{B}(\tau_3,\tau_4)\big\rangle_{\text{S}} \\
&\times \frac{\xi_V(\tau_1)\xi_V(\tau_2)\xi_W(\tau_3)\xi_W(\tau_4)}{\big\{2\sin\big[(\tau_1-\tau_2)/2\big]\big\}^{2\Delta}\big\{2\sin\big[(\tau_3-\tau_4)/2\big]\big\}^{2\Delta}} + \mathcal{O}(G^2)\,,
\end{aligned} \tag{5.47}$$

where the sources ξ_V, ξ_W are dual to the operators V, W, respectively, and $\langle\ldots\rangle_{\text{S}}$ denotes averaging over the linearized Schwarzian action (5.34):

$$\langle O\rangle_{\text{S}} \equiv \frac{\int\mathcal{D}\delta\varphi\, O\exp\big(-I_{\text{Sch}}[\delta\varphi]\big)}{\int\mathcal{D}\delta\varphi\,\exp\big(-I_{\text{Sch}}[\delta\varphi]\big)}\,. \tag{5.48}$$

Note that $\langle\mathcal{B}(\tau_1,\tau_2)\rangle_{\text{S}} = 0$, because $\mathcal{B}$ is linear in $\delta\varphi$. Differentiating the effective generating functional, we find the connected four-point function:

$$\begin{aligned}
\mathcal{F}(\tau_1,\tau_2,\tau_3,\tau_4) &= \frac{\partial^4\exp\big(-I_{\text{eff}}[\xi_V,\xi_W]\big)}{\partial\xi_V(\tau_1)\partial\xi_V(\tau_2)\partial\xi_W(\tau_3)\partial\xi_W(\tau_4)}\bigg|_{\xi_V=0,\,\xi_W=0} \\
&= \frac{\big\langle\mathcal{B}(\tau_1,\tau_2)\mathcal{B}(\tau_3,\tau_4)\big\rangle_{\text{S}}}{\big\{2\sin\big[(\tau_1-\tau_2)/2\big]\big\}^{2\Delta}\big\{2\sin\big[(\tau_3-\tau_4)/2\big]\big\}^{2\Delta}}\,.
\end{aligned} \tag{5.49}$$

Thus, we need to calculate the expectation value of the product of two $\mathcal{B}$s. Using propagator (5.35) and taking into account that

$$\begin{aligned}
\big\langle\delta\varphi'(\tau_1)\delta\varphi(\tau_2)\big\rangle_{\text{S}} &= \operatorname{sgn}(\tau_1-\tau_2)\big\langle\delta\varphi(\tau_1)\delta\varphi(\tau_2)\big\rangle'_{\text{S}}\,, \\
\big\langle\delta\varphi'(\tau_1)\delta\varphi'(\tau_2)\big\rangle_{\text{S}} &= \big\langle\delta\varphi(\tau_1)\delta\varphi(\tau_2)\big\rangle''_{\text{S}}\,,
\end{aligned} \tag{5.50}$$

we find that this average significantly depends on the order of the Euclidean times due to sign factors. As in the SYK model, there are two essentially different orderings (expressions for other orderings follow from the symmetries of $\mathcal{F}$ discussed in Section 4):

$$\begin{aligned}
&\text{OPE}: \quad 2\pi > \tau_1 > \tau_2 > \tau_3 > \tau_4 > 0\,, \\
&\text{OTO}: \quad 2\pi > \tau_1 > \tau_3 > \tau_2 > \tau_4 > 0\,.
\end{aligned} \tag{5.51}$$

For the first type of ordering, the connected four-point function is as follows:

$$\frac{\mathcal{F}(\tau_1,\tau_2,\tau_3,\tau_4)}{G(\tau_1,\tau_2)G(\tau_3,\tau_4)} = \frac{16G\Delta^2}{\bar\phi_{\text{r}}}\left(\frac{\tau_{12}}{2\tan(\tau_{12}/2)} - 1\right) \times \left(\frac{\tau_{34}}{2\tan(\tau_{34}/2)} - 1\right) + \mathcal{O}(G^2)\,. \tag{5.52}$$

Here, $G(\tau_1,\tau_2)$ denotes the tree-level two-point functions (5.42) of operators V and W. For the second type of ordering, the expression for the connected four-point function is more cumbersome:

$$\begin{aligned}
\frac{\mathcal{F}(\tau_1,\tau_2,\tau_3,\tau_4)}{G(\tau_1,\tau_2)G(\tau_3,\tau_4)} &= \frac{16G\Delta^2}{\bar\phi_{\text{r}}}\left(\frac{\tau_{12}}{2\tan(\tau_{12}/2)} - 1\right) \\
&\times \left(\frac{\tau_{34}}{2\tan(\tau_{34}/2)} - 1\right) \\
&\times \frac{8\pi G\Delta^2}{\bar\phi_{\text{r}}}\left(\frac{\sin\big[(\tau_{12}+\tau_{34})/2\big] - \sin\big[(\tau_{13}+\tau_{24})/2\big]}{\sin(\tau_{12}/2)\sin(\tau_{34}/2)}\right. \\
&\left. + \frac{\tau_{23}}{\tan(\tau_{12}/2)\tan(\tau_{34}/2)}\right) + \mathcal{O}(G^2)\,.
\end{aligned} \tag{5.53}$$

In a similar way, we also find the $\mathcal{O}(G)$ correction to the two-point functions:

$$\begin{aligned}
\frac{\langle V(\tau_1)V(\tau_2)\rangle}{G(\tau_1,\tau_2)} &= 1 + \frac{G\Delta}{\bar\phi_{\text{r}}}\frac{1}{\big[\sin(\tau_{12}/2)\big]^2}\Big[2 + 4\Delta \\
&+ \tau_{12}(\tau_{12}-2\pi)(\Delta+1) + \big(\Delta\tau_{12}(\tau_{12}-2\pi) - 4\Delta - 2\big)\cos\tau_{12} \\
&+ 2(\pi-\tau_{12})(2\Delta+1)\sin\tau_{12}\Big] + \mathcal{O}(G^2)\,.
\end{aligned} \tag{5.54}$$

The corrections to the $\langle WW\rangle$ correlator are the same.

Finally, we restore β, substitute appropriate Euclidean times into correlator (5.43), and analytically continue (5.52) and (5.53) to nonzero Lorentzian times to obtain the TOC and OTOC. For the OTOC, we consider the following set of complex times:

$$\tau_1 = \frac{\beta}{4} + \mathrm{i}t\,, \quad \tau_2 = -\frac{\beta}{4} + \mathrm{i}t\,, \quad \tau_3 = 0\,, \quad \tau_4 = -\frac{\beta}{2}\,. \tag{5.55}$$

In the pure imaginary case ($t = 0$), this choice corresponds to OTO ordering, so we need to analytically continue (5.53):

$$\begin{aligned}\mathrm{OTOC}(t) &\equiv \mathrm{tr}\left[\rho^{1/4}V(t)\rho^{1/4}W(0)\rho^{1/4}V(t)\rho^{1/4}W(0)\right]\\ &= \mathcal{F}\left(\frac{\beta}{4}+\mathrm{i}t,\,-\frac{\beta}{4}+\mathrm{i}t,\,0,\,-\frac{\beta}{2}\right)\\ &+\left\langle V\left(\frac{\beta}{2}\right)V(0)\right\rangle\left\langle W\left(\frac{\beta}{2}\right)W(0)\right\rangle\\ &\approx\left(\frac{\pi}{\beta}\right)^{4\Delta}\left[1-2\Delta^2\,\frac{\beta G}{\bar{\phi}_\mathrm{r}}\exp\left(\frac{2\pi t}{\beta}\right)\right]\ \text{for}\ \ \beta\ll t\ll\beta\log\frac{\bar{\phi}_\mathrm{r}}{\beta G}\,.\end{aligned}\tag{5.56}$$

Here, ρ denotes the density matrix in the corresponding boundary CFT. Note that we disregard the $\mathcal{O}(G)$ contributions from (5.53) and (5.54) which do not grow with t. It is required that $t\gg\beta$ to rule out possible contributions from 'mixed' correlators of the form $\langle VW\rangle$, which decay at such times. Also note that the Gaussian approximation that we used to obtain this result works well only for relatively small times, i.e., until the decay of the OTOC is saturated. For larger times, this correlator should be calculated more carefully.

For the TOC, we consider a different set of times,

$$\tau_1=\frac{\beta}{2}+\mathrm{i}t\,,\quad \tau_2=\mathrm{i}t\,,\quad \tau_3=0\,,\quad \tau_4=-\frac{\beta}{2}\,,\tag{5.57}$$

which corresponds to OPE ordering at the beginning of the Lorentzian time evolution, $t=0$. Thus, we analytically continue correlator (5.52) and obtain the following expression:

$$\begin{aligned}\mathrm{TOC}(t) &\equiv \mathrm{tr}\left[V(t)\rho^{1/2}V(t)W(0)\rho^{1/2}W(0)\right]\\ &\approx\left(\frac{\pi}{\beta}\right)^{4\Delta}\left[1+\mathrm{const}\,\frac{G}{\bar{\phi}_\mathrm{r}}\right],\end{aligned}\tag{5.58}$$

which weakly deviates from the tree-level value even for large evolution times.

6. Examples of chaotic behavior (in lieu of a conclusion)

Instead of a conclusion, let us briefly review the most notable examples of chaotic systems, i.e., models with exponentially growing $C(t)$ commutators and rapidly decaying OTOCs. All these models are considered in the quasiclassical limit (large N or small G limit) and somehow model all-to-all couplings; furthermore, only small fluctuations above the equilibrium state are usually considered, so calculations of the correlation functions are similar in all cases. In particular, in these models the leading contribution to the OTOC is ensured by ladder diagrams.

6.1 Sachdev–Ye–Kitaev model/ two-dimensional dilaton gravity

First of all, let us briefly recall the main properties of the SYK model. This is a quantum mechanical model of $N\gg 1$ Majorana fermions with all-to-all couplings J_{ijkl} which are distributed randomly and independently, i.e., according to a Gaussian distribution with an average square $\overline{J_{ijkl}^2}=3!J^2/N^3$ (no sum assumed). Such a choice of couplings allows introducing a kind of $1/N$ expansion for the disorder averaged correlation functions. Notably, disorder averaged corrections to two-point and four-point functions are determined by so-called 'melonic' (see Fig. 1) and 'ladder' (see Fig. 7) diagrams.

Using such diagrammatics, one finds that in the limit $1\ll\beta J\ll N$, which corresponds to small but nonzero temperature ($T=1/\beta$), the exact two-point correlation function exponentially decays in Lorentzian time:

$$\begin{aligned}&G_\mathrm{c}^\beta(t)\approx\frac{\pi^{1/4}}{\sqrt{2\beta J}}\,\frac{\operatorname{sgn}t}{\left|\sinh\left(\pi t/\beta\right)\right|^{1/2}}\sim\exp\left(-\frac{t}{t_\mathrm{d}}\right)\\ &\text{for}\quad t\gg t_\mathrm{d}=\frac{2\beta}{\pi}\,,\end{aligned}\tag{6.1}$$

the time-ordered correlator is approximately equal to the product of two-point functions:

$$\mathrm{TOC}(t)\approx G_\mathrm{c}^\beta\left(-\frac{\mathrm{i}\beta}{2}\right)G_\mathrm{c}^\beta\left(-\frac{\mathrm{i}\beta}{2}\right)\approx\frac{\sqrt{\pi}}{2\beta J}\quad\text{for}\quad t\gg t_\mathrm{d}\,,\tag{6.2}$$

and the out-of-time-ordered correlator is rapidly saturated:

$$\begin{aligned}&\mathrm{OTOC}(t)\approx\frac{\sqrt{\pi}}{2\beta J}\left[1-\frac{\Delta^2}{2C}\,\frac{\beta J}{N}\exp\left(\kappa t\right)\right]\\ &\text{for}\quad t_\mathrm{d}\ll t\ll t_*=\beta\log\frac{N}{\beta J}\,,\end{aligned}\tag{6.3}$$

where C is some positive numerical constant, $\Delta=1/4$ is the effective conformal dimension of fermions, and $\kappa\approx(2\pi/\beta)(1-6.05/(\beta J)+\ldots)$ is the Lyapunov exponent. Thus, the expectation value of the square of the commutator grows exponentially:

$$\begin{aligned}C(t)&=2\,\mathrm{TOC}(t)-\mathrm{OTOC}\left(t-\frac{\mathrm{i}\beta}{4}\right)-\mathrm{OTOC}\left(t+\frac{\mathrm{i}\beta}{4}\right)\\ &\approx\frac{\mathrm{const}}{N}\,2\cos\left(\frac{\beta\kappa}{4}\right)\exp\left(\kappa t\right)\approx\frac{\mathrm{const}}{N}\,\frac{6\pi}{\beta J}\exp\left(\kappa t\right).\end{aligned}\tag{6.4}$$

Note that the prefactor of the growing exponent is nonzero, because κ is not exactly equal to the maximal value $2\pi/\beta$.

One can find the detailed derivation of these identities in Sections 3 and 4 of the present paper, papers [4–8, 103, 104], and talks [1].

It is worth stressing that a pure boson analog of the SYK model,

$$I=\int\mathrm{d}\tau\left[\frac{1}{2}\sum_{i=1}^{N}\left(\frac{\mathrm{d}\phi^i}{\mathrm{d}\tau}\right)^2+\sum_{i,\,j,\,k,\,l=1}^{N}J_{ijkl}\,\phi^i\phi^j\phi^k\phi^l\right],\tag{6.5}$$

is not self-consistent; in particular, it has no reasonable exact solution [79]. At the same time, supersymmetric analogs of the SYK model are well defined [79, 80].

The SYK model is also closely related to Jackiw–Teitelboim (JT) gravity, i.e., two-dimensional 'near-AdS_2' gravity with a dilaton [10–12]. It can be shown that this theory is effectively one-dimensional, since its dynamics is determined by the shape of the boundary curve. Furthermore, in the IR limit, the effective action of this theory exactly coincides with the effective action of the SYK model. In both cases, this action appears due to the symmetry with respect to $\mathrm{SL}(2,\mathbb{R})$ transformations. Therefore, it is not surprising that in the semiclassical limit the behavior of correlation functions in JT gravity is similar to that of corresponding quantities in the SYK model:

$$G(t)\approx\left(\frac{\pi}{\beta\sinh\left(\pi t/\beta\right)}\right)^{2\Delta}\sim\exp\left(-\frac{t}{t_\mathrm{d}}\right)\quad\text{for}\quad t\gg t_\mathrm{d}=\frac{\beta}{2\pi\Delta}\,,\tag{6.6}$$

$$\mathrm{TOC}(t) \approx \left(\frac{\pi}{\beta}\right)^{4\Delta} \quad \text{for} \quad t \gg t_{\mathrm{d}}\,, \tag{6.7}$$

$$\mathrm{OTOC}(t) \approx \left(\frac{\pi}{\beta}\right)^{4\Delta}\left[1 - 2\Delta^2\frac{\beta G}{\bar{\phi}_{\mathrm{r}}}\exp(\kappa t)\right] \quad \text{for} \quad t_{\mathrm{d}} \ll t \ll t_* = \beta\log\frac{\bar{\phi}_{\mathrm{r}}}{\beta G}\,, \tag{6.8}$$

where Δ is the conformal dimension of operators dual to free matter fields in the bulk, G is a two-dimensional Newton constant, $\bar{\phi}_{\mathrm{r}}$ is the boundary value of the dilaton, and $\kappa \approx 2\pi/\beta$ is the Lyapunov exponent.

Details regarding the derivation of the correlation functions and other properties of two-dimensional dilaton gravity can be found in Section 5, papers [10–13, 103], and talks [1].

Note that JT gravity can be derived as a near-horizon limit of an extremal black hole [139, 134], and AdS_2 space exhibits the same causal properties as higher-dimensional AdS black holes. This opens the way to use JT gravity and the SYK model as toy models of many complex black hole phenomena, e.g., as toy models of a traversable wormhole [17–20].

However, it is worth stressing that JT gravity incorporates only the lowest-energy features of the SYK model (which are described by the Schwarzian action) and, hence, cannot be considered a complete gravity dual of this model. Moreover, at the present moment, such a dual is far from known. The main problem is that the complete gravity dual should reproduce the nonlocal action (3.46) that describes the dynamics of the bilinear fields G and Σ. This requires coupling the theory to an infinite number of massive bulk fields (each with $\mathcal{O}(1)$ mass), but it is not known how to do this. A more detailed discussion of the putative SYK gravity dual can be found in [103, 122, 123].

6.2 Generalizations of the Sachdev–Ye–Kitaev model

All the remarkable properties of the SYK model, including solvability in the large N limit, the emergence of conformal symmetry in the IR limit, and saturation of the 'bound on chaos,' are based on the averaging of correlation functions over the quenched disorder, i.e., over random implementations of coupling constants. This means that the SYK model is not really a quantum mechanical model; in particular, one cannot find a unitary operator that generates time evolution in this model. Thus, generalizations of the SYK model, which mimic it in the large N limit without quench disorder, are of great interest. Here, we present three examples of such models.

The first example is the Gurau–Witten model proposed in [106, 107]:

$$I_{\mathrm{GW}} = \int_0^\beta \mathrm{d}\tau\left[\frac{1}{2}\sum_{c=0}^{3}\left(\sum_{\mathbf{a}^c}\chi^c_{\mathbf{a}^c}\,\frac{\mathrm{d}}{\mathrm{d}\tau}\,\chi^c_{\mathbf{a}^c}\right) + \frac{J}{N^{3/2}}\sum_{\mathbf{a}^0\mathbf{a}^1\mathbf{a}^2\mathbf{a}^3}\chi^0_{\mathbf{a}^0}\chi^1_{\mathbf{a}^1}\chi^2_{\mathbf{a}^2}\chi^3_{\mathbf{a}^3}\prod_{c_1<c_2}\delta_{a^{c_1c_2}a^{c_2c_1}}\right], \tag{6.9}$$

where χ^c are real fermionic fields and τ is Euclidean time. For every color c, the field χ^c lives in a vector representation of $\mathrm{O}(N^3)$, i.e., it is a rank-three tensor with indices $\mathbf{a}^c = \{a^{cd}, d \neq c\}$, each of which runs in the range $1,\ldots,N$. The full symmetry group of the model is $\mathrm{O}(N^6)$. For simplicity, we present only the model with a four-fermion vertex; general expressions can be found in [106, 107].

The second example is the uncolored fermionic tensor model, or Klebanov–Tarnopolsky model [108–110]:

$$I_{\mathrm{KT}} = \int_0^\beta \mathrm{d}\tau\left[\frac{\mathrm{i}}{2}\sum_{abc}\chi^{abc}\,\frac{\mathrm{d}\chi^{abc}}{\mathrm{d}\tau} - \frac{g}{4}\sum_{a_1a_2b_1b_2c_1c_2}\chi^{a_1b_1c_1}\chi^{a_1b_2c_2}\chi^{a_2b_1c_2}\chi^{a_2b_2c_1}\right], \tag{6.10}$$

where χ^{abc} is a rank-three fermionic tensor, and indices a, b, c are indistinguishable and run in the range $1,\ldots,N$. The full symmetry group of the model is $\mathrm{O}(N^3)$.

The third example (Nishinaka–Terashima model [111]) mimics the SYK model by replacing random couplings J_{ijkl} with a light bosonic tensor field:

$$I_{\mathrm{NT}} = \int_0^\beta \mathrm{d}\tau\sum_{i<j<k<l}\frac{1}{2\epsilon}\left[\left(\frac{\mathrm{d}\phi_{ijkl}}{\mathrm{d}\tau}\right)^2 + m^2(\phi_{ijkl})^2\right] + I_{\mathrm{SYK}}\,, \tag{6.11}$$

where $\epsilon = (3!/\pi)(mJ^2/N^3)$, $m\beta \ll 1$, and I_{SYK} is the standard SYK action (3.1) with $J_{ijkl} = \phi_{ijkl}$.

We will not review models (6.9)–(6.11) in detail; the only important point for us is that they reproduce the SYK diagrammatics in the large N limit. Therefore, one can expect that these models are described by the same effective action and have the same properties as the original SYK model. The derivation of this and other remarkable properties of SYK-like tensor models can be found in [106–111, 152–164].

The other notable extension of the SYK model is the complex SYK model (CSYK) [23, 165, 166]:

$$I_{\mathrm{CSYK}} = \int_0^\beta \mathrm{d}\tau\left[\sum_{i=1}^{N}\chi_i^\dagger(\tau)\dot{\chi}_i(\tau) - \sum_{j_1<j_2,\,k_1<k_2}J_{j_1j_2,k_1k_2}\mathcal{A}\{\chi^\dagger_{j_1}\chi^\dagger_{j_2}\chi_{k_1}\chi_{k_2}\}\right], \tag{6.12}$$

where $\mathcal{A}\{\ldots\}$ denotes the antisymmetrized product of operators, and randomly distributed couplings $J_{j_1j_2,k_1k_2}$ have a zero mean and variance

$$\overline{|J_{j_1j_2,k_1k_2}|^2} = \frac{2J^2}{N^3}\,.$$

This theory has both $\mathrm{SL}(2,\mathbb{R})$ and $\mathrm{U}(1)$ symmetries. Similarly to its pure real predecessor, in the IR limit the CSYK model is described by the Schwarzian action with an additional term corresponding to the $\mathrm{U}(1)$ mode. A thorough discussion of the CSYK model and its applications can be found in [23, 165–167].

6.3 Two-dimensional conformal field theory with large central charge/shock waves in three-dimensional anti-de Sitter space

BTZ black hole and 2D CFT with a large central charge were among the first systems where OTOCs were calculated [26, 35, 74–76]. Let us briefly review the main ideas of this calculation.

First of all, in Section 2.2, we noticed that the OTOC of local operators V and W can be represented as a two-sided correlation function in a perturbed thermofield double state (see formulas (2.20) and (2.21)). If the left and right systems are CFTs with AdS duals, then the pure state (2.18) is dual to an eternal AdS Schwarzschild black hole with inverse

temperature β [168]. In particular, if both systems are 2D CFTs, $|\mathrm{TFD}\rangle$ describes a BTZ black hole.

In this picture, operator $V_L(t)$ acting on the pure $|\mathrm{TFD}\rangle$ is dual to a particle injected near the left boundary at moment t in the past. According to holographic terminology [147–150], the mass of the particle is $m_V = \Delta_V/(2L)$, where L is the radius of AdS space and Δ_V is the conformal dimension of V (we assume that $\Delta_V \gg 1$). In general, such a perturbation distorts the geometry of the space. Hence, one needs to estimate this distortion in order to evaluate the two-sided correlator and OTOC.

Without going into detail, we discover that the distorted geometry is described by a so-called shock wave [26, 75, 169]. In a nutshell, this solution is obtained by gluing the metrics of the initial black hole (of mass M) and the black hole that swallowed the injected particle (of mass $M + m_V$) in such a way that the time at the boundary flows continuously and the radius of the unit circle is continuous across the glued surface. For small masses of the injected particle, $m_V \ll M$, the metric of the shock wave is as follows:

$$\begin{aligned} \mathrm{d}s^2 = &-\frac{4L^2}{(1+UV)^2}\,\mathrm{d}U\,\mathrm{d}V + R^2\left(\frac{1-UV}{1+UV}\right)^2\mathrm{d}\phi^2 \\ &+\frac{4L^2}{(1+UV)^2}\,\frac{m_V}{4M}\exp\left(\frac{Rt}{L^2}\right)\delta(U)\,\mathrm{d}U^2\,, \end{aligned} \tag{6.13}$$

where $U = u$, $V = v + m_V/(4M)\exp(Rt/L^2)\theta(u)$, u and v are standard Kruskal coordinates, and R is the radius of the black hole. In this metric, the geodesic distance between two points close to the left and right boundaries is

$$\begin{aligned} \frac{d}{L} \approx 2\log\frac{2r}{R} + 2\log\Bigg[&\cosh\frac{R(t_\mathrm{R}-t_\mathrm{L})}{2L^2} \\ &+\frac{m_V}{8M}\exp\left(\frac{Rt}{L^2}-\frac{R(t_\mathrm{R}+t_\mathrm{L})}{2L^2}\right)\Bigg]\,, \end{aligned} \tag{6.14}$$

where $t_\mathrm{L}, t_\mathrm{R}$ are time coordinates and r is the radial coordinate of the left and right end points of the geodesic. For simplicity, we assume that the angular coordinates of the end points coincide. Subtracting the divergent contribution and setting $t_\mathrm{L} = t_\mathrm{R} = 0$, we obtain the following two-sided correlation function in the semiclassical limit ($G \to 0$):

$$\begin{aligned} &\mathrm{OTOC}(t) \approx \left\langle \mathrm{TFD}\middle| V_\mathrm{L}^\dagger(t) W_\mathrm{L}(0) W_\mathrm{R}(0) V_\mathrm{L}(t)\middle|\mathrm{TFD}\right\rangle \\ &\quad\sim \exp(-m_W d) \sim \left[1+\frac{m_V}{8M}\exp\left(\frac{Rt}{L^2}\right)\right]^{-2Lm_W} \\ &\quad\sim \left[1+C_1\,\frac{m_V L}{S}\exp\left(\frac{2\pi t}{\beta}\right)\right]^{-2Lm_W} \\ &\text{for}\quad t \ll t_* = \frac{\beta}{2\pi}\log S\,, \end{aligned} \tag{6.15}$$

where $m_W = \Delta_W/(2L)$, $\Delta_W \gg 1$ is the conformal dimension of W, and C_1 is a positive numerical constant. Here, we have used identities for the temperature $\beta = 2\pi L^2/R$, mass $M = R^2/(8GL^2)$, and entropy $S = \pi R/(2G)$ of a BTZ black hole. We also assumed that the black hole is large, $R \sim L$, so that $S \sim R^2/(GL)$ and $C_1 = \mathcal{O}(1)$. A detailed derivation of (6.15) and related discussions can be found in [26, 74, 76].

Finally, under these assumptions, one can obtain the correlation function in the boundary CFT with large central charge $c = 3L/(2G)$:

$$\begin{aligned} &\mathrm{OTOC}(t) \sim \left[1 + C_2\,\frac{\Delta_V}{c}\exp\left(\frac{2\pi t}{\beta}\right)\right]^{-\Delta_W} \\ &\text{for}\quad t \ll t_* \sim \frac{\beta}{2\pi}\log c\,, \end{aligned} \tag{6.16}$$

where C_2 is another positive $\mathcal{O}(1)$ numerical constant. One can also obtain this answer without holography, considering different analytical continuations of the Euclidean four-point function and using the Virasoro conformal block of the identity operator [35, 77, 78].

Note that both black hole entropy and central charge measure the number of degrees of freedom of the corresponding systems; hence, for both (6.15) and (6.16) scrambling time $t_* \sim \beta\log N$. This saturates the bound of the fast scrambling conjecture. The Lyapunov exponent $\kappa = 2\pi/\beta$ also saturates the corresponding bound. However, let us keep in mind that (6.15) reproduces only the leading contribution in the limit $G \to 0$, while the complete answer must capture quantum corrections too. As was shown in [76], such corrections increase the scrambling time and reduce the growth rate of OTOCs.

6.4 Hermitian matrix model with quartic interaction in the limit of a large number of degrees of freedom

A remarkable example of a chaotic, but not maximally chaotic, model is the large N matrix scalar quantum field theory with quartic self-interaction which was considered in [83]:

$$I = \int \mathrm{d}^4x\,\frac{1}{2}\,\mathrm{tr}\left[(\partial_\mu\Phi)^2 - m^2\Phi^2 - g^2\Phi^4\right], \tag{6.17}$$

where Φ is a Hermitian $N \times N$ matrix, $N \gg 1$. The 't Hooft coupling is $\lambda = g^2N \ll 1$. Summing the leading contributions in the limit $N \to \infty$, $g \to 0$, $\lambda = \mathrm{const}$ and taking the integral over the spatial coordinates, one obtains an integro-differential equation for the averaged square of the commutator:

$$\frac{\mathrm{d}C(t)}{\mathrm{d}t} = M \circ C(t)\,, \tag{6.18}$$

where M is some integral operator specified in [83], and

$$\begin{aligned} C(t) = \frac{1}{N^4}\sum_{abcd}\int \mathrm{d}^3\mathbf{x}\;\mathrm{tr}\Big(&\rho^{1/2}\left[\Phi_{ab}(\mathbf{x}), \Phi_{cd}(0)\right] \\ &\times \rho^{1/2}\left[\Phi_{ab}(\mathbf{x}), \Phi_{cd}(0)\right]\Big)\,. \end{aligned} \tag{6.19}$$

As in the conformal part of the SYK four-point function (see Section 4.2), the leading contribution to (6.19) is provided by ladder diagrams, with operator M adding an extra rung to the ladder. The largest eigenvalue of Eqn (6.18) is nothing but the Lyapunov exponent κ, which determines the growth rate of $C(t) \sim \exp(\kappa t)$. Numerically diagonalizing (6.18), one can show that for small inverse temperatures, $m\beta \ll 1$, the exponent is as follows:

$$\kappa \approx 0.025\,\frac{\lambda^2}{\beta^2 m}\,. \tag{6.20}$$

In the case of zero bare mass, $m = 0$, one should substitute into (6.20) the thermal mass $m_\mathrm{th}^2 = 2\lambda/(3\beta^2)$ which is

generated by one-loop corrections to two-point functions:

$$\kappa \approx 0.025\,\frac{\lambda^2}{\beta^2 m_{\rm th}} \approx 0.031\,\frac{\lambda^{3/2}}{\beta}\,. \tag{6.21}$$

There is also another way to find Lyapunov exponent (6.20), which relies on an analogy between epidemic growth and scrambling. Let us consider the theory (6.17) as a gas of N^2 interacting particles. The one-particle distribution function $f(t,\mathbf{p})$ of this gas satisfies (in the leading order) the linearized Boltzmann equation,

$$\frac{\partial f(t,\mathbf{p})}{\partial t} = \int \frac{\mathrm{d}^3\mathbf{q}}{(2\pi)^3}\,\frac{1}{2E_{\mathbf{q}}}\left[R^{\wedge}(\mathbf{p},\mathbf{q}) - R^{\vee}(\mathbf{p},\mathbf{q})\right] f(t,\mathbf{q})\,, \tag{6.22}$$

where $E_{\mathbf{p}} = \sqrt{m^2+\mathbf{p}^2}$, $\mathbf{p}$ is three-dimensional momentum, and functions $R^{\wedge}(\mathbf{p},\mathbf{q})$ and $R^{\vee}(\mathbf{p},\mathbf{q})$ measure the increase and decrease in the particle density in the phase space cell $\mathbf{p}$ associated with the phase space cell $\mathbf{q}$. Note that the loss of particles is caused by two distinct processes: annihilation and outflow of particles to other cells. These processes are described by functions $2\Gamma_{\mathbf{p}}\delta(\mathbf{p}-\mathbf{q})$ and $R^{\vee}(\mathbf{p},\mathbf{q}) - 2\Gamma_{\mathbf{p}}\delta(\mathbf{p}-\mathbf{q})$, respectively. The gain is only due to the inflow from other cells. For simplicity, we assume that the system is spatially homogeneous.

Now, let us use this qualitative model to estimate how quickly a local perturbation spreads throughout the system (i.e., estimate how quickly the system scrambles). Imagine that we injected into the system a contagious particle which infects other particles when they collide. In the early stages of the epidemic, the rate of its growth is determined by the gross flow passing through the phase space cell, i.e., by the sum of inflow and outflow:

$$\frac{\partial}{\partial t}\,f_{\rm OTOC}(t,\mathbf{p}) = \int \frac{\mathrm{d}^3\mathbf{q}}{(2\pi)^3}\,\frac{1}{2E_{\mathbf{q}}}\,\frac{\sinh\left(\beta E_{\mathbf{q}}/2\right)}{\sinh\left(\beta E_{\mathbf{p}}/2\right)}$$

$$\times\left[R^{\wedge}(\mathbf{p},\mathbf{q}) + R^{\vee}(\mathbf{p},\mathbf{q}) - 4\Gamma_{\mathbf{p}}\delta(\mathbf{p}-\mathbf{q})\right] f_{\rm OTOC}(t,\mathbf{q})\,. \tag{6.23}$$

To obtain this equation, we changed the sign of the outflow term in (6.22) and divided the function $f(t,\mathbf{p})$ by $\sinh\left(\beta E_{\mathbf{p}}/2\right)$. The function $f_{\rm OTOC}(t,\mathbf{p})$ measures the infected particle density. If this qualitative picture is applicable to system (6.17) and infected particles are analogs of particles affected by a perturbation, then the epidemic growth is equivalent to scrambling. Hence, one expects that the growth rate of $f_{\rm OTOC}(t,\mathbf{p})$ coincides with the growth rate of $C(t)$.

Indeed, it was shown in [84, 170] that equation (6.23) can be deduced from the IR limit of the Bethe–Salpeter equation for the OTOC (in this limit, Bethe–Salpeter equations decouple). Therefore, one can evaluate the Lyapunov exponent by diagonalizing (6.23) instead of (6.18). In particular, this method reproduces result (6.20) in the limit $N \gg 1$, $m\beta \ll 1$. Of course, this approach can also be applied to other weakly coupled systems.

Acknowledgements

The author would like to thank F K Popov, A Milekhin, A Yu Morozov, V A Rubakov, P I Arseev, V V Losyakov, U Moschella, A S Gorsky, A Dymarsky, D Grumiller, D A Galante, L A Akopyan, E N Lanina, R O Sharipov, and E S Trunina for their useful comments and discussions. I would especially like to thank E T Akhmedov for sharing his ideas and support throughout the work. I would also like to thank Hermann Nicolai and Stefan Theisen for their hospitality at the Albert Einstein Institute, Golm, where the work on this project was partly done. This study was supported by a grant from the Foundation for the Advancement of Theoretical Physics and Mathematics, BASIS.

7. Appendices

A. One-dimensional Majorana fermions

Let us consider representations of one-dimensional Majorana fermions [1, 103, 171, 172]:

$$\{\chi_i,\chi_j\} = \delta_{ij}, \quad i,j = 1,\ldots,N\,, \tag{A.1}$$

where $\chi_i = \chi_i^{\dagger}$. For convenience, we restrict ourselves to the even number[31] $N = 2K$. In this case, we can combine even and odd operators into non-Hermitian ones,

$$c_i = \frac{1}{\sqrt{2}}\left(\chi_{2i} - \mathrm{i}\chi_{2i+1}\right), \quad c_i^{\dagger} = \frac{1}{\sqrt{2}}\left(\chi_{2i} + \mathrm{i}\chi_{2i+1}\right), \quad i = 1,\ldots,K\,, \tag{A.2}$$

which obey the standard anticommutation relations as a corollary of (A.1):

$$\{c_i,c_j\} = \{c_i^{\dagger},c_j^{\dagger}\} = 0\,, \quad \{c_i,c_j^{\dagger}\} = \delta_{ij}\,. \tag{A.3}$$

In fact, they are the creation and annihilation operators of the fermion field. Hence, we can build the standard representation for the fermionic modes using these operators. Namely, we define the vacuum state as the state that is annihilated by all annihilation operators, $c_i|0\rangle = 0$, and build k-particle states using creation operators: $(c_1^{\dagger})^{n_1},\ldots,(c_K^{\dagger})^{n_K}|0\rangle$, where $n_i = 0,\ 1$, and $n_1 + \ldots + n_K = k$. There are 2^K such states. Moreover, we can also build an explicit representation for these operators using $2^K \times 2^K$ matrices [103], but we do not need it in what follows.

Let us calculate finite-temperature two-point correlation functions using this representation. We recall that in the free theory (3.1), $J_{ijkl} = 0$, the Hamiltonian is identically zero, so we rewrite the thermal average as follows:

$$\left\langle \mathcal{T}\chi_i(\tau)\chi_j(0)\right\rangle_{\beta} = \frac{\mathrm{tr}\left[\mathcal{T}\exp\left(-\beta H_0\right)\chi_i(\tau)\chi_j(0)\right]}{\mathrm{tr}\left[\exp\left(-\beta H_0\right)\right]}$$

$$= \frac{\mathrm{tr}\left[\mathcal{T}\chi_i(\tau)\chi_j(0)\right]}{\mathrm{tr}\left[1\right]} = \theta(\tau)\,\frac{\mathrm{tr}\left[\chi_i\chi_j\right]}{\mathrm{tr}\left[1\right]} + \theta(-\tau)\,\frac{\mathrm{tr}\left[\chi_j\chi_i\right]}{\mathrm{tr}\left[1\right]}\,, \tag{A.4}$$

where the trace denotes summation over all possible quantum states. The last identity is valid for $\tau \in [-\beta/2,\beta/2)$; for other times, we use the antiperiodicity of the propagator under the change $\tau \to \tau+\beta$ to restore the correct answer. Obviously, the average (A.4) equals zero if $|i-j| > 1$, because in this case it contains averages of different creation and annihilation operators which anticommute with each other (e.g., $\langle c_1 c_2\rangle_{\beta}$ or $\langle c_1 c_2^{\dagger}\rangle_{\beta}$). The case $|i-j| \leqslant 1$ is more subtle. Let us separately consider four averages that correspond to this case:

$$\mathrm{tr}\left[\chi_{2i}\chi_{2i}\right] = \frac{1}{2}\,\mathrm{tr}\left[c_i c_i^{\dagger} + c_i^{\dagger}c_i\right]$$

$$= \frac{1}{2}\,2^{K-1}\left[\langle 0|c_i c_i^{\dagger} + c_i^{\dagger}c_i|0\rangle + \langle 1_i|c_i c_i^{\dagger} + c_i^{\dagger}c_i|1_i\rangle\right] = 2^{K-1}, \tag{A.5}$$

[31] As was shown in [120, 173], the spectrum of the SYK model is different for different $N \bmod 8$, but we will not discuss this point here.

$$\operatorname{tr}[\chi_{2i+1}\chi_{2i+1}] = \frac{1}{2}\operatorname{tr}\left[c_i c_i^\dagger + c_i^\dagger c_i\right] \tag{A.6}$$
$$= \frac{1}{2}2^{K-1}\left[\langle 0|c_i c_i^\dagger + c_i^\dagger c_i|0\rangle + \langle 1_i|c_i c_i^\dagger + c_i^\dagger c_i|1_i\rangle\right] = 2^{K-1},$$

$$\operatorname{tr}[\chi_{2i}\chi_{2i+1}] = \frac{\mathrm{i}}{2}\operatorname{tr}\left[c_i c_i^\dagger - c_i^\dagger c_i\right] \tag{A.7}$$
$$= \frac{i}{2}2^{K-1}\left[\langle 0|c_i c_i^\dagger - c_i^\dagger c_i|0\rangle + \langle 1_i|c_i c_i^\dagger - c_i^\dagger c_i|1_i\rangle\right] = 0,$$

$$\operatorname{tr}[\chi_{2i+1}\chi_{2i}] = \frac{\mathrm{i}}{2}\operatorname{tr}\left[c_i^\dagger c_i - c_i c_i^\dagger\right] \tag{A.8}$$
$$= \frac{i}{2}2^{K-1}\left[\langle 0|c_i^\dagger c_i - c_i c_i^\dagger|0\rangle + \langle 1_i|c_i^\dagger c_i - c_i c_i^\dagger|1_i\rangle\right] = 0,$$

where we denoted $|1_i\rangle \equiv c_i^\dagger|0\rangle$ and used relations (A.2). It is now easy to find the free Wightman function:

$$\langle\chi_i\chi_j\rangle_\beta = \frac{\operatorname{tr}[\chi_i\chi_j]}{\operatorname{tr}[1]} = \frac{1}{2}\delta_{ij}. \tag{A.9}$$

Taking the formal limit $\beta\to\infty$, we find the free zero-temperature Feynman propagator:

$$\left\langle\mathcal{T}\chi_i(\tau)\chi_j(0)\right\rangle = \frac{1}{2}\operatorname{sgn}\tau\,\delta_{ij}. \tag{A.10}$$

This expression is also valid for the finite-temperature Feynman propagator for $\tau\in[-\beta/2,\beta/2)$. At the same time, the propagator is antiperiodic under the change $\tau\to\tau+\beta$, which allows the finite-temperature correlation function to be restored for all Euclidean τ:

$$\left\langle\mathcal{T}\chi_i(\tau)\chi_j(0)\right\rangle = \frac{1}{2}\operatorname{sgn}\left(\sin\frac{\pi\tau}{\beta}\right)\delta_{ij}. \tag{A.11}$$

Finally, Wick's theorem can be proven for n-point correlation functions using representation (A.2) and a standard textbook argumentation [112, 174]. However, note that for a non-equilibrium initial state this theorem does not work (see, e.g., [175]). This is a peculiarity of the $(0+1)$-dimensional quantum field theory.

B. Functional integral over Majorana fermions

Different one-dimensional Majorana fermions anticommute, but the square of the single fermion is not zero (see relations (3.2)). Hence, these fermions cannot be described by either normal or Grassmann numbers. This means that a naive definition of the functional integral over Majorana fermions (e.g., Eqn (3.38)) is unclear: how can one integrate over the variables χ_i if one does not even know what algebra they obey?

However, in Appendix A, we showed that the set of $N=2K$ one-dimensional Majorana fermions can be rewritten in terms of ordinary Dirac fermions:

$$\chi_{2i} = \frac{1}{\sqrt{2}}\left(\psi_i+\bar\psi_i\right),\quad \chi_{2i+1} = \frac{\mathrm{i}}{\sqrt{2}}\left(\psi_i-\bar\psi_i\right),\quad i=1,\ldots,K, \tag{B.1}$$

which become Grassmanian upon quantization (A.3). Therefore, the measure of the integration can be defined as

$$\mathcal{D}\chi_{2i}\mathcal{D}\chi_{2i+1} = \left|\frac{\partial(\chi_{2i},\chi_{2i+1})}{\partial(\psi_i,\bar\psi_i)}\right|\mathcal{D}\psi_i\mathcal{D}\bar\psi_i = \mathcal{D}\psi_i\mathcal{D}\bar\psi_i. \tag{B.2}$$

Using these definitions, we calculate the Gaussian integral from Section 3.4. Instead of a puzzling integral over Majorana fermions, we can work with an ordinary integral over Grassmann variables:

$$\int\left(\prod_{i=1}^{2K}\mathcal{D}\chi_i\right)\exp\left[-\frac{1}{2}\sum_{i=1}^{2K}\int\mathrm{d}\tau\,\mathrm{d}\tau'\,\chi_i(\tau)A(\tau,\tau')\chi_i(\tau')\right]$$
$$= \int\left(\prod_{i=1}^{K}\mathcal{D}\psi_i\mathcal{D}\bar\psi_i\right)\exp\left[-\sum_{i=1}^{K}\int\mathrm{d}\tau\,\mathrm{d}\tau'\,\bar\psi_i(\tau)A(\tau,\tau')\psi_i(\tau')\right]$$
$$= \operatorname{tr}\log\sqrt{A(\tau,\tau')}. \tag{B.3}$$

Here, we used the fact that the function $A(\tau,\tau') = -\delta(\tau-\tau')\partial_\tau - \Sigma(\tau,\tau')$ is antisymmetric under the change $\tau\leftrightarrow\tau'$. Note that the factor $1/2$ is canceled, as expected.

C. Correlator of energy fluctuations in the Sachdev–Ye–Kitaev model

Following [5], in this appendix we show that expression (4.24) is nothing but the correlator of the energy fluctuations. In order to do this, we need the following thermodynamic relation:

$$-\log Z = \beta F = N\left[-S_0 - \frac{2\pi^2 C}{\beta J} + \mathcal{O}\left(\frac{1}{(\beta J)^2}\right)\right]$$
$$+\beta E_0 + \frac{3}{2}\log(\beta J) + \text{const} + \mathcal{O}\left(\frac{1}{N}\right), \tag{C.1}$$

where E_0 is the ground state energy, S_0 is the zero-temperature entropy (per site), and C is the coefficient from the Schwarzian action (3.64). The derivation of this identity can be found in [5, 8, 120].

Varying (C.1), in the leading order in N and βJ we find that

$$\delta E = 4\pi^2 C\,\frac{N\delta\beta}{\beta^3 J}. \tag{C.2}$$

Now, let us consider a small variation in the temperature in the propagator (3.34):

$$\frac{G_{\mathrm{c}}^{\beta+\delta\beta}(\tau)}{G_{\mathrm{c}}^{\beta}(\tau)} = 1 - \frac{2\Delta}{\beta}\left[1 - \frac{\pi\tau}{\beta\tan(\pi\tau/\beta)}\right]\delta\beta. \tag{C.3}$$

Substituting (C.2) and averaging over the quantum fluctuations, we obtain the connected four-point function:

$$\frac{\left\langle G_{\mathrm{c}}^{\beta+\delta\beta}(\tau_1,\tau_2)G_{\mathrm{c}}^{\beta+\delta\beta}(\tau_3,\tau_4)\right\rangle}{G_{\mathrm{c}}^{\beta}(\tau_1,\tau_2)G_{\mathrm{c}}^{\beta}(\tau_3,\tau_4)} - 1 = \frac{\Delta^2}{4\pi^4C^2}$$
$$\times\left[1 - \frac{\pi\tau_{12}}{\beta\tan(\pi\tau_{12}/\beta)}\right]\left[1 - \frac{\pi\tau_{34}}{\beta\tan(\pi\tau_{34}/\beta)}\right]\frac{\beta^4J^2}{N^2}\left\langle(\delta E)^2\right\rangle. \tag{C.4}$$

On the other hand, the average square of the energy fluctuation can be found from (C.1):

$$\left\langle(\delta E)^2\right\rangle = \partial_\beta^2\log Z = \frac{4\pi^2C}{\beta^3J}, \tag{C.5}$$

so the correlation function is as follows:

$$\frac{\left\langle G_{\mathrm{c}}^{\beta+\delta\beta}(\tau_1,\tau_2)G_{\mathrm{c}}^{\beta+\delta\beta}(\tau_3,\tau_4)\right\rangle}{G_{\mathrm{c}}^{\beta}(\tau_1,\tau_2)G_{\mathrm{c}}^{\beta}(\tau_3,\tau_4)} - 1$$
$$= \frac{\Delta^2}{\pi^2C}\,\frac{\beta J}{N}\left[1 - \frac{\pi\tau_{12}}{\beta\tan(\pi\tau_{12}/\beta)}\right]\left[1 - \frac{\pi\tau_{34}}{\beta\tan(\pi\tau_{34}/\beta)}\right]. \tag{C.6}$$

This expression coincides with (4.24) for $\Delta = 1/4$.

D. Integral over the product of two eigenfunctions

To deduce the explicitly $\mathrm{SL}(2,\mathbb{R})$-invariant decomposition for the identity operator and four-point function, we need to calculate the following integral:

$$A(h) = \int_{-\infty}^{\infty} \frac{\mathrm{d}\omega}{2\pi}\, \Psi_{h\omega}(\tau_1,\tau_2)\Psi^*_{h\omega}(\tau_3,\tau_4)\,. \tag{D.1}$$

Using the symmetry of the integral under the changes $h \to 1-h$, $\omega \to -\omega$ and substituting eigenfunctions (4.47), we obtain the following expression:

$$A(h) = \frac{2}{\pi}\int_0^{\infty} \mathrm{d}\omega\, \cos\left[\omega(\tau_{13}+\tau_{24})\right] \times \begin{cases} \dfrac{\cos^2(\pi h/2)}{\cos^2(\pi h)}\, J_{h-1/2}(\omega|\tau_{12}|)J_{h-1/2}(\omega|\tau_{34}|) + (h \to 1-h)\,, & h = 2n\,, \\ \dfrac{\sin^2(\mathrm{i}\pi s/2)}{\sin(\mathrm{i}\pi s)}\, J_{\mathrm{i}s}(\omega|\tau_{12}|)J_{\mathrm{i}s}(\omega|\tau_{34}|) + (s \to -s)\,, & h = 1/2 + \mathrm{i}s\,. \end{cases} \tag{D.2}$$

We then use the identity established in Appendix D of [4] as a generalization of equation 6.612 from [125],

$$\int_0^{\infty} \mathrm{d}x\, \cos(ax)\, J_\nu(bx)\, J_\nu(cx) = \frac{1}{\pi\sqrt{bc}} \begin{cases} Q_{\nu-1/2}(z)\,, & z > 1\,, \\ \tilde{Q}_{\nu-1/2}(z)\,, & |z| < 1\,, \\ -\sin(\pi\nu) Q_{\nu-1/2}(z)\,, & z < -1\,, \end{cases} \tag{D.3}$$

where we have introduced the variable

$$z = \frac{-a^2+b^2+c^2}{2bc} \tag{D.4}$$

and defined the function $\tilde{Q}_\nu(z)$, which is analytic in the real interval $z \in (-1,1)$:

$$\tilde{Q}_\nu(z) \equiv \frac{1}{2}\left[Q_\nu(z+\mathrm{i}0) + Q_\nu(z-\mathrm{i}0)\right]. \tag{D.5}$$

Here, $Q_\nu(z)$ is the usual Legendre function of the second kind, while $\tilde{Q}_\nu(z)$ is referred to as the Legendre function on the cut. Applying this identity to integral (D.2) and using equations 8.335, 8.820, 9.134 from [125], we obtain the required formula:

$$A(h) = \frac{1}{\sqrt{|\tau_{12}\tau_{34}|}} \times \begin{cases} \dfrac{\Gamma(h/2)\Gamma\big((1-h)/2\big)}{\sqrt{\pi}}\, {}_2F_1\left[\dfrac{h}{2}, \dfrac{1-h}{2}, \dfrac{1}{2}, \left(\dfrac{2-\chi}{\chi}\right)^2\right], & \text{if } \chi > 1\,, \\ \dfrac{\cos^2(\pi h/2)}{\cos(\pi h)}\, \dfrac{\Gamma^2(h)}{\Gamma(2h)}\, \chi^h\, {}_2F_1(h,h,2h,\chi) + (h \to 1-h)\,, & \text{if } 0 < \chi < 1\,, \end{cases} \tag{D.6}$$

where χ is the $\mathrm{SL}(2,\mathbb{R})$-invariant cross-ratio. Note that function (D.6) is invariant with respect to the transformation $\chi \to \chi/(\chi-1)$, which allows calculating $A(h)$ for negative cross-ratios.

References

1. Kitaev A "Hidden correlations in the Hawking radiation and thermal noise", in *Fundamental Physics Prize Symp., November 10, 2014*; https://www.youtube.com/embed/OQ9qN8j7EZI; "A simple model of quantum holography, Pt. 1", in *Kavli Institute for Theoretical Physics, Univ. of California, Santa Barbara, CA, USA, April 7, 2015*; https://online.kitp.ucsb.edu/online/entangled15/kitaev/; "A simple model of quantum holography, Pt. 2", in *Kavli Institute for Theoretical Physics, Univ. of California, Santa Barbara, CA, USA, May 7, 2015*, https://online.kitp.ucsb.edu/online/entangled15/kitaev2/
2. Sachdev S, Ye J *Phys. Rev. Lett.* **70** 3339 (1993); cond-mat/9212030
3. Sachdev S *Phys. Rev. Lett.* **105** 151602 (2010); arXiv:1006.3794
4. Polchinski J, Rosenhaus V *J. High Energ. Phys.* **2016** 1 (2016); arXiv:1601.06768
5. Maldacena J, Stanford D *Phys. Rev. D* **94** 106002 (2016); arXiv:1604.07818
6. Kitaev A, Suh S J *J. High Energ. Phys.* **2018** 183 (2018); arXiv:1711.08467
7. Jevicki A, Suzuki K, Yoon J *J. High Energ. Phys.* **2016** 7 (2016); arXiv:1603.06246
8. Jevicki A, Suzuki K *J. High Energ. Phys.* **2016** 046 (2016); arXiv:1608.07567
9. Maldacena J, Shenker S H, Stanford D *J. High Energ. Phys.* **2016** 106 (2016); arXiv:1503.01409
10. Maldacena J, Stanford D, Yang Z *Prog. Theor. Exp. Phys.* **2016** 12C104 (2016); arXiv:1606.01857
11. Jensen K *Phys. Rev. Lett.* **117** 111601 (2016); arXiv:1605.06098
12. Almheiri A, Polchinski J *J. High Energ. Phys.* **2015** 14 (2015); arXiv:1402.6334
13. Engelsöy J, Mertens T G, Verlinde H *J. High Energ. Phys.* **2016** 139 (2016); arXiv:1606.03438
14. Sekino Y, Susskind L *J. High Energ. Phys.* **2008** (10) 065 (2008); arXiv:0808.2096
15. Susskind L, arXiv:1101.6048
16. Lashkari N et al. *J. High Energ. Phys.* **2013** 22 (2013); arXiv:1111.6580
17. Maldacena J, Stanford D, Yang Z *Fortschr. Phys.* **65** 1700034 (2017); arXiv:1704.05333
18. Maldacena J, Qi X-L, arXiv:1804.00491
19. Maldacena J, Milekhin A, Popov F, arXiv:1807.04726
20. Maldacena J, Milekhin A, arXiv:1912.03276
21. Hartnoll S A, Lucas A, Sachdev S, arXiv:1612.07324
22. Song X-Y, Jian C-M, Balents L *Phys. Rev. Lett.* **119** 216601 (2017); arXiv:1705.00117
23. Sachdev S *Phys. Rev. X* **5** 041025 (2015); arXiv:1506.05111
24. Larkin A I, Ovchinnikov Yu N *Sov. Phys. JETP* **28** 1200 (1969); *Zh. Eksp. Teor. Fiz.* **55** 2262 (1968)
25. Almheiri A et al. *J. High Energ. Phys.* **2013** 18 (2013); arXiv:1304.6483
26. Shenker S H, Stanford D *J. High Energ. Phys.* **2014** 67 (2014); arXiv:1306.0622
27. Gur-Ari G, Hanada M, Shenker S H *J. High Energ. Phys.* **2016** 91 (2016); arXiv:1512.00019
28. Eichhorn R, Linz S J, Hänggi P *Chaos Solitons Fractals* **12** 1377 (2001)
29. de Wijn A S, Hess B, Fine B V *Phys. Rev. Lett.* **109** 034101 (2012); arXiv:1205.2901
30. Fine B V et al. *Phys. Rev. E* **89** 012923 (2014); arXiv:1305.2817
31. Aleiner I L, Larkin A I *Phys. Rev. B* **54** 14423 (1996); cond-mat/9603121
32. Silvestrov P G, Beenakker C W J *Phys. Rev. E* **65** 035208(R) (2002); nlin/0111042
33. Berman G P, Zaslavsky G M *Physica A* **91** 450 (1978)
34. Zaslavsky G M *Phys. Rep.* **80** 157 (1981)
35. Roberts D A, Stanford D *Phys. Rev. Lett.* **115** 131603 (2015); arXiv:1412.5123
36. Romero-Bermúdez A, Schalm K, Scopelliti V *J. High Energ. Phys.* **2019** 107 (2019); arXiv:1903.09595

37. Polyakov A M *Gauge Fields and Strings* (Chur: Harwood Acad. Publ., 1987); Translated into Russian: *Kalibrovochnye Polya i Struny* (Izhevsk: Udmurtskii Univ., 1999)
38. Makeenko Y, in *M-Theory and Quantum Geometry* (NATO Science Ser. C, Vol. 556, Eds L Thorlacius, T Jonsson) (Dordrecht: Kluwer Acad. Publ., 2000) p. 285; hep-th/0001047
39. Cotler J S, Ding D, Penington G R *Ann. Physics* **396** 318 (2018); arXiv:1704.02979
40. Xu T, Scaffidi T, Cao X *Phys. Rev. Lett.* **124** 140602 (2020); arXiv:1912.11063
41. Hashimoto K, Murata K, Yoshii R *J. High Energ. Phys.* **2017** 138 (2017); arXiv:1703.09435
42. Gharibyan H et al. *J. High Energ. Phys.* **2018** 124 (2018); arXiv:1803.08050; *J. High Energ. Phys.* **2019** 197 (2019) Erratum
43. Haake F *Quantum Signatures of Chaos* (Berlin: Springer, 2010)
44. Ott E *Chaos in Dynamical Systems* (Cambridge: Cambridge Univ. Press, 2012)
45. Stöckmann H-J *Quantum Chaos*: *An Introduction* (Cambridge: Cambridge Univ. Press, 1999)
46. Srednicki M *Phys. Rev. E* **50** 888 (1994); cond-mat/9403051
47. Deutsch J M *Rep. Prog. Phys.* **81** 082001 (2018); arXiv:1805.01616
48. D'Alessio L et al. *Adv. Phys.* **65** 239 (2016); arXiv:1509.06411
49. Foini L, Kurchan J *Phys. Rev. E* **99** 042139 (2019); arXiv:1803.10658
50. Murthy C, Srednicki M *Phys. Rev. Lett.* **123** 230606 (2019); arXiv:1906.10808
51. Parker D E et al. *Phys. Rev. X* **9** 041017 (2019); arXiv:1812.08657
52. Avdoshkin A, Dymarsky A *Phys. Rev. Res.* **2** 043234 (2020); arXiv:1911.09672
53. Huang Y, Brandão F G S L, Zhang Y-L *Phys. Rev. Lett.* **123** 010601 (2019); arXiv:1705.07597
54. Sonner J, Vielma M *J. High Energ. Phys.* **2017** (11) 149 (2017); arXiv:1707.08013
55. Nayak P, Sonner J, Vielma M *J. High Energ. Phys.* **2019** (10) 19 (2019); arXiv: 1903.00478
56. Anous T, Sonner J *SciPost Phys.* **7** 003 (2019); arXiv:1903.03143
57. Page D N *Phys. Rev. Lett.* **71** 1291 (1993); gr-qc/9305007
58. Nishioka T, Ryu S, Takayanagi T *J. Phys. A* **42** 504008 (2009); arXiv:0905.0932
59. Anninos D, Galante D A, Hofman D M *J. High Energ. Phys.* **2019** (07) 38 (2019); arXiv:1811.08153
60. Aalsma L, Shiu G *J. High Energ. Phys.* **2020** (05) 152 (2020); arXiv:2002.01326
61. Hayden P, Preskill J *J. High Energ. Phys.* **2007** (09) 120 (2007); arXiv:0708.4025
62. Almheiri A et al. *J. High Energ. Phys.* **2013** (02) 62 (2013); arXiv:1207.3123
63. Mathur S D *Class. Quantum Grav.* **26** 224001 (2009); arXiv:0909.1038
64. Roberts D A, Stanford D, Streicher A *J. High Energ. Phys.* **2018** (06) 122 (2018); arXiv:1802.02633
65. Qi X-L, Streicher A *J. High Energ. Phys.* **2019** (08) 12 (2019); arXiv:1810.11958
66. Hartman T, Maldacena J *J. High Energ. Phys.* **2013** (05) 14 (2013); arXiv:1303.1080
67. Asplund C T et al. *J. High Energ. Phys.* **2015** (09) 110 (2015); arXiv:1506.03772
68. Aref'eva I Ya, Khramtsov M A, Tikhanovskaya M D *J. High Energ. Phys.* **2017** (09) 115 (2017); arXiv:1706.07390
69. Camanho X O et al. *J. High Energ. Phys.* **2016** (02) 20 (2016); arXiv:1407.5597
70. Roberts D A, Swingle B *Phys. Rev. Lett.* **117** 091602 (2016); arXiv:1603.09298
71. Hosur P et al. *J. High Energ. Phys.* **2016** (02) 4 (2016); arXiv:1511.04021
72. Nahum A, Vijay S, Haah J *Phys. Rev. X* **8** 021014 (2018); arXiv:1705.08975
73. Mezei M, Stanford D *J. High Energ. Phys.* **2017** (05) 65 (2017); arXiv:1608.05101
74. Roberts D A, Stanford D, Susskind L *J. High Energ. Phys.* **2015** (03) 51 (2015); arXiv:1409.8180
75. Shenker S H, Stanford D *J. High Energ. Phys.* **2014** (12) 46 (2014); arXiv:1312.3296
76. Shenker S H, Stanford D *J. High Energ. Phys.* **2015** (05) 132 (2015); arXiv:1412.6087
77. Turiaci G J, Verlinde H *J. High Energ. Phys.* **2016** (12) 110 (2016); arXiv:1603.03020
78. Fitzpatrick A L, Kaplan J *J. High Energ. Phys.* **2016** (05) 70 (2016); arXiv:1601.06164
79. Murugan J, Stanford D, Witten E *J. High Energ. Phys.* **2017** (08) 146 (2017); arXiv:1706.05362
80. Fu W et al. *Phys. Rev. D* **95** 026009 (2017); *Phys. Rev. D* **95** 069904 (2017) Erratum; arXiv:1610.08917
81. Gross D J, Rosenhaus V *J. High Energ. Phys.* **2017** (02) 93 (2017); arXiv:1610.01569
82. Gu Y, Qi X-L, Stanford D *J. High Energ. Phys.* **2017** (05) 125 (2017); arXiv:1609.07832
83. Stanford D *J. High Energ. Phys.* **2016** (10) 9 (2016); arXiv:1512.07687
84. Aleiner I L, Faoro L, Ioffe L B *Ann. Physics* **375** 378 (2016); arXiv:1609.01251
85. Yao N Y et al., arXiv:1607.01801
86. Huang Y, Zhang Y-L, Chen X *Ann. Physik* **529** 1600318 (2017); arXiv:1608.01091
87. Swingle B, Chowdhury D *Phys. Rev. B* **95** 060201(R) (2017); arXiv:1608.03280
88. Shen H et al. *Phys. Rev. B* **96** 054503 (2017); arXiv:1608.02438
89. Dóra B, Moessner R *Phys. Rev. Lett.* **119** 026802 (2017); arXiv:1612.00614
90. Bohrdt A et al. *New J. Phys.* **19** 063001 (2017); arXiv:1612.02434
91. Patel A A, Sachdev S *Proc. Natl. Acad. Sci. USA* **114** 1844 (2017); arXiv:1611.00003
92. Patel A A et al. *Phys. Rev. X* **7** 031047 (2017); arXiv:1703.07353
93. Lin C-J, Motrunich O I *Phys. Rev. B* **97** 144304 (2018); arXiv:1801.01636
94. von Keyserlingk C W et al. *Phys. Rev. X* **8** 021013 (2018); arXiv:1705.08910
95. Arseev P I *Phys. Usp.* **58** 1159 (2015); *Usp. Fiz. Nauk* **185** 1271 (2015)
96. Kamenev A *Field Theory of Non-Equilibrium Systems* (Cambridge: Cambridge Univ. Press, 2011); cond-mat/0412296
97. Krotov D, Polyakov A M *Nucl. Phys. B* **849** 410 (2011); arXiv:1012.2107
98. Akhmedov E T *Int. J. Mod. Phys. D* **23** 1430001 (2014); arXiv:1309.2557
99. Akhmedov E T, Godazgar H, Popov F K *Phys. Rev. D* **93** 024029 (2016); arXiv:1508.07500
100. Akhmedov E T et al. *Phys. Rev. D* **96** 025002 (2017); arXiv:1701.07226
101. Akhmedov E T, Moschella U, Popov F K *Phys. Rev. D* **99** 086009 (2019); arXiv:1901.07293
102. Haehl F M et al. *SciPost Phys.* **6** 001 (2019); arXiv:1701.02820
103. Sárosi G *PoS* **Modave2017** 001 (2018); arXiv:1711.08482
104. Rosenhaus V *J. Phys. A* **52** 323001 (2019); arXiv:1807.03334
105. Krajewski T et al. *Phys. Rev. D* **99** 126014 (2019); arXiv:1812.03008
106. Witten E *J. Phys. A* **52** 474002 (2019); arXiv:1610.09758
107. Gurau R *Nucl. Phys. B* **916** 386 (2017); arXiv:1611.04032
108. Klebanov I R, Tarnopolsky G *Phys. Rev. D* **95** 046004 (2017); arXiv:1611.08915
109. Klebanov I R, Popov F, Tarnopolsky G *PoS* **TASI2017** 004 (2018); arXiv:1808.09434
110. Klebanov I R, Pallegar P N, Popov F K *Phys. Rev. D* **100** 086003 (2019); arXiv:1905.06264
111. Nishinaka T, Terashima S *Nucl. Phys. B* **926** 321 (2018); arXiv:1611.10290
112. Peskin M E, Schroeder D V *An Introduction to Quantum Field Theory* (Reading, Mass.: Addison-Wesley Publ. Co., 1995); Translated into Russian: *Vvedenie v Kvantovuyu Teoriyu Polya* (Izhevsk: RKhD, 2001)
113. Bonzom V, Nador V, Tanasa A *Lett. Math. Phys.* **109** 2611 (2019); arXiv:1808.10314
114. Gurau R *Europhys. Lett.* **119** 30003 (2017); arXiv:1702.04228

115. Parcollet O, Georges A *Phys. Rev. B* **59** 5341 (1999); cond-mat/9806119
116. Lunkin A V, Tikhonov K S, Feigel'man M V *Phys. Rev. Lett.* **121** 236601 (2018); arXiv:1806.11211
117. Bagrets D, Altland A, Kamenev A *Nucl. Phys. B* **911** 191 (2016); arXiv:1607.00694
118. Aref'eva I et al. *J. High Energ. Phys.* **2019** (07) 113 (2019); arXiv:1811.04831
119. Wang H et al. *J. High Energ. Phys.* **2019** (09) 57 (2019); arXiv:1812.02666
120. Cotler J S et al. *J. High Energ. Phys.* **2017** (05) 118 (2017); *J. High Energ. Phys.* **2018** (09) 2 (2018) Erratum; arXiv:1611.04650
121. Kitaev A, arXiv:1711.08169
122. Gross D J, Rosenhaus V *J. High Energ. Phys.* **2017** (12) 148 (2017); arXiv:1710.08113
123. Gross D J, Rosenhaus V *J. High Energ. Phys.* **2017** (05) 92 (2017); arXiv:1702.08016
124. Reed M, Simon B *Methods of Modern Mathematical Physics* Vol. 1 *Functional Analysis* (New York: Academic Press, 1980)
125. Gradshteyn I S, Ryzhik I M *Tables of Integrals, Series, and Products* (San Diego, CA: Associated Press, 2007); Translated from Russian: *Tablitsy Integralov, Ryadov i Proizvedenii* (St. Petersburg: BKhV-Peterburg, 2011)
126. Bagrets D, Altland A, Kamenev A *Nucl. Phys. B* **921** 727 (2017); arXiv:1702.08902
127. Streicher A *J. High Energ. Phys.* **2020** (02) 48 (2020); arXiv:1911.10171
128. Choi C, Mezei M, Sárosi G, CERN-TH-2019-206 (Geneva: CERN, 2019); arXiv:1912.00004
129. Thomi P, Isaak B, Hajicek P *Phys. Rev. D* **30** 1168 (1984)
130. Nayak P et al. *J. High Energ. Phys.* **2018** (09) 48 (2018); arXiv:1802.09547
131. Grumiller D, Kummer W, Vassilevich D V *Phys. Rep.* **369** 327 (2002); hep-th/0204253
132. Jackiw R *Nucl. Phys. B* **252** 343 (1985)
133. Teitelboim C *Phys. Lett. B* **126** 41 (1983)
134. Kolekar K S, Narayan K *Phys. Rev. D* **98** 046012 (2018); arXiv:1803.06827
135. Akhmedov E T, Moschella U, Popov F K *J. High Energ. Phys.* **2018** (03) 183 (2018); arXiv:1802.02955
136. Spradlin M, Strominger A *J. High Energ. Phys.* **1999** (11) 021 (1999); hep-th/9904143
137. Akhmedov E T *Phys. Lett. B* **442** 152 (1998); hep-th/9806217
138. de Boer J, Verlinde E P, Verlinde H L *J. High Energ. Phys.* **2000** (08) 003 (2000); hep-th/9912012
139. Skenderis K *Class. Quantum Grav.* **19** 5849 (2002); hep-th/0209067
140. Grumiller D, McNees R *J. High Energ. Phys.* **2007** (04) 074 (2007); hep-th/0703230
141. Grumiller D et al. *J. High Energ. Phys.* **2017** (10) 203 (2017); arXiv:1708.08471
142. Cvetič M, Papadimitriou I *J. High Energ. Phys.* **2016** (12) 008 (2016); *J. High Energ. Phys.* **2017** (01) 120 (2017) Erratum; arXiv:1608.07018
143. Davis J L, McNees R *J. High Energ. Phys.* **2005** (09) 072 (2005); hep-th/0411121
144. González H A, Grumiller D, Salzer J *J. High Energ. Phys.* **2018** (05) 83 (2018); arXiv:1802.01562
145. Grumiller D, Leston M, Vassilevich D *Phys. Rev. D* **89** 044001 (2014); arXiv:1311.7413
146. Grumiller D, Salzer J, Vassilevich D *J. High Energ. Phys.* **2015** (12) 015 (2015); arXiv:1509.08486
147. Maldacena J *Int. J. Theor. Phys.* **38** 1113 (1999); *Adv. Theor. Math. Phys.* **2** 231 (1998); hep-th/9711200
148. Gubser S S, Klebanov I R, Polyakov A M *Phys. Lett. B* **428** 105 (1998); hep-th/9802109
149. Aharony O et al. *Phys. Rep.* **323** 183 (2000); hep-th/9905111
150. Witten E *Adv. Theor. Math. Phys.* **2** 253 (1998); hep-th/9802150
151. Freedman D Z et al. *Nucl. Phys. B* **546** 96 (1999); hep-th/9804058
152. Krishnan C, Sanyal S, Bala Subramanian P N *J. High Energ. Phys.* **2017** (03) 56 (2017); arXiv:1612.06330
153. Bonzom V, Lionni L, Tanasa A *J. Math. Phys.* **58** 052301 (2017); arXiv:1702.06944
154. Choudhury S et al. *J. High Energ. Phys.* **2018** (06) 94 (2018); arXiv:1707.09352
155. Bulycheva K et al. *Phys. Rev. D* **97** 026016 (2018); arXiv:1707.09347
156. Klebanov I R et al. *Phys. Rev. D* **97** 106023 (2018); arXiv:1802.10263
157. Giombi S et al. *Phys. Rev. D* **98** 105005 (2018); arXiv:1808.04344
158. Pakrouski K et al. *Phys. Rev. Lett.* **122** 011601 (2019); arXiv:1808.07455
159. Popov F K *Phys. Rev. D* **101** 026020 (2020); arXiv:1907.02440
160. Gaitan G et al. *Phys. Rev. D* **101** 126002 (2020); arXiv:2002.02066
161. Ferrari F *Ann. Inst. Henri Poincaré D* **6** 427 (2019); arXiv:1701.01171
162. Azeyanagi T et al. *Ann. Physics* **393** 308 (2018); arXiv:1710.07263
163. Ferrari F, Rivasseau V, Valette G *Commun. Math. Phys.* **370** 403 (2019); arXiv:1709.07366
164. Azeyanagi T, Ferrari F, Schaposnik Massolo F I *Phys. Rev. Lett.* **120** 061602 (2018); arXiv:1707.03431
165. Gu Y et al. *J. High Energ. Phys.* **2020** (02) 157 (2020); arXiv:1910.14099
166. Bulycheva K *J. High Energ. Phys.* **2017** (12) 69 (2017); arXiv:1706.07411
167. Davison R A et al. *Phys. Rev. B* **95** 155131 (2017); arXiv:1612.00849
168. Maldacena J *J. High Energ. Phys.* **2003** (04) 021 (2003); hep-th/0106112
169. Cornalba L et al. *J. High Energ. Phys.* **2007** (08) 019 (2007); hep-th/0611122
170. Grozdanov S, Schalm K, Scopelliti V *Phys. Rev. E* **99** 012206 (2019); arXiv:1804.09182
171. Kitaev A Yu *Phys. Usp.* **44** (10S) 131 (2001); *Usp. Fiz. Nauk* **171** (Suppl. 10) 131 (2001); cond-mat/0010440
172. Kourkoulou I, Maldacena J, arXiv:1707.02325
173. García-García A M, Verbaarschot J J M *Phys. Rev. D* **94** 126010 (2016); arXiv:1610.03816
174. Evans T S, Steer D A *Nucl. Phys. B* **474** 481 (1996); hep-ph/9601268
175. Trunin D A *Int. J. Mod. Phys. A* **33** 1850140 (2018); arXiv:1805.04856